Greener alternatives open a wide scope of alternatives to a world based on fossil resources. In this context biomass and more exactly lignin is going to be the source for the production of value added chemicals.During this thesis the influence of the raw materials on the lignin structure, the different extraction methods to extract lignin, different pathways for the production of aromatic acids and polyol production from lignin are going to be studied more in detail.

Ane Sequeiros

EUSKO JAURLARITZA
GOBIERNO VASCO

EKONOMIAREN GARAPEN
ETA LEHIAKORTASUN SAILA

DEPARTAMENTO DE DESARROLLO
ECONÓMICO Y COMPETITIVIDAD

2016

Universidad del País Vasco

Euskal Herriko Unibertsitatea

STUDY OF LIGNIN TO VALUE ADDED CHEMICALS

Ane Sequeiros

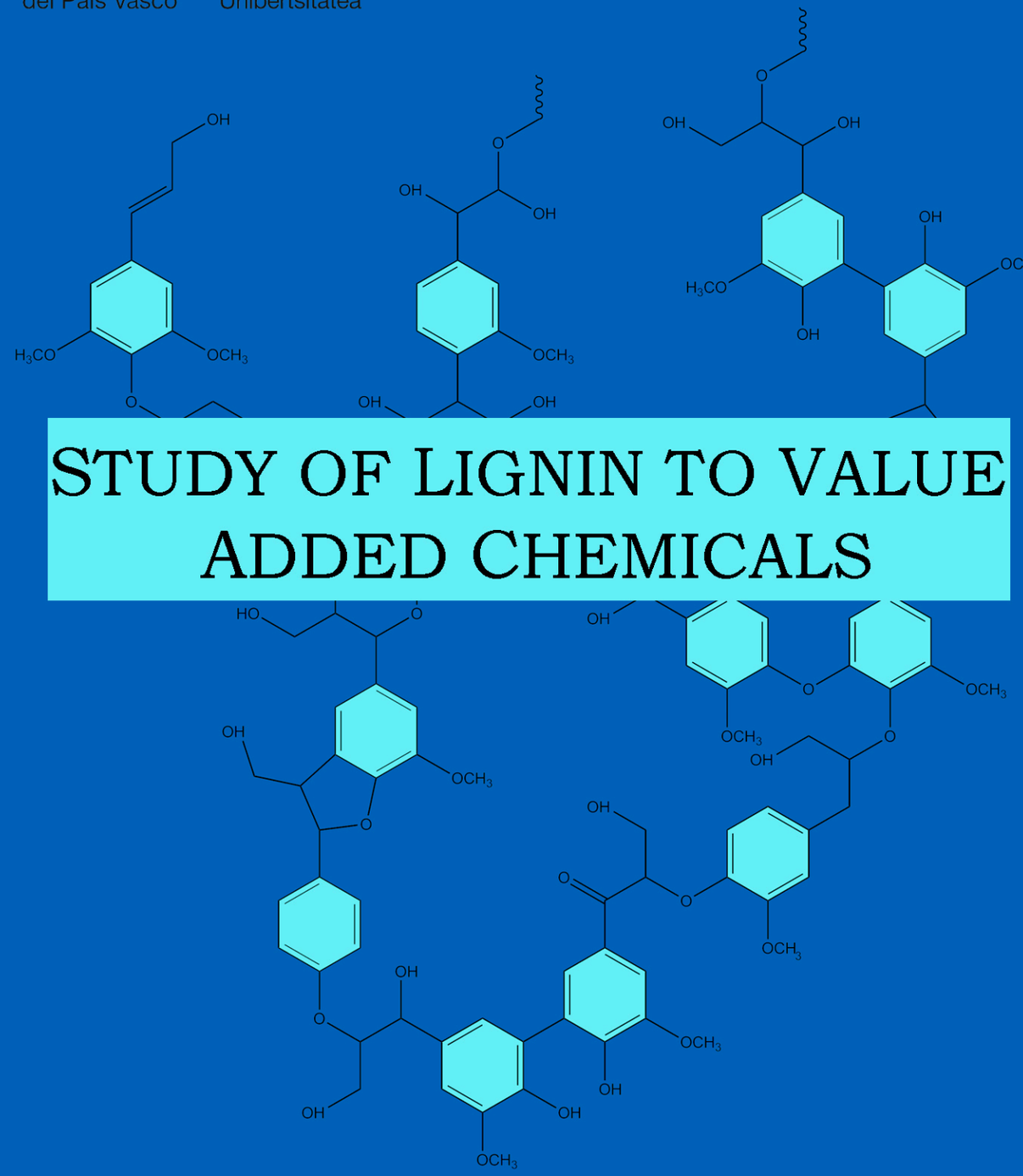

STUDY OF LIGNIN TO VALUE ADDED CHEMICALS

Ane Sequeiros Echeverria 2016

eman ta zabal zazu

UPV EHU

STUDY OF LIGNIN TO VALUE ADDED CHEMICALS

Thesis by

Ane Sequeiros Echeverria

For the degree of

Doctor in Renewable Material Engineering

Director: Jalel Labidi

Chemical and Environmental Engineering Department

Faculty of Engineering of Gipuzkoa

Donostia-San Sebastian 2016

Agradecimientos

Me gustaría agradecer en primer lugar a mi director de tesis el Dr. Jalel Labidi la oportunidad de realizar esta tesis doctoral bajo su dirección en estos 4 años. Además, también me gustaría agradecerle las numerosas oportunidades que me ha dado para asistir a congresos y cursos.

Agradezco al Departamento de Desarrollo Económico y Competitividad del Gobierno Vasco la oportunidad que me han brindado al ser beneficiaria de la beca de formación de jóvenes investigadores.

Más en concreto me gustaría agradecer a todos mis compañeros del grupo de "procesos de biorefinería" por ayudarme en el plano laboral y personal durante estos 4 años para ir avanzando en mi investigación y hacer más ameno cada día en el laboratorio.

Durante mi tesis he tenido la oportunidad de realizar una estancia en el extranjero para completar mi investigación. Tuve el placer de estar 3 meses en el Leibniz Instute for Catalysis (Rostock-Alemania) bajo la supervisión del profesos Hans de Vries. Agradecer a todo el grupo de investigación la paciencia que tuvieron al introducirme en el mundo de la catálisis y ayudarme con todas mis dudas.

No quisiera terminar sin agradecer a mi familia y a mis amigos por todo lo que han tenido que aguantar durante este proceso de aprendizaje. A mi pareja que ha escuchado con paciencia todos mis comentarios y dudas que he tenido y ayudarme a seguir adelante en los momentos más oscuros.

En definitiva; gracias a todos porque sin vosotros esta tesis no hubiera sido posible.

Summary

The depletetion of the fossil resources arise several challenges that are trying to be addressed by greener alternatives such the biomass. In this thesis one of the main components of the biomass and due to its aromatic scructure was selected to be studied extensively.

During the development of this thesis several lignin extraction methods were studied to seek for the purest lignin. Afterwars, three agro-forestal raw materials and an industrial residue were analyzed by pyrolysis to know which raw material was the one with the highest syringyl and guaiacyl groups for further depolymerization. During this stage, lignin was used to produce polyols from microwave heating; experimental conditios were applied with the objective of polyol with high yield and high hydroxyl groups. Finally, syringol and guaiacol two main monomers that could be obtained from the depolimerization of lignin under mild conditionds were used as raw materials to produce aromatic acids. For this target three different pathways were subjected to a test being the fist one the alkoxy carbonylation the second the oxidative carbonylation and the third one the bromination followed by the Grignard reaction.

Table of content

Objectives and methodology

The depletion of fossil recourse arise several global challenges to a society which is based on few energy sources such as petroleum. In addition, the ecological disadvantages have come into prominence as the use of fossil energy sources produces a number of severe consequences for the environment, including the greenhouse gas emission, air pollution, acid rain, etc… that are causing the climate change. Trying to give an alternative to the fossil resources renewable sources and technologies are investigated. One of these technologies is the conversion of biomass to fuels and chemicals in the so-called "Integrated Biorefinery".

The aim of this thesis was to revalorize an agricultural and industrial residue such as lignin and to obtain high value added chemicals that could be used in several chemical reactions.

The specific objectives are:

- To extract lignin from almond shell by different methods to determine the treatment that allows the obtaining of the purest lignin.

- Full chemical characterization of three agro-forestal residues and an industrial residue and determination of the syringyl and guaiacyl groups by Py/GC-MS with the aim to know the lignin with the highest content of those two groups for further depolymerization.

- Polyol production by liquefaction of lignin from olive tree pruning under microwave heating. Determination of polyols with high yields and high hydroxyl numbers by screening different experimental conditions (time, temperature and catalyst concentration).

- Production of aromatic acids starting from two main monomers that could be obtained from lignin depolymerization. The treatments that were employed were the alkoxy carbonylation, the oxidative carbonylation and the bromination followed by the Grignard reaction.

The thesis is structured in five chapters, described briefly in the following paragraphs.

The first chapter is a literature review of the current issue about petrochemistry which is used for fuels and chemicals and the lignocellulosic biomass as an alternative to deal with the decreasing source of petroleum. At the same time there is a brief description of the main components of the lignocellulosic biomass (cellulose, hemicelluloses and lignin) and a description of the chosen the raw materials that were used during the development of this research work. Among the main components of lignocellulosic biomass, due to its aromatic structure lignin is one most attractive component.

This thesis is focus on the revalorization of one of the main components of biomass, lignin. In the second chapter the main lignin fractionation processes to extract lignin are described. The experimental work of extracting lignin from almond shell using different extraction methods such as alkaline and organosolv processes was made to study the differences between the extracted lignins. The methodology followed was to analyze the liquid fraction by performing analysis of pH, density; total dissolved solid, organic and inorganic matter and lignin content. At the same time lignin was also analyzed by measuring acid insoluble and soluble lignin, total sugars, ashes, FTIR, molecular weight, total phenolic content, antioxidant power and ^{13}C NMR.

The third chapter deals with the importance of the H:G:S ratio and the different method that exist to measure it. In

this chapter the pyrolysis methods was the chosen to measure the guaiacyl and syringyl groups of different lignins to know which has the highest ratio to be further depolymerized. Moreover in this chapter three agro-forestal residues such as apple tree pruning, olive tree pruning and almond shell with and industrial residue, kraft lignin, were fully characterized taking into accound the raw materials, the liquid fractions of each extraction process and the lignin that was recovered.

In the fourth chapter lignin from olive tree pruning was subjected to liquefaction under microwave heating to obtain polyols. Experimental conditions (time, temperature, catalyst concentration) were modified with the aim to obtain the highest reaction yields and hydroxyl number. The statistical studies revealed bad regression values for the hydroxyl number equation. As a consequence this equation was not taken into account and based on literature the hydroxyl number had to be between 300-800 mgKOH/g. Applying this limitations two optical conditions were obtained (polyol an and 24).

In the fifth chapter guaiacol and syringol the two main monomers that are obtained from the depolimerization of lignin are chemically transformed into aromatic acids by different methods. In the first part of this chapter activated guaiacol and syringol were alkoxy carbonylated in an autoclabe reactor with different experimental conditions, catalysts that was palladium acetate, ligands, bases that were DABCO, potassium carbonate and sodium acetate, the temperate was varied between 100-125ºC, pressure loading and time was set at 15 hours. Once the reaction was over the autoclave was colded down and samples were analyzed by GC to ackwoledge the yield and the conversion of each reaction. In the second part of this chapter oxidative carbonylation of guaiacol and syringol in an autoclave reactor using different substrates, catalyst potassium

persultate, oxidants such as benzoquinone and potassium persulfate, temperature room temperature-50 ºC and 100 ºC, different pressure loading of carbon monoxide (1 bar; 5 bars) and time was set for 20 hours. After the reaction was over the reactor was colded down and samples were collected to be analyzed by HPLC that gave the yield and the conversion of each reaction. In the third part of this chapter another methodology to convert guaiacol and syringol into aromatic acid was studied. In these two steps process guaiacol and syringol were firstly brominated and secondly Grignard reaction took place to create the aromatic acids. The bromination reaction was performed by an ionic liquid 1-butyl-3-methylimidazoliumbromide that was dried by microwave heating in combination of N-bromosuccinimide. Once the substrate was brominated liquid-liquid extractions were done to the mixture by ethyl acetate and diethyl ether. The results were analyzed by GC-MS and 13C-NMR. The Grignard reaction was performed with a mixture of brominated guaiacol and syringol in a nitrogen fluxed gas made assembly to which magnesium turning were added as well as diethyl ether. Once the raction was started and controlled dry ice was added to the mixture. The liquid-liquid extractions were done with sodium hydroxide after that the organic face was precipitated with chloridric acid. The analyses of the final products were made by HPLC.

Chapter 1

Introduction

1.1 Overview

Up to the 19th century mankind used renewable resources not only for food but also for functional applications. In the 19th century there was a fundamental change, brought about by the emergence of carbochemistry (based on coal, aromatics and synthesis of gas) and in the 20th century by the development of petrochemistry. The use of renewable raw materials declined significantly, mainly as consequence of the extremely low prices for petrochemical resources. During this period, the strongly developing chemical industry was nearly systematically based on petrochemical resources [1].

Nowadays, the conventional resources are still mainly nonrenewable and according to the World Energy Council, up to 82% of the world's energy needs are currently covered by fossil resources such as petroleum, natural gas and coal [2, 3].

Fossil resources are not only use for energy and fuel needs, but also for more than 2500 different oil-based products that are on the market. Crude oil represents the major source for plastics, fibers and colors. At presents, 10% of world-wide natural gas consumption, 21% of the natural gas liquids and 4% or crude oil are used for chemicals [4].

Moreover, the supply of these fossil resources is inherently finite. It is generally agreed that we will be running out of petroleum within 50 years, natural gas within 65 years and coal in about 200 years. The world's crude oil reserves will not last forever. With regard of fossil reserves, the crude oil is being consumed faster than what is produced (Figure 1.1). Furthermore, the largest parts of petroleum reserves are located in politically unstable countries or regions. Therefore, the cost for extracting the crude oil rises continuously, reflected in increasing oil prices. Also, the ecological disadvantages have come to prompt from the use

of fossil sources include the greenhouse gas emissions, air pollution, acid rain, etc [2]. These growing concerns have stimulated intense research to investigate the potential of renewable alternatives for fuel, energy and chemical production [5]. The energy consumption can be based on various alternative raw materials (wind, sun, water, biomass, nuclear fission and fusion) with the advantage of forming smaller amounts of greenhouse gases compared to the conversion of fossil fuels, as the carbon dioxide generated during the energy conversion is consumed during subsequent biomass re-growth [6]. However, simply providing sustainable and non-polluting energy will not be enough. In our life, clothes, shelter, tools, medications and so on are all, to a greater or lesser degree, dependent on organic carbon. The challenge is to find replacements not only for current usage, but also for the even future greater energy consumption, with a likely concomitant increase in biomass demand for manufacturing [7].

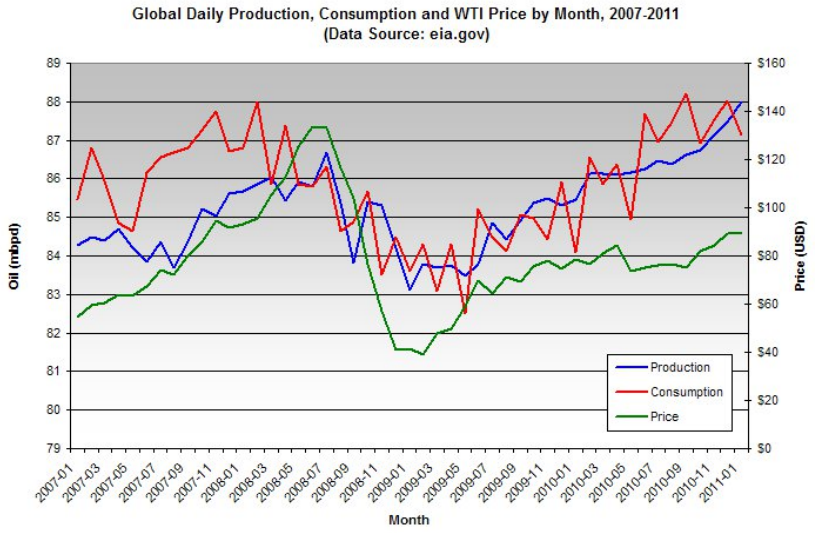

Figure 1.1 Global production, consumption and price of oil by month

In this context our government is taking some measures for the replacement of the fossil resources. The renewable energy directive of the European Union (EU) has established an overall policy for the production and promotion of energy from renewable resources in the EU. It is required to the EU to fulfill at least 20% of its total energy needs with renewable by 2020 to be achieved through the attainment of individual national targets. A mandatory 10% minimum target of their transport fuels to come from renewable sources by 2020 for all Member States [8].

1.2 Biomass as a renewable resource

These goals have contributed to the intensification in the development of technology and processes for biomass valorization in terms not only for energy production, but also to yield biofuels and biomaterials (Figure 1.2).

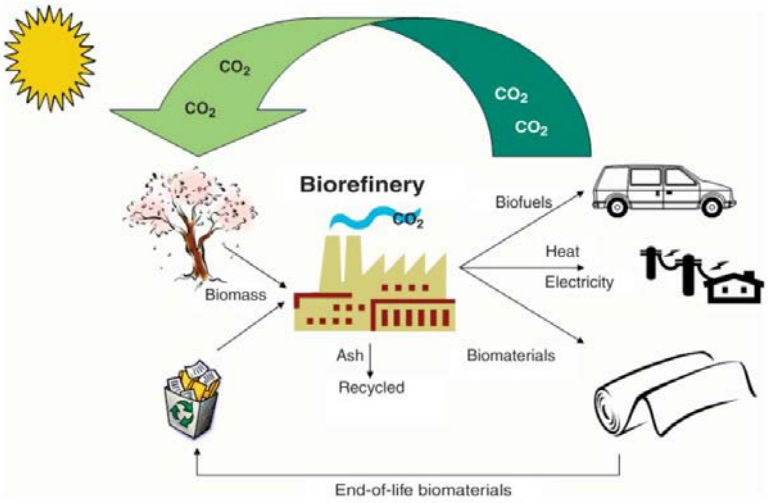

Figure 1.2 Biomass based biorefinery scheme.

The term biomass (Greek *bio* meaning *life* + *maza* meaning *mass*) refers to non fossilized and biodegradable organic material originated from plants, animals and microorganisms. The biomass includes products,

byproducts, residues and waste from agriculture, forestry and related industrial as well as the non-fossilized and biodegradable organic fractions of industrial and municipal solid wastes. Biomass also includes gases and liquids recovered from the decomposition of non-fossilized and biodegradable organic material [9].

Biomass is produced via photosynthesis, which converts light energy to chemical energy, stores it in carbohydrates as "6 CO_2 + 6 H_2O C_6H_{12} + 6 O_2" and fixed atmospheric carbon into biomass (living carbon) [10] (Figure 1.3).

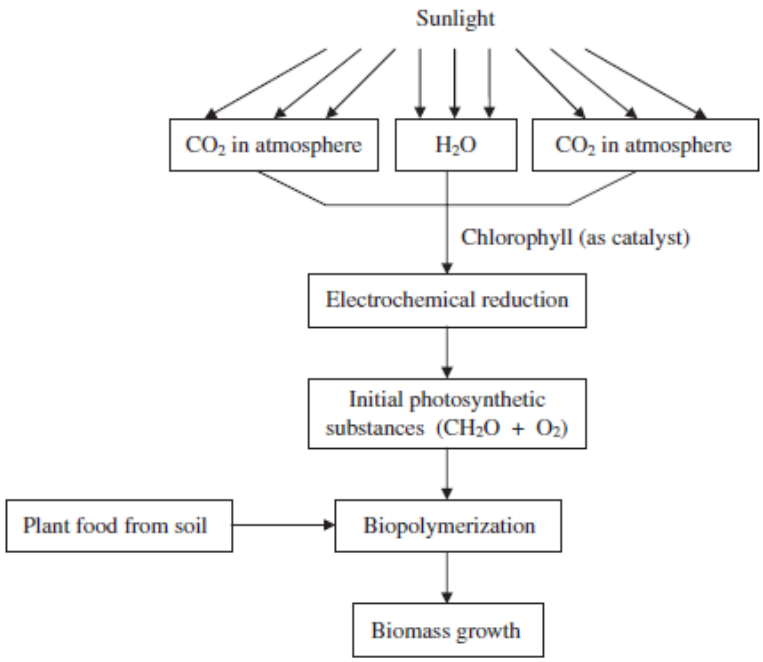

Figure 1.3 The main steps of photosynthetic biomass growth (adapted from [9])

Lignocellulosic feedstock is by far less costly that other feedstocks (crude oil, natural gas, corn kernels, and soy oil). For example, crude oil price varying from $40 to $80 per barrel is much higher that the price of lignocellulose [10].

Biomass appears to be an attractive feedstock for three main reasons. First, it is a renewable resource that could be sustainably developed in the future. Second, it appears to have formidably positive environmental properties by reducing Green House Gas emissions, possibly reducing NO_x and SO_x depending on the fossil fuel displaced. Third, it appears to have significant economic potential provided that fossil fuel prices increase in the future [9].

1.3 Lignocellulosic biomass

Lignocellulose is the material that makes up the cell walls of woody plants such as trees, shrubs and grasses. It is a composite material, with three biopolymers, cellulose, hemicelluloses and lignin, making up 90% of the dry matter (Figure 1.4) [11] along with smaller amounts of pectin, protein, extractives (soluble nonstructural materials) and ash [12]. The exact composition of lignocelluloses depends on the species, the plant tissue and the growth conditions.

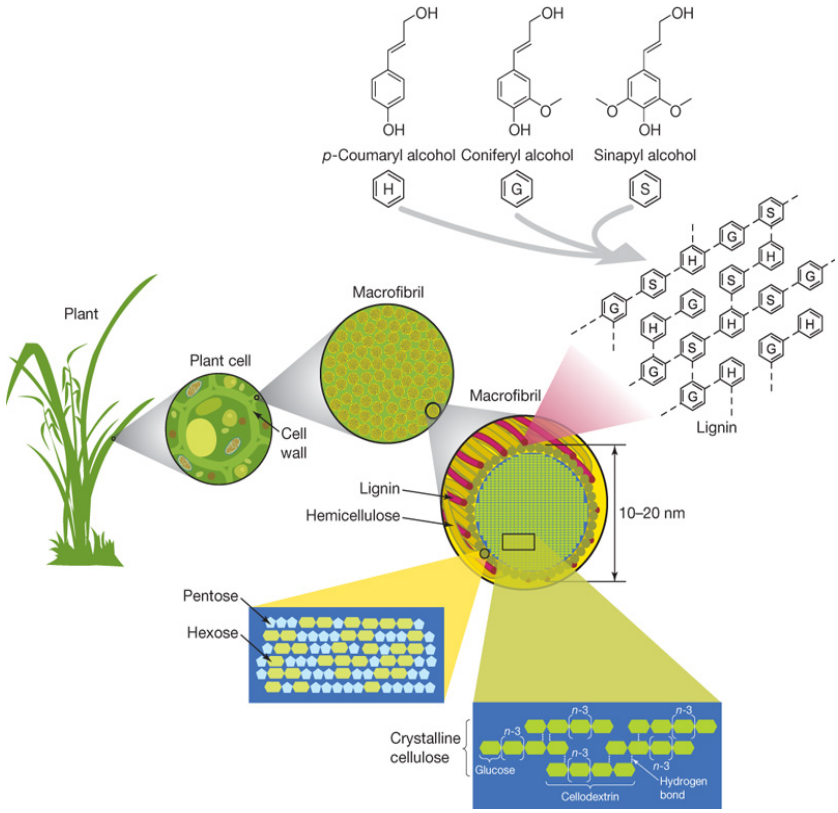

Figure 1.4 Scheme of structural components of plant cell wall [13]

1.3.1. Non structural components

Extractives

The extractives are a group of cell wall chemicals manly consisting of fats, fatty acids, fatty alcohols, phenols, terpenes, steroids, resin acids, rosin, waxes, etc. these chemicals exist as monomers, dimmers and polymers [14]. The extractives possess both fungicidal activity as well as being excellent antioxidants [15].

Proteins

Plant cell wall proteins comprise less than 10% of cell wall dry weight, but play crucial roles in cell wall structure and architecture, cell wall metabolism, cell enlargement, signaling, responses to abiotic and biotic stresses, and many other physiological processes [16].

Ashes

The presence of ash-forming elements in trees is the result of biochemical processes, the mineral uptake from soil and the element transport within the trees. Some of the main ash-forming elements are essential for plant growth. These are divided in macronutrients (K, Ca, Mg, P and S) and micronutrients (Fe, Mn and Cl) after their level of occurrence. Si, Al and Na are non-essential for plant growth [17]. In general the ash content of fibrous raw material is between 1 and 20%, while in softwood and hardwoods contain almost negligible amounts of minerals [18].

1.3.2. Cellulose

Cellulose is the largest single component of lignocelluloses. Although the cellulose content of different biomass feedstocks varies significantly, it is typically in the range of 35-50 wt% [11]. A cellulose molecule has the generic chemical formula $(C_6H_{12}O_5)_n$. It consists of a skeletal linear polysaccharide, in which glucose based monomers units are joined together through β-1,4-glycosidic linkages. The glucose units are further tightly bound by extensive intramolecular and intermolecular hydrogen bonding networks and Van der Walls forces [19] (Figure1.5). Cellulose is usually organized into microfibrils, each measuring about 3 to 6 nm in diameter and containing up to 36 glucan chains having thousands of glucose residues. According to

the degree of crystallinity, cellulose is classified into crystalline and amorphous [20].

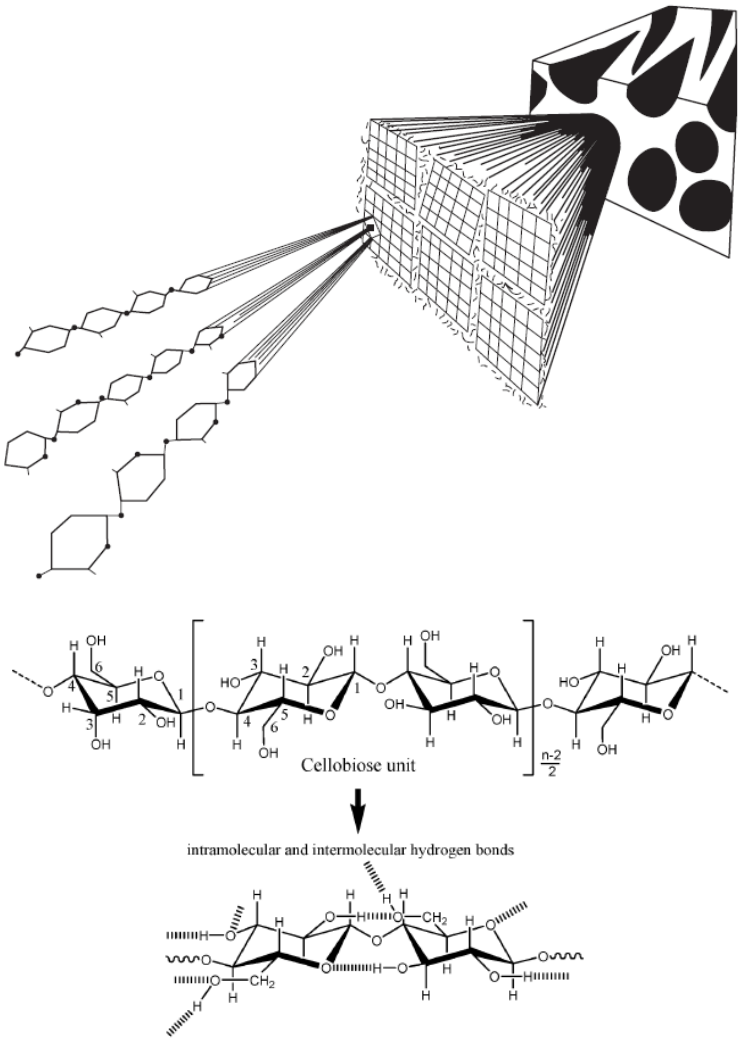

Figure1.5 Schematic view of the components of cellulose fiber [18, 21]

Although the monomer (glucose) and short oligomers are water-soluble, cellulose is not. The reasons for this are the high molecular weight of cellulose and the comparatively low flexibility of cellulose polymer chains [11].

In industry cellulose has been used not only for pulp and paper production but also, for the production of regenerated materials (fibers, films, food casings, membranes, sponges) and cellulose derivatives (ether and esters) [22].

Other cellulose applications imply the hydrolysis of cellulose to obtain glucose which can subsequently modified via liquefaction, gasification pyrolysis or hydrogenation to obtain a variety of products including ethanol, sorbitol, furfural malic acid, lactic acid and so on [19].

1.3.3. Hemicelluloses

Hemicelluloses are a large group of polysaccharides found in the primary and secondary cell walls and constitute about 20-40% of the total mass. They are classically defined as alkali soluble material after removal of pectic substances, and have a much lower degree of polymerization (100-200) compared with that of cellulose (10,000-14,000). The principal sugar components are both hexose and pentose sugars; the C6 sugars glucose, mannose, galactose and the C5 sugars xylose and arabinose (Figure 1.6) [23].

The main backbone of a hemicellulosic macromolecule is formed of either the same monomeric unit (homopolymer) or of two or more different units (heteropolymer). In general terms, hemicelluloses could be classified in four groups:

- Xylans (β-1,4- linked D-xylone)
- Mannans (β-1,4-linked D-mannose)
- Arabinans (α-1,5-linked L-arabinose)
- Galactans (β-1,3- linked D-galactose)

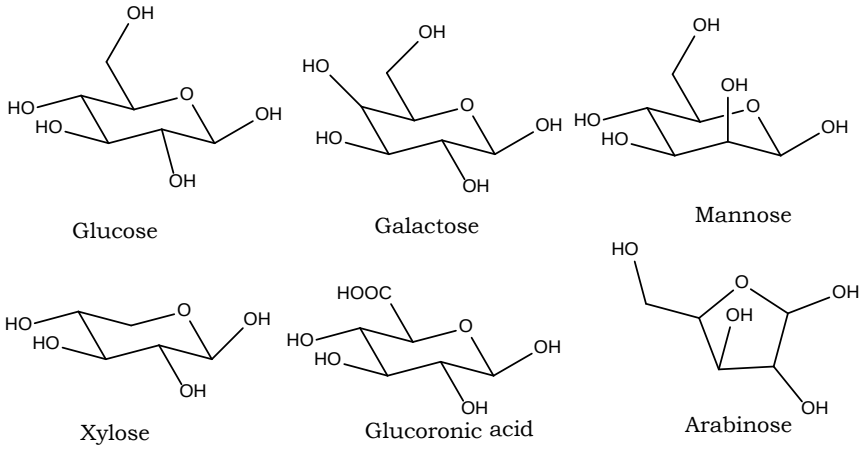

Figure 1.6 Hemicellulose main monomeric sugars

Xylans are the main hemicelluloses in hardwood and they also predominate in annual plants and cereals making up to 30% of the cell wall material, whereas galactomannans represent the largest hemicelluloses fraction in softwoods. Hardwood xylan (*O*-acetyl -4-methyl-glucuronoxylan) is substituted at irregular intervals with 4-*O*-methyl-α-D-glucuronic acid groups joined to xylose by α-1,2-glycosidic linkages (Figure 1.7). On average, every tenth xylose unit has an uronic acid group attached at C2 or C3 of the xylopyronose [24].

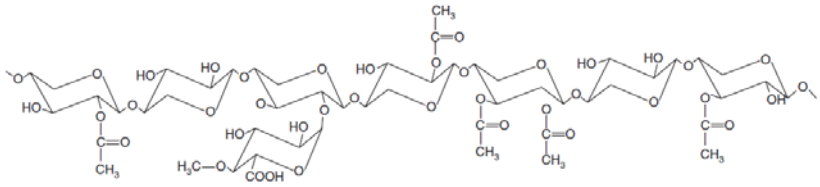

Figure 1.7 Structure of *O*-acetyl-(4-methyl-glucuro)xylan in hardwood [22].

1.3.4. Lignin

Lignin is among the most abundant biopolymers on earth, constituting approximately 30% of the dry weight of softwoods and 20% of hardwood. The term lignin is derived from the Latin word *lignum* which means wood [25] and its functions encompass the strengthening of plant cell walls, providing resistance against microbial attack, and playing a crucial part in water transport by reducing cell wall permeability [26].

Lignin is a three-dimensional, complex biopolymer comprised of three phenylpropanoid units (monolignols), namely synapyl alcohol (S), coniferyl alcohol (G), and *p*-coumaryl alcohol (H) (Figure 1.8). The initial dehydrogenation reaction of the monolignols (H, G or S) is promoted by peroxidases and laccases, and consists in the removal of the phenolic hydrogen atom from the precursors leading to phenyl radicals, which by non-enzymatic and random radical-radical coupling produce a three dimensional amorphous polymer which forms a randomized structure inside the cell walls [27].

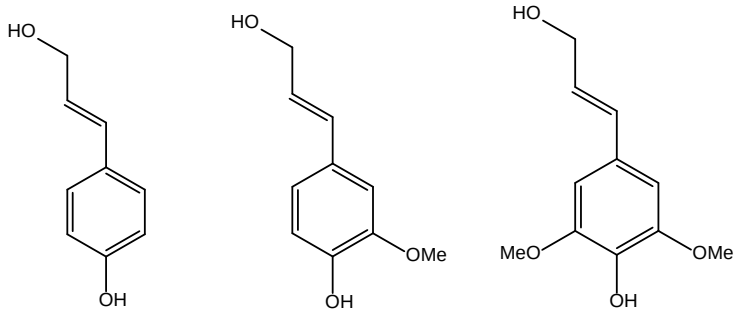

Figure 1.8 Most common monolignols in lignin

Despite of having a randomized structure, there are some common linkages that are repeated in the lignin structure: β-O-4 aryl ether bonds, β-5-phenylcourmaran, 5-5´biphenyl, 4-O-5-diarylether, β-1(1,2-diarylpropane), α-O-4-aryl ether and β-β´-resinol linkages which are depicted in Figure 1.9.

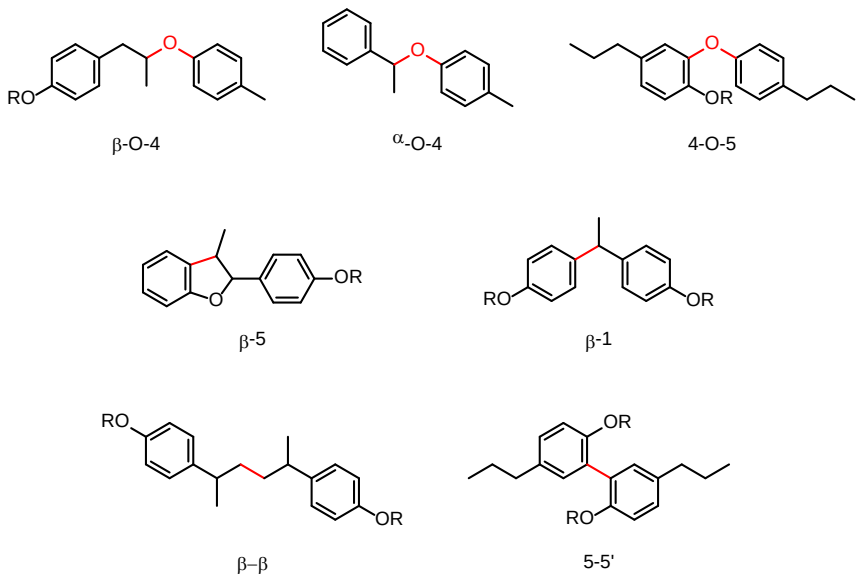

Figure 1.9 Most common lignin linkages

Depending on its source lignin structure presents different concentrations of phenylpronanoid units. In softwood lignin (Figure 1.10 b), usually referred as guaiacyl lignin, the structural elements are derived principally from coniferyl alcohol (G) and trace amount of *p*-coumaryl alcohol (H). On the other hand, hardwood lignin (Figure 1.10 a), known as guaiacyl-syringyl lignin, is comprised of coniferyl alcohol and sinapyl alcohol (S) -derived units in varying ratios. Although grass lignins are also classified as guaiacyl-syringyl lignins they additionally contain small but significant amounts of structural elements derived from *p*-coumaryl alcohol [28].

The proportion of the linkages also varies among lignin of different sources as it could be seen in Table 1.1.

Table 1.1 Types and frequencies of interunitary linkages

Linkage type	Softwood (%)	Hardwood (%)
β-O-4	45-48	60
α-O-4	6-8	6-8
4-O-5	3.5-8	6.5
5-5´	9.5-11	4.5
β-1	7-10	8
β-5	9-12	6
β-β´	2	3

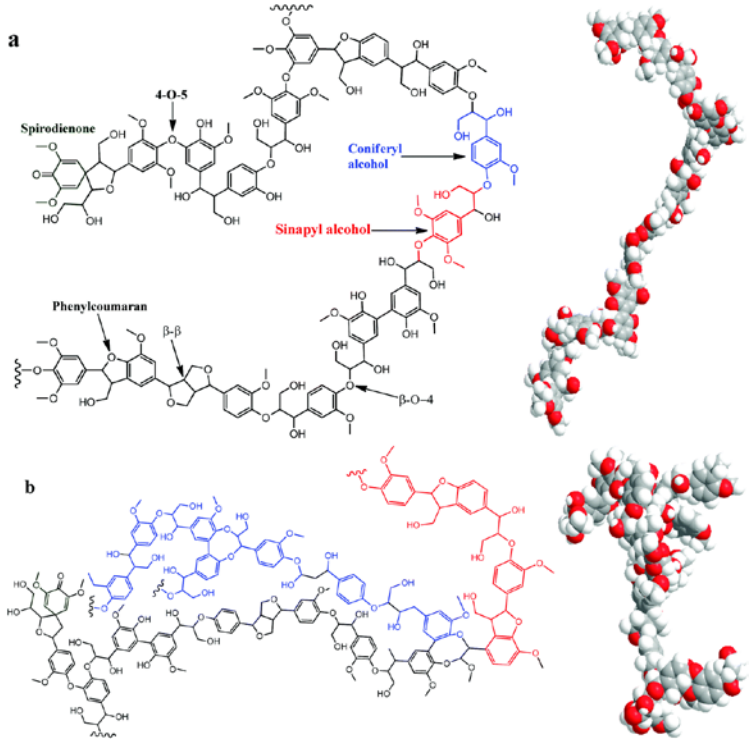

Figure 1.10 (a) Lignin structure of hardwood and (b) softwood [29].

1.3.5. Lignin applications

Lignin is produced extensively as a co-product in the bio-ethanol and paper and pulp industries. Although the amount of lignin extracted in pulping operation around the word is estimated to be over 70 million tons per year, less than 2% is actually recovered for utilization as a chemical product [30]. Lignin is undervalued as a by-product and it is not utilized significantly [31]. Besides being fuel for the boilers, lignin finds very limited applications. Therefore, there is an increasing demand for new processes that could provide new means to use this resource in a more efficient manner, not only as a fuel but also as a starting material for our chemical industry with the aim of producing commodity and fine chemicals (Figure 1.11) [32].

Based on the variety of functional groups provided by the structure of lignin it finds application in the areas, such as polymer additives, surfactant, UV stabilizer and coloring agent, and as base material for the production of chemicals, dyes, adhesives and fertilizers, etc. There has been limited research on the utilization of lignin for value added products. However, some reports are available on the usage of lignin as a reinforcing phase or filler for polymeric systems. Moreover, lignin can be used as polyols for the production of certain polymers due to its hydroxyl content (Figure 1.11).

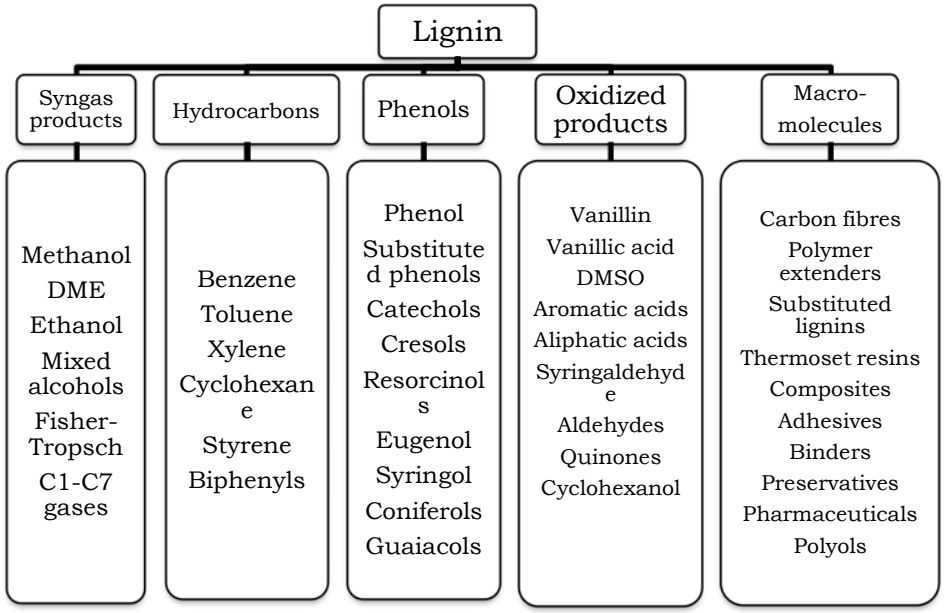

Figure 1.11 Potential lignin applications

Lignins are used as fillers in phenol formaldehyde resins, polyurethane, polyvivylchlorides (PVC), and to a lesser extent, in polypropylenes, polyethylenes, polyhydroxyalkanoates and polylactides [31].

Moreover, lignin has been demonstrated as antioxidants, acting as free radical scavengers. This activity allows the use of lignin for cosmetic formulations such as topical applications [33]. There are studies that demonstrated the

influence of the obtaining process of lignin on the antioxidant activity [34].

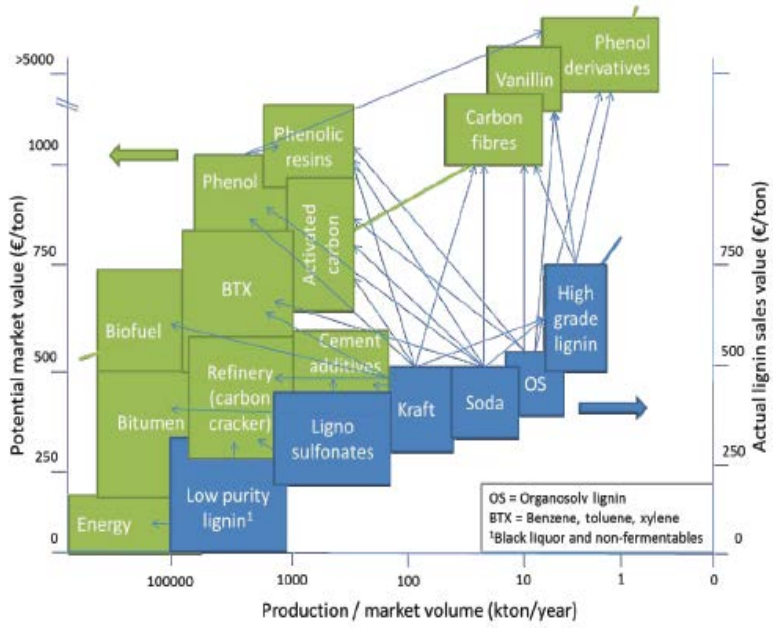

Figure 1.12 Lignin production and potential lignin derived product market value [25]

1.4 Raw materials

1.4.1. Olive tree pruning

The olive tree (*Olea Europea)* is one of the most important tree crop species of the Mediterranean basin for the production of edible fruit and oil. It is an evergreen tree with broad crown and twisted trunk and can measure up to 15 meters. The bark is finely fissured and it is gray or silver. Its opposite leaves have a length of 2-8 cm and have lanceolate shape with slightly pointed apex green/dark gray on the top and paler and densely scaly on the underside. The Mediterranean olive tree comprises varieties the wild *oleaster* (var. *sylvestris*) and the cultivated (var. *sativa*) [35].

The olive tree is one of the oldest cultivated species in the world. This fact, together with the ease of vegetative propagation, cross-pollination, mutation and clonal selection has contributed to the high number of varieties of this species in the word. Nowadays there are more than 2000 varieties of this tree [36].

Figure 1.13 Olive tree cultivation field

Olive growing was introduced in Spain during the maritime domination of the Phoenicians (1050 BC) but did not develop to a noteworthy extent until the arrival of Scipio (212 BC) and Roman rule (45 BC). After the third Punic War, olives occupied a large stretch of the Baetica valley and spread towards the central and Mediterranean coastal areas of the Iberian Peninsula including Portugal. The Arabs brought their varieties with them to the south of Spain and influence the spread of cultivation so much that the Spanish word for olive (aceituna), oil (aceite), and wild olive tree (acebuche) have Arabic roots [37]. Currently, about 90% of olive trees

are grown in the Mediterranean countries, especially in Spain, Italy and Grecee. The cultivation of olive tree has expanded into Australia, China, Latin America, South Africa and the USA [37, 38].

Olive tree cultivation (Figure 1.13) is a periodical culture operation by means of which less productive branches are cut off and trees are rejuvenated. This action generates an annual volume of lignocellulosic residues estimated at 3000 kg/ha [39] thus constituting a widely available and renewable resource. Just in Spain, the main olive oil producer in the world, some $7*10^6$ t/year of olive tree pruning biomass are available. A typical pruning lot includes leaves, branches and wood. To prevent propagation of vegetal diseases, these residues are commonly burnt with associated costs, environmental concern and until now, no economical alternatives [40].

1.4.2. Apple tree pruning

There is known data to determine the origin of the apple tree and the cider in the Basque Country. However, it is true that over centuries the cider has been one of the most important drinks in the Basque Country. Cider is a natural drink, resulting from the fermentation of apple juice, with low alcohol content. Annual cider production in this region is around 9000 m^3 for which both local and imported apples are used by Natural Cider Association of Gipúzkoa [41]. Figure Figure 1.14 shows cider apple tree field.

The growing of apples for cider production has been an important activity in the Basque Country. Normally, the picking period lasts from the end of September-beginning of October until the middle of November, depending on the variety of apple.

Figure 1.14 Apple tree

Apple trees are pruned after the collection, in a period from the end of January until the end of February. Due to the fact in farms there is not enough space to store apple tree pruning, farmers tend to burn this reside [42].

This agricultural residue is a suitable as lignocellulosic material, to produce cellulose, hemicelluloses and lignin which could be converted to value added chemicals. Working with this residue could offer new opportunities for the apple tree pruning.

1.4.3. Almond shell

Almond coming from the almond tree (*prunus amigdalus)* (Figure 1.15) is one of the most common tree nuts on a world-wide basis and ranks number one in tree nut production. They are typically used as snack foods and

ingredients in a variety of processes foods, especially in bakery and confectionary products. Almond production is located mainly in countries with Mediterranean climates such as, Italy, Spain and California. After EE.UU, Spain is the largest producer of this nut with a production of 63,000 tm of grain 2005 [43].

Figure 1.15 Almond tree

Spain produces more than 100 varieties, but three of them are the botanically native varieties, Marcona, Larqueta and Planeta. Almond shell is the name given to the ligneous material forming the thick endocarp or husk of the almond tree fruit. The shell a lignocellulosic agricultural bio-product was traditionally employed as a source of energy due to its high calorific power [44, 45]. Moreover, the high content of lignin made almond husk an appropriate residue for lignin extraction [44, 46].

1.5 References

1. W. Soetaert, E. Vandamme. The impact of industrial biotechnology. *Biotechnology Journal*, (2006), *1*(7-8), 756-769.
2. W. Soetaert, E.J. Vandamme. Biofuels in perspective. *Biofuels. John Wiley & Sons, Ltd., London, UK (2009).*
3. C. Baskar, S. Baskar, R.S. Dhillon, (Eds.). Biomass conversion: The interface of biotechnology, chemistry and materials science, *Springer Science & Business Media,* (2012).
4. H. Danner, R. Braun. Biotechnology for the production of commodity chemicals from biomass. Chem. *Soc. Rev.*, (1999), 28(6), 395-405.
5. K.B. Finch, R.M. Richards, A. Richel, A.V. Medvedovici, N.G. Gheorghe, M. Verziu, V.I. Parvulescu. Catalytic hydroprocessing of lignin under thermal and ultrasound conditions. *Catalysis today*, (2012), *196*(1), 3-10.
6. B. Kamm, M. Kamm. Principles of biorefineries. *Applied microbiology and biotechnology*, (2004), *64*(2), 137-145.
7. H. Wang, L. Cheng. "Lignocelluloses Feedstock Biorefiney as Petrorefinery Substitutes". Chapter 14 of Biomass now-Sustainable Growth and Use, Ed: M.D. Matovic,Intech, (2013), 347-388.
8. Directive 2009/28/EC of the European Parliament of the council of 23 April 2009 on "the promotion of the use of energy from renewable sources and amending and subsequently repealing Directives 2001/177/ED and 2003/30/EC".
9. A. Demirbas. Chapter 2: Fuels from biomass. *Biohydrogen*. Springer London (UK), (2009), pp 43-59.
10. Y.H.P. Zhang. Reviving the carbohydrate economy via multi-product lignocellulose

biorefineries. *Journal of industrial microbiology & biotechnology*, (2008), *35*(5), 367-375.

11. A. Brandt, J. Gräsvik, J.P. Hallett, T. Welton. Deconstruction of lignocellulosic biomass with ionic liquids. *Green chemistry*, (2013), *15*(3), 550-583.
12. P. Kumar, D.M. Barrett, M.J. Delwiche, P. Stroeve. Methods for pretreatment of lignocellulosic biomass for efficient hydrolysis and biofuel production. *Industrial & Engineering Chemistry Research*, (2009), *48*(8), 3713-3729.
13. E.M., Rubin. Genomics of cellulosic biomass. *Nature*, (2008), 454 (7206), 841-845.
14. J.S. Han, J.S. Rowell. *Chemical composition of fibers.* In: Rowell R.M., Young R.A., Rowell J.K. editors. Paper and Composites from Agro-Based Resources, Boca Raton (Florida): CRC Press Inc. (1997), pp. 83-134.
15. T.P. Schultz, D.D. Nicholas. Naturally durable heartwood: evidence for a proposed dual defensive function of the extractives. *Phytochemistry*, (2000), *54*(1), 47-52.
16. J. Zhu, S. Chen, S. Alvarez, V.S. Asirvatham, D.P. Schachtman, Y. Wu, R.E. Sharp. Cell wall proteome in the maize primary root elongation zone. I. Extraction and identification of water-soluble and lightly ionically bound proteins. *Plant physiology*, (2006), *140*(1), 311-325.
17. J. Werkelin, B.J. Skrifvars, M. Hupa. Ash-forming elements in four Scandinavian wood species. Part 1: Summer harvest. *Biomass and Bioenergy*, (2005), *29*(6), 451-466.
18. F. Xu. Chapter 2: Structure, ultrastructure, and chemical composition. In: R.C. Sun editor. Cereal straw as a resource of sustainable biomaterials and biofuels: chemistry, extractives, lignins, hemicelluloses and cellulose, Amsterdam. Elsevier B.V. (2010), 9-47.

19. C.H. Zhou, X. Xia, C.X. Lin, D.S. Tong, J. Beltramini. Catalytic conversion of lignocellulosic biomass to fine chemicals and fuels. *Chemical Society Reviews*, (2011), *40*(11), 5588-5617.
20. Y. Zheng, Z. Pan, R. Zhang. Overview of biomass pretreatment for cellulosic ethanol production. *International journal of agricultural and biological engineering*, (2009), *2*(3), 51-68.
21. A. Gandini, M.N., Belgacem. The state of the art. In: M.N. Belgacem, A. Gandini. Editors. *Monomers, polymers and composites from renewable resources*. Amsterdam, Elsevier, B.V. (2008), 1-16.
22. Y. Cao, J. Wu, J. Zhang, H. Li, Y. Zhang, J. He. Room temperature ionic liquids (RTILs): a new and versatile platform for cellulose processing and derivatization. *Chemical Engineering Journal*, (2009), *147*(1), 13-21.
23. B. Xiao, X. Sun, R. Sun. Chemical, structural, and thermal characterizations of alkali-soluble lignins and hemicelluloses, and cellulose from maize stems, rye straw, and rice straw. *Polymer Degradation and Stability*, (2001), *74*(2), 307-319.
24. I. Spiridon, V.I. Popa. Chapter 13: Hemicelluloses: major sources, properties and applications. In: M.N. Belgacem, A. Gandini. Editors. *Monomers, polymers and composites from renewable resources*. Amsterdam, Elsevier, B.V. (2008), *1*, 289-304.
25. R.J.A. Gosselink. Lignin as a renewable aromatic resource for the chemical industry. 2011. Doctoral Thesis. University of Twente.
26. J.S. Lupoi, S. Singh, R. Parthasarathi, B.A. Simmons, R.J. Henry. Recent innovations in analytical methods for the qualitative and quantitative assessment of lignin. *Renewable and Sustainable Energy Reviews*, (2015), *49*, 871-906.

27. O. Lanzalunga, M. Bietti. Photo-and radiation chemical induced degradation of lignin model compounds. *Journal of Photochemistry and Photobiology B: Biology*, (2000), *56*(2), 85-108.
28. C.W. Dence, S.Y. Lin. Chapter 1: Introduction. In: T.E. Timell, editor. Method in lignin chemistry. Springer-Verlag Berlin Heidelberg, (1992), pp.1-17.
29. W.J. Liu, H., Jiang, & H.Q., Yu. Thermochemical conversion of lignin to functional materials: a review and future directions. *Green Chemistry*, (2015), *17*(11), 4888-4907.
30. J. Lora. Industrial commercial lignins: sources, properties and applications. In : B.M. Naceur, A. Gandini, editors. Monomers, polymers and composites from renewable resources. Elsevier, Amsterdam (2008), pp. 225-241.
31. S. Sahoo, M.Ö. Seydibeyoğlu, A.K. Mohanty, M. Misra, M. Characterization of industrial lignins for their utilization in future value added applications. *Biomass and bioenergy*, (2011), *35*(10), 4230-4237.
32. I. Kilpeläinen, H. Xie, A. King, M. Granstrom, S. Heikkinen, D.S. Argyropoulos. Dissolution of wood in ionic liquids. *Journal of agricultural and food chemistry*, (2007), *55*(22), 9142-9148.
33. M.P. Vinardell, V. Ugartondo, M. Mitjans. Potential applications of antioxidant lignins from different sources. *Industrial crops and products*, (2008), *27*(2), 220-223.
34. A. García, M.G. Alriols, G. Spigno, J. Labidi. Lignin as natural radical scavenger. Effect of the obtaining and purification processes on the antioxidant behaviour of lignin. *Biochemical Engineering Journal*, (2012), *67*, 173-185.
35. E. Rugini, C. De Pace,P. Gutiérrez-Pesce, R. Muleo. *Olea*. In : C. Kole. Editor. Wild Crop Relatives: Genomic and Breeding Resouces: Temperature

Fruits, New York: Springer-Verlang Berlin Heidelberg, (2011), 79-117.
36. J.D. Rejón, C.G. Suárez, J.D. Alché, A.J. Castro, M.I. Rodríguez-García. Evaluation of different methods to determine pollen quality in several olive (*Olea europea L.*) cultivars. *Polen* (2012), 20, 61-72
37. International olive council, http://internationaloliveoil.org
38. W. Wang, F. Tai, X. Hu. Current initiatives in proteomics of the olive tree. In: V.R. Preedy, R.R. Watson, editors. *Olives and olive oil in health and disease prevetion*, Amsterdam: Elsevier (2010), 25-32.
39. S. Sánchez, A.J. Moya, M. Moya, I. Romero, R. Torreno, V. Bravo, M.P. San Miguel. Aprovechamiento del residuo de poda del olivar. *Ingeniería Química,* (2002), 34, 194-202.
40. I. Romero, E. Ruiz, E. Castro, M. Moya. Acid hydrolysis of olive tree biomass. *Chemical Engineering Research and Design*, (2010), 88, 633-664.
41. http://sagardotegiak.com
42. L. Serrano, G. Spigno, A. García, D. Amendola, J. Labidi. Properties of Soda and Organosolv Lignins from Apple Tree Pruning. *Journal of Biobased Materials and Bioenergy*, (2012), *6*(3), 329-335.
43. http://fao.org, FAO-Food and Agricultural Organization of the Unitated Nations.
44. A.J. Esfahlan,R. Jamei, R.J. Esfahlan. The importance of almond (Prunus amygdalus L.) and its by-products. *Food Chemistry*, (2010), *120*(2), 349-360.
45. M. Urrestarazu, G.A. Martínez, M. del Carmen Salas, M. Almond shell waste: possible local rockwool substitute in soilless crop culture. *Scientia Horticulturae*, (2005), *103*(4), 453-460.

46. J. Quesada, F. Teffo-Bertaud, J.P. Croué, M. Rubio. Ozone oxidation and structural features of an almond shell lignin remaining after furfural manufacture. *Holzforschung*, (2002), *56*(1), 32-38.

Chapter 2

Lignin extraction and characterization

2.1 Lignin extraction processes

Lignin is one of the main components of lignocellulosic biomass. Lignocellulosic fractionation (Figure 2.16) breakes down the cell wall structure to separate each component (cellulose, hemicelluloses and lignin) by using chemicals, physical and/or mechanical methods that weaken the linkages among the different components (Figure 2.16). Pretreatments also have great potential for improvement of efficiency and lowering of cost through research and development [1].

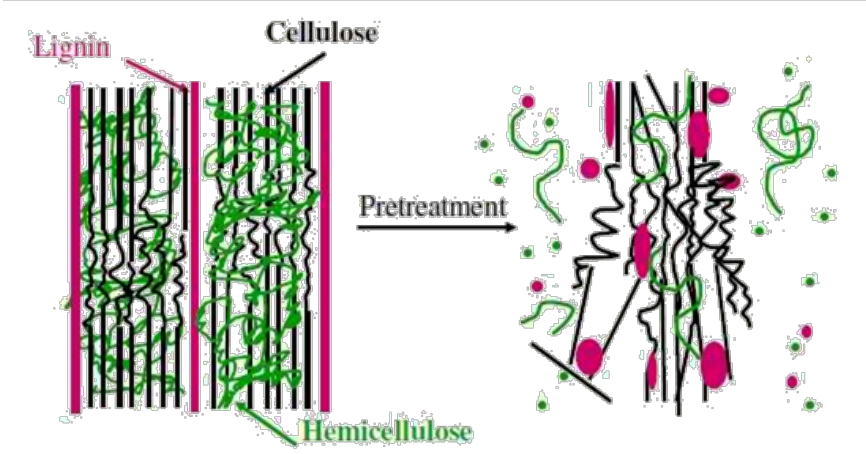

Figure 2.16 Schematic goal of pretreatment of lignocellulosic biomass [1]

There are several methods by which lignin can be isolated from biomass. These processes can be classified into two general groups: (1) processes in which lignin is degraded into soluble fragments and removed by separating the solid residue from the spent liquor and (2) processes that selectively hydrolyze polysaccharides and leave lignin along with some condensed carbohydrate deconstruction products as a solid residue. The example of the former would be the pulping processes: such as kraft, sulphite, soda and organosolv; an example of the latter would be dilute acid

hydrolysis of lignocellulose to yield sugar monomers, furfural and levulinic acid. In this case the most common methods for the lignin extraction belong to the first group which are described below [2].

2.1.1. Sulphite process

It was in 1874 when Ekman, a Swedish chemist marketed the first sulphite process. Almost simultaneously with A. Ekman, Mitschelich in Germany worked on the sulphite cooking process of wood and, in 1880 he started a sulphite pulp mill in Zell in south Germany [3].

In sulphite pulping, usually conducted under acid or neutral conditions, but in principle it can operate over the entire pH range simply by changing the pulping chemicals and adjusting the dosage. Sulphite pulping is based on sulphur dioxide and/or bisulphite ions as well as calcium (Ca^{+2}), magnesium (Mg^{+2}) or sodium (Na^{+2}) as counter ions which react with lignin to produce water-soluble sulphonated lignins that are degraded by acid hydrolysis reactions. Nowadays only 10% of the pulp is produced by this method as the Kraft process has become the dominant one [2, 4].

2.1.2. Kraft process

The Kraft process (Figure 2.17) is the dominant pulping process in the pulp and paper industry. About 130 million tons per year of Kraft pulp are produced globally, accounting for two-thirds of the world's virgin pulp production and over 90% of chemical pulp [5]. In this process, cellulose fibers are isolated through dissolution of lignin and hemicelluloses of the wood chips in a solution of sodium hydroxide (NaOH) and sodium sulphite (Na_2S) that is known as white liquor [2].

The white liquor and the chips are heated to a cooking temperature of about 170 °C and are allowed to cook at that temperature for about two hours. During this treatment, the hydroxide and hydrosulphite anions react with the lignin, causing the polymer fragmentation into smaller water/alkali-soluble fragments. Consequently, the kraft lignin is dissolved in the pulping liquors whereas cellulose can be filtered off in the form of pulp (Figure 2.17).

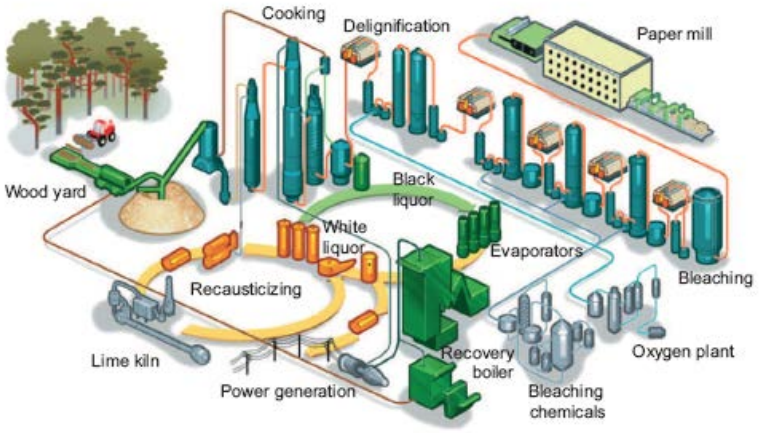

Figure 2.17 Overview of a kraft process in the paper industry

The resulting so-called kraft "black liquor" from the kraft treatment is in the next stages concentrated by evaporation and is used as fuel in the recovery boilers. Although this precipitated kraft lignin is often used as additional solid fuel in other areas of the pulp mill, it represents a marketable product and an important raw material for chemical valorization [6]. Presently less than 100,000 tons per year of kraft lignin are valorized instead of being burned [7].

2.1.3. Alkaline treatment

Soda pulping of annual plants accounts for nearly 5% of the total pulp production [2]. Pretreatment with alkali such as NaOH, KOH, $Ca(OH)_2$, hydrazine and anhydrous ammonia cause swelling of biomass, which increases the internal surface area of the biomass, and decreases both the degree of polymerization, and cellulose crystallinity. Alkaline pretreatment disrupt the lignin structure and breaks the linkage between lignin and the other carbohydrate fraction in lignocellulosic biomass, thus making the carbohydrates in the hetero-matrix more accessible [8].

Alkaline pretreatment is most effective with low lignin content biomass like agricultural residues but becomes less effective as lignin content increases [8]. When lignin content in the biomass is low, only 10-15% NaOH is required for delignification.

It is expected that soda pulping may become more important in the context of biorefinery as the precipitated lignin would be sulphur-free and could be used for further applications. However, in alkaline pretreatment together with lignin, solubilization of carbohydrates, extractives and other non-desired reactions occur. Hence, it is essential the application of purification steps for the subsequent utilization of lignin [9].

2.1.4. Organosolv process

Since 1970s, organosolv pulping has attracted much interest because processes, kraft and sulphite pulping the convetional procecces, have some serious shortcomings such as air and water pollution [10]. In organosolv treatments lignin is extracted from lignocellulosic feedstock by lignin

dissolution using organic solvents or aqueous solutions of them. The most commonly used solvents for organosolv delignification include alcohols such as methanol and ethanol (usually mixed with 50% of water), and organic acid such as formic and acetic acid, amines, ketones, phenols [2]. For most of the operated organosolv processes the temperature range is wide ranging from 100°C to 250°C. Furthermore, the addition of acid catalyst could increase the delignification range. Mineral acid such as hydrochloric acid, sulfuric acid and phosphoric acid are good catalysts [10].

Organosolv was proven to be a very selective pretreatment method yielding three separate fractions: dry lignin, and aqueous hemicelluloses stream, and a pure cellulose fraction [8]. It is important to note that owing to its sulfur-free and less-condensed structure, the organosolv lignin is one of the most suitable types of technical lignin for further conversion and valorization. It is anticipated that the organosolv method will find more interest in the future for biomass fractionation. Figure 2.18 shows the rising research activities with regard to organosolv methods as represented by the number of annually published papers [2].

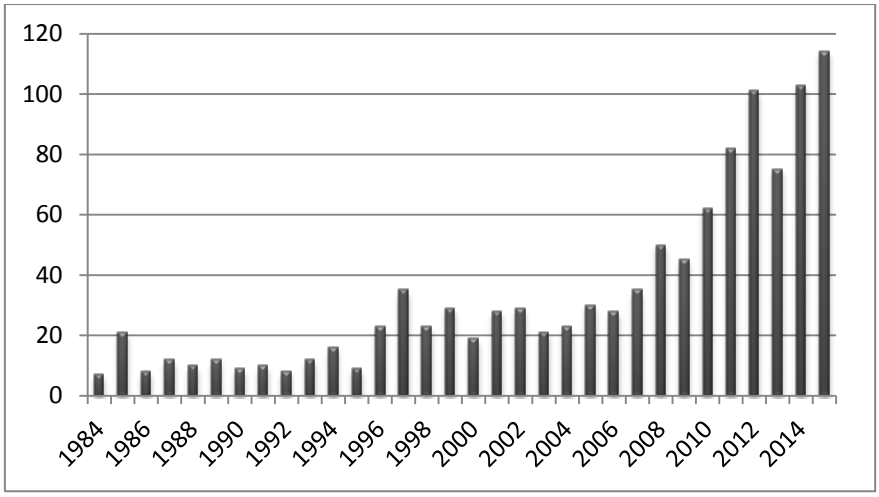

Figure 2.18 Number of papers published on organosolv biomass fractionation

2.4.1.1. Alcohol organosolv processes

Alcohols, especially the lowest molecular weight aliphatic alcohols, are the most frequently used solvents in organosolv pretreatments. Regarding the type of alcohol, it was found that normal primary alcohols were better agents that the secondary or tertiary alcohols for delignification, although the mixture of *n*-butyl-alcohol-water appeared to be the most efficient in removing lignin from wood. However, due to low cost and ease of recovery, methanol and ethanol seem to be the most favored alcohols from alcohol-based organosolv pretreatment.

Methanol improves penetration of the pulping liquor into the lignocellulosic material and therefore increases the degree of delignification. Methanol is a low boiling alcohol, and therefore, it can be relatively easy recovered by distillation. However, methanol is a poisonous chemical and

forms inflammable vapors at relatively low temperatures. Therefore, methanol pretreatment process has to be carefully designed and operated.

Ethanol pretreatment on the other hand, is safer because is less toxic than methanol and can be performed with less solvent concentration. Ethanol also can be easily recovered by distillation, but the higher price of ethanol leads to a slightly higher cost for ethanol pretreatment process than that for methanol pretreatment. For low boiling point solvent, the attribute of volatility results in the easy recovery of solvent after pretreatment, which benefits the reduction of energy consumption. Whereas, very high pressure is needed for low boiling point solvents pretreatment with required high equipment costs with associated maintenance and safety problems [10].

2.4.1.2. Acid organosolv processes

Delignification of wood in organic solvents is facilitated at higher hydrogen ion contents. It has been demonstrated that formic acid and acetic acid are fairly suitable for the cleavage of lignin α-ether linkages and dissolving the subsequent lignin fragments at low to moderate temperatures. Low temperature pulping is carried out at atmospheric or low operating pressures but requiring the presence of peroxides or catalyst such as HCl. Delignification in presence of formic acid was found to proceed faster than in presence of acetic acid [2].

2.1.5. Ionic liquid process

Ionic liquids are salts that are liquid at, or close to, room temperature with melting points below an arbitrary set point of 100°C. They often have tunable physical properties based

on the choice of cation and anion pair, a negligible vapor pressure, and good thermal stability [11]. Ionic liquids have been used as lignocellulosic material solvents, as a greener alternative to fractionation processes used until now. Other advantage of ionic liquids is that they are easily recovered and reutilized, so it is reduced the amount of wastes generated on the process.

2.2 Objective

The main goal of this chapter was to study the delignification of almond shell under different extraction treatments such as alkaline and organosolv processes.

2.3 Chemical characterization of almond shell

In this study almond shell was collected from La Rioja (Spain) originated from almond tree (*Prunus amygdalus*) belonging to the varieties called Marcona and Larqueta.

The almond shell was chemically characterized according to the TAPPI methodology described in the **Appendix I**. The obtained results are shown in Table 1.2.

Table 1.2 Chemical composition on dry basis (wt, %) of the characterized almond shell

	Almond shell
Moisture	10.77 ± 0.10
Ash	0.89 ± 0.01
Extractives	0.07 ± 0.01
Lignin	52.59 ± 3.71
Hemicelluloses	8.57 ± 0.80
Cellulose	41.29 ± 2.19

As it can be observed, the almond shell showed high content of cellulose that represented nearly half of the composition of the raw materials. The most abundant component was the lignin and hemicelluloses showed low percentage. The low percentage of extractives was in agreement with the results published by other authors as well as the overall results [10].

2.4 Materials and methods

2.4.1. Lignin extraction by different methods

Organosolv treatment was carried out based on the conditions of previous works [13]. Almond shell was treated with a mixture of ethanol/water (70:30, v/v). The solid:liquid ratio was 1:6 and the reaction was carried out at 180 ºC for 90 minutes in a 4 L pressure stainless steel batch reactor (ELO723 Iberfluid) controlled by Adkir software. The black liquor was treated with 2 volumes of acidified water (pH 2), and the precipitated lignin was recovered by centrifugation (5500 rpm, 15 min) and then vacuum dried at 50ºC until constant weight (from now on OE)[13].

Formosolv treatment was carried out based on the conditions of previous works [15, 16]. The almond shell was treated with 80 wt.% formic acid solution with 0.2% of HCl as catalyst. The solid:liquid ratio was 1:10 and the reaction was carried out at 130 ºC for 90 minutes the same pressure reactor as the organosolv process. The black liquor was treated with 5 volumes of water and recovered by centrifugation. The obtained lignin will be called OF from now on.

Acetosolv and formosolv treatments were carried out together. The concentration and the pulping media were chosen from previous works [17, 15, and 18]. The almond shell was treated with a solution of acetic acid-formic acid-water (60/30/10, v/v/v) and 0.2% of HCl as catalyst. The other parameters of the treatment and the separation of lignin (called OAF from now on) were the same as the previous pulping process.

Alkaline treatment was performed based on previous studies [19]. The almond shell was treated with a sodium hydroxide solution (15:85, v/v). The solid:liquid ratio was 1:10 and the reaction was carried out at 90 ºC for 90 minutes in a 23 L atmospheric reactor. The black liquor was treated with sulphuric acid (96% w/w) until pH 2 (from now on AS) was isolated by centrifugation and was washed several times with acidified water (pH 2) to remove the impurities [20, 14].

2.4.2. Liquid fraction characterization

Liquid fractions recovered from each of the organosolv and alkaline treatments were characterized according to the TAPPI methodology described in the **Appendix II**.

2.4.3. Lignin characterization

The four different lignins recovered were characterized by different techniques described in the **Appendix III** and **Appendix IV**.

The chemical structure of the different lignin was characterized by Fourier Transformed Infrared Spectroscopy (FT-IR) and nuclear magnetic resonance (NMR).

Lignins were subjected to gel permeation chromatography (GPC) to evaluate lignin average molecular weight (Mw) and molecular weight distribution (IP). Acid insoluble lignin (AL) was determined by subjecting lignin to an acid hydrolysis and acid soluble lignin (ASL) was determined by spectrophotometry (UV absorption at 205 nm). Different sugar content was determined injecting the obtained filtrate from AS analysis into a high performance liquid chromatography (HPLC). A thermogravimetric analysis (TGA) was carried out to determine the ash content.

The total phenolic content (GAE%) of the analyzed lignins was determined by Folin-Ciocalteau spectrophotometric method and the antioxidant capacity (AOP%) was measured by the ABTS assay.

2.5 Different treatment study results

2.5.1. Liquid fraction

The liquid fraction obtained after the different organosolv and alkaline treatments were characterized in order to evaluate some parameters. The results are shown in Table 2.3.

The pH and density of the recovered liquid fractions depended on the nature of solvents as well as of the media that were used for the extraction process. It could be observed that for the alkaline treatment the pH was basic

and for the rest of the organosolv treatments the pH was acid, being the formosolv and acetosolv/formosolv the most acid ones.

Table 2.3 Physicochemical properties of the obtained liquid fractions

Paramenter	Organosolv	Formosolv	Acetosolv/Formosolv	Alkaline
pH	4.76 ± 0.01	1.00 ± 0.00	1.00 ± 0.00	13.70 ± 0.07
Density (g/mL)	0.89 ± 0.00	1.16 ± 0.00	1.10 ± 0.00	1.14 ± 0.00
TDS (wt, %)	5.43 ± 0.14	4.94 ± 0.47	5.24 ± 0.02	23.16 ± 0.70
IM (wt, %)	0.05 ± 0.02	0.34 ± 0.03	0.17 ± 0.02	14.56±0.04
OM (wt,%)	5.31 ± 0.07	4.60 ± 0.44	5.08 ± 0.02	17.20±1.15
Lignin (wt,%)	2.03 ± 0.03	1.48 ± 0.10	2.00 ± 0.12	5.52±2.39

Otherwise, organosolv and acetosolv/formosolv treatment had more quantity of both organic matter and lignin. This indicates that the mixture of the two acids and ethanol water had higher impact on the solubilisation of lignin and other compounds of the almond shell.

In the case of the alkaline treatment it showed the highest content in lignin and inorganic matter than the rest of the liquid fractions. However, the precipitation of the black liquor revealed the formation of sodium sulphate salts in the medium. These salts were removed by washing the liquid fraction several times with acidified water [13]. After the purification step the lignin content decreased about 75% in the AS samples.

2.5.2. Lignin characterization

The chemical composition of the obtained four lignin samples is shown in Table 2.4.

Table 2.4 Chemical composition of the different lignins in dry basis (wt.%)

	OE	**OF**	**OAF**	**AS**
IL (%)	67.41 ± 2.92	80.86 ± 3.06	71.13 ± 0.93	13.25 ± 3.72
ASL (%)	1.72 ± 0.27	2.74 ± 0.48	2.10 ± 0.27	3.70 ± 0.48
TLC (%)	69.13 ± 2.66	83.60 ± 2.64	73.24 ± 0.66	16.95 ± 3.89
Total sugar (%)	3.40 ± 0.25	1.89 ± 0.25	2.25 ± 0.13	27.62 ± 1.49
Glucose (%)	0.56 ± 0.01	0.07 ± 0.11	0.25 ± 0.01	-
Arabinose (%)	0.03 ± 0.18	0.05 ± 0.01	0.09 ± 0.01	-
Xylose (%)	2.80 ± 0.18	1.78 ± 0.29	1.91 ± 0.13	27.36 ± 1.53
Ash (%)	4.04	3.28	3.18	35.39

OE and OAF had a similar quantity of acid insoluble lignin; around 70% and AS showed a low quantity of lignin 13%. These results are in agreement with others obtained by other authors that have worked with organosolv and alkaline extraction methods [17, 21, 22]. On the other hand, OF purity was the highest one with 80.86% of acid insoluble lignin. Moreover, in accordance with these purity results, the most carbohydrates contaminated sample was AS while OF lignin presented very low sugar contamination.

Among carbohydrates, xylose was the major sugar present in all samples, especially in AS which revealed the highest percentage of this sugar. Otherwise, arabinose was very low

for all analyzed lignins due to low selectivity of organic acid in the extraction of arabinoxylans [22].

Lignin ash content was in concordance with other organosolv and alkaline lignins [21]. AS lignin showed a high content of ashes due to the formation of sodium sulphate salts during the precipitation [32]. Due to the purification stage applied to this lignin the inorganic content is lower than the results reported by other authors [24].

2.5.3. Lignin structure and molecular weight

FTIR spectra of different almond shell lignin samples (Figure 2.19) showed some changes in the peak intensity and form. The wide band observed around 3400 cm^{-1} represented the stretching of OH and hydrogen bonding and this band was higher in the case of OE and AS methods due to the higher content of hydroxyl groups of the lignin. The peaks at 2940 cm^{-1} and 2850 cm^{-1} were assigned to –CH stretching of methyl and methylene groups. The band at 1720 and 1650 cm^{-1} associated with the carbonyl group might be able to establish a difference between organic acid and organic alcohol treatments. As it could be observed in the band 1650 cm^{-1} of the OE spectra, this band had a stronger peak demonstrating a higher presence of conjugated carbonyl groups in lignins treated with organic alcohols that with organic acids [17]. In addition, the band at 1374 cm^{-1} attributed to the -CH stretching of methyl group was of lower intensity in OE spectra than in OF and OAF [16]. On the other hand, a vibration band appeared at 1648 cm^{-1} which corresponds to the carbonyl stretching in γ-lactone. The bands which were observed at 1600 cm^{-1} and 1470 cm^{-1} correspond to the aromatic skeletal vibration on lignin samples. The band intensity at 1600 cm^{-1} in the AS lignin was lower than the other lignin due to the lower amount

lignin extracted by alkaline methods. Other lignin characteristic band are also shown such as band at 1320 cm^{-1} was assigned to syringyl breathing with CO stretching, band at 1223 $cm^{-1}$was assigned to guaiacyl ring breathing with CO stretching, band at 1113 cm^{-1} was assigned to CH in plane deformation in syringyl, band at 899 cm^{-1} was assigned to CH in plane deformation un guaiacyl and bat at 829 cm^{-1} was assigned to CH deformation in aromatic rings. The AS lignin revealed the polysaccharide and salt contamination. The sharp band around 1100 cm^{-1} was an overlapping band for the sodium sulphate salts that formed during the precipitation with sulphuric acid and the band for xylan. Also, the band at 895 cm^{-1} was assigned to the ß-glycosidic linkages (1 →4) between xylose units in hemicelluloses [25, 26].

a)

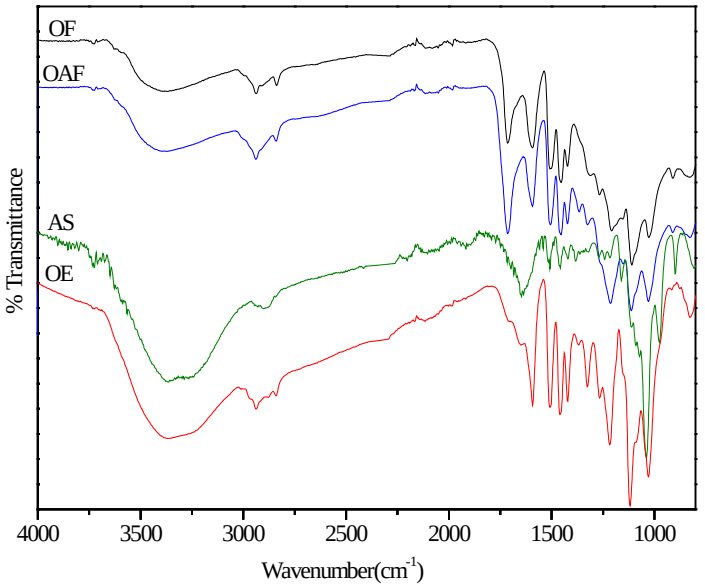

b)

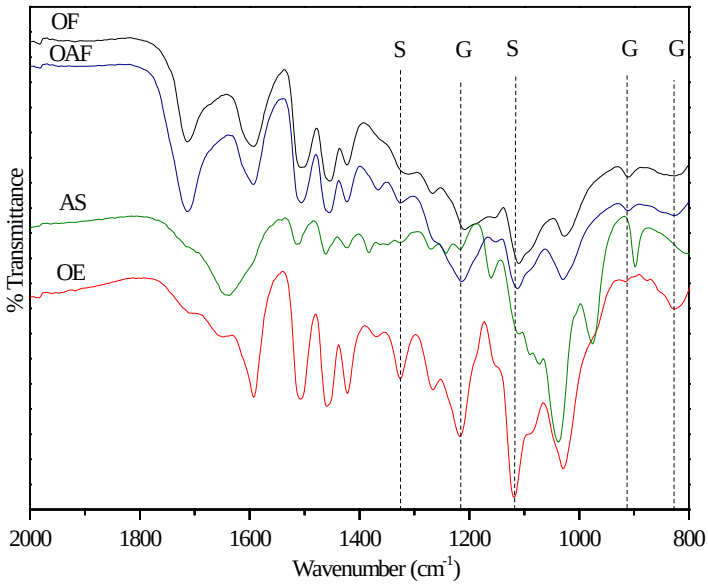

Figure 2.19 FTIR spectra of obtained different lignins. (a) wave number from 4000 to 700 $cm^{-1}$and (b) magnification of 2000-700 cm^{-1} region.

Molecular weight distribution of the obtained almond shell lignins and weight average (M_w), number average (M_n) molecular weights and polydispersity (M_w/M_n) of the different extracted lignin are shown in Table 2.5 and Figure 2.20. First of all the values obtained for the AS lignin are approximate due to a 43% of solubility results of this sample towards the DMF. This result suggests that the particles with the highest molecular weight were not soluble in DMF.

Table 2.5 Weight average (M_w) molecular weight, number average (M_n) molecular weight and polydispersity (M_w/M_n) of the different lignins.

	OE	**OF**	**OAF**	**AS**
M_w	15,7500	8,000	12,500	7,500[a]
M_n	3,900	1,800	2,850	4,200[a]
M_w/M_n	4.04	4.44	4.40	1.81[a]

Note: [a] Approximate values due to the low solubility of the sample in DMF

Organosolv treatments treated with organic acids, may suffer from condensation reaction which would raise the molecular weight, besides acidic depolymerisation reactions. As proposed by Li et al. [27], the Cα of the side chain is prone to form highly unstable carbonium ions, which can then bind with electron-rich carbon atoms in the aromatic ring of another lignin unit to form new stable carbon-carbon units. On the other hand, extraction conditions also affect the lignin size. Zhang et al. [21] claimed that higher temperature and longer residence times increase the degree of cleavage of other bonds in the lignin macromolecule, and therefore lower lignin sizes could be obtained when the extraction process becomes more severe.

This way OF lignin had the lowest molecular weight due to the severity of the treatment with formic acid. The effect of the repolymerization could be observed in the OAF lignin with the highest molecular weight.

The polydispersity results were unexpectedly similar as it could also be observed in Figure 2.20 were all peaks presented nearly equal width. Moreover, the OF shoulder started at higher retention times indicating the presence of low molecular weight fractions of lignin.

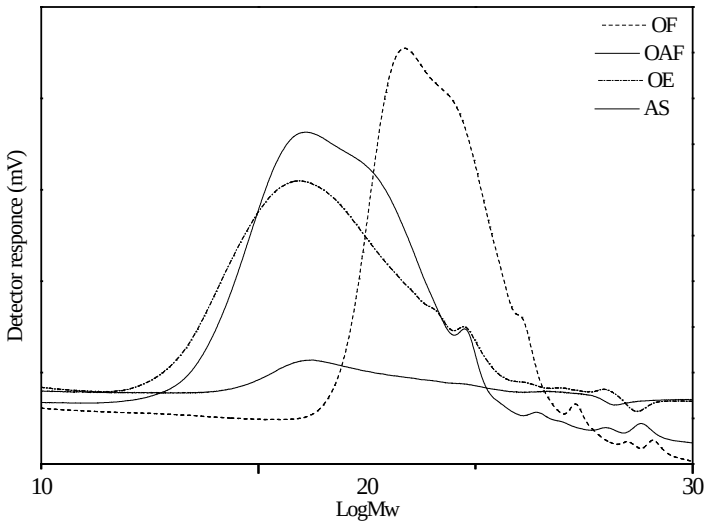

Figure 2.20 Molecular weight distribution of different lignins.

Table 2.6 Total phenolic content (GAE%) and antioxidant power (AOP%) of the studied lignins

Samples	GAE(%)	AOP(%)	AOP_{sample} (%/µg of sample)	AOP_{GAE} (%/µg of GAE)
OE	24.17 ± 1.58	86.83 ± 0.75	1.74 ± 0.02	7.21 ± 0.55
OF	43.21 ± 0.06	93.82 ± 0.16	1.88 ± 0.00	4.35 ± 0.00
OAF	24.27 ± 0.04	90.85 ± 0.28	1.82 ± 0.06	7.48 ± 0.04
AS	12.25 ± 0.02	51.24 ± 1.61	1.02 ± 0.03	8.38 ± 0.27

The antioxidant power (AOP%) values of the analyzed lignin samples are shown in Table 2.6. The antioxidant activities of lignin fractions were determined by measuring the rate of disappearance of the ABTS radical in the presence of lignin. OF sample showed the highest scavenging activity against the ABTS radical and the AS lignin performed the lowest

activity. This antioxidant values are strongly correlated with the purity of the samples being the purest lignin sample (OF) the one with the highest antioxidant power.

The total phenolic content (GAE%) values of the lignin fractions are also summed up in Table 2.6. It could be observed that the method used for the fractionation of the raw material clearly affected the phenolic content. In general, mild acidic conditions favored higher content of phenolic groups in lignin [27]. In this context, organosolv lignin fractions revealed higher phenolic values than those extracted by alkaline treatments. Moreover, the low phenolic value of the alkaline lignin was also due to the negative effect of the high hemicellulosic and inorganic type of impurities present in the sample.

The AOP_{sample} can be considered as a lignin purity indicator. The purest lignin sample OF, which contained a 4.17% of inorganic and hemicellulosic impurities, had an AOP_{sample} 1.88%/µg of sample, whereas the AS lignin presented the lowest AOP_{sample} value 1.02%/µg of sample due to the highest contamination. The parameter of AOP_{GAE} could be used to denote the inhibition efficacy of the phenolic groups present in the sample. The results suggested that the phenolic structure of the analyzed sample exhibit similar inhibition efficacy, except for the OF sample that showed the lowest value.

Lignin chemical structures were also analyzed by ^{13}C NMR showed in the Figure 2.21.

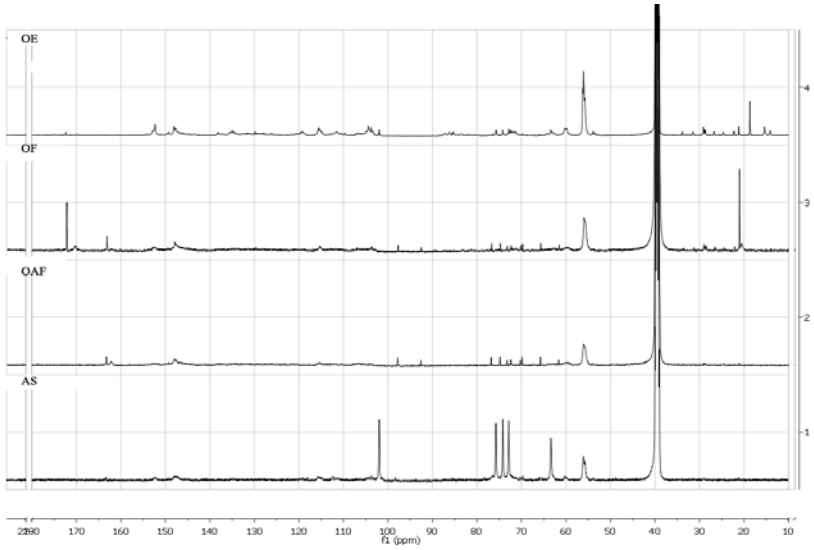

Figure 2.21 ^{13}C NMR spectra of the obtained different lignins.

The OE, OAF and OF spectra presented similar identified signals and intensities. This way, all samples showed signals in the aromatic region that ranges from 103.9 to 168.0 ppm. The $C_3$and C_5 in etherified and non etherified syringyl (S) residues were identified at 153013, 152.78, 152.31, 148.36, 147.93 and 104.41ppm. C_6 guaiacyl (G) residues were verified by signals at 119.33 ppm. These signals confirmed that the lignins could be of GS type of lignin. The signals at 163.56, 163.12, 115.85 ppm are attributed to esterified *p*-coumaric acid.

The signals at 172.57 ppm the OAF spectra could be attributed to the acetate group due to presence of residual solvent. Also, OE and OAF spectrum at around 21.50 ppm showed a signal attributed to the methyl (-CH_3) in the acetyl groups coming from the residual solvents.

The OE, OAF and OF lignins presented signals at 115.50, 101.95, 74.20, 74.75, 69.81, 65.68 ppm related to the presence of polysaccharide presence in the lignin samples. Moreover, the AS lignin at 101.95 (C-1), 75.73 ppm, 74.18 ppm, 72.86 ppm (C2, C3, C4) and at 63.37 ppm (C5) showed signals corresponding to 1-4 linkage of ß-*D*-xyl residue [18, 22].

2.6 Conclusions

In this chapter different organosolv and alkaline treatments were used to extract lignin from almond shell. The results showed that almond shell is a suitable raw material for the lignin extraction and recovery. In general organosolv treatments revealed to be more effective for the delignification of almond shell that alkaline treatment, being the organic acid conditions the best ones.

In order to study the adequacy of the obtained lignins (OE, OF, OAF and AS) for further applications, these were analyzed by different techniques to elucidate their structure and chemical composition. The purity of organosolv samples was high (more than 70% of AIL) with low content of inorganics and sugars. As for the AS lignin the results showed low purity of lignin and high carbohydrates and ashes. Otherwise, all lignin samples, except for the AS lignin, had a very high antioxidant power and were average in total phenolic content.

The average molecular weight was high in all cases, which was in concordance with the applied conditions. However, the average molecular weight was very different between the three lignin samples. The polydispersity values were in general medium values.

2.7 References

1. N. Mosier, C. Wyman, B. Dale, R. Elander, Y.Y. Lee, M. Holtzapple, M. Ladisch. Features of promising technologies for pretreatment of lignocellulosic biomass. *Bioresource technology*, (2005), *96*(6), 673-686.
2. P. Azadi, O.R. Inderwildi, R. Farnood, D.A. King. Liquid fuels, hydrogen and chemicals from lignin: A critical review. *Renewable and Sustainable Energy Reviews*, (2013), *21*, 506-523.
3. H.F.J. Wenzel. The chemical technology or wood. Chapter VII: The sulphite pulp cooking process 358-390, (1970) New York: Academic Press.
4. H.L. Hintz. *Paper: Pulping and Bleaching*. In: Buschow K.H.J., Cahn R.W., Flemings M.C., Ilschner B., Kramer E.J., Mahajan S., Veyssière P. editors, Encyclopedia of Materials: Science and Technology, Amsterdam: Elsevier (2001), pp. 6707-6711
5. H. Tran, E.K. Vakkilainnen. The kraft chemcial recovery process (2008).
6. H. Werhan. *A process for the complete valorization of lignin into aromatic chemicals based on acidic oxidation* .Doctoral dissertation, Diss., Eidgenössische Technische Hochschule ETH Zürich, (2013), Nr. 21132.
7. R.J.A. Gosselink, E. De Jong, B. Guran, A. Abächerl. Co-ordination network for lignin—standardisation, production and applications adapted to market requirements (EUROLIGNIN). *Industrial Crops and Products*, (2004), *20*(2), 121-129.
8. V.B. Agbor, N. Cicek, R. Sparling, A. Berlin, D.B. Levin. Biomass pretreatment: fundamentals toward application. *Biotechnology advances*, (2011), *29*(6), 675-685.

9. I. Egüés, C. Sanchez, I. Mondragon, J. Labidi. Effect of alkaline and autohydrolysis processes on the purity of obtained hemicelluloses from corn stalks. *Bioresource technology*, (2012), *103*(1), 239-248.
10. X. Zhao, K. Cheng, D. Liu, D. Organosolv pretreatment of lignocellulosic biomass for enzymatic hydrolysis. *Applied microbiology and biotechnology*, (2009), *82*(5), 815-827.
11. J. Zakzeski, P.C. Bruijnincx, A.L. Jongerius, B.M. Weckhuysen. The catalytic valorization of lignin for the production of renewable chemicals. *Chemical reviews*, (2010), 110(6), 3552-3599.
12. L. Chen, X. Wang, H. Yang, Q. Lu, D. Li, Q. Yang, H. Chen, Study on pyrolysis behaviors of non-woody lignins with TG-FTIR and Py-GC/MS, Journal of Analytical Applied Pyrolysis. (2015), 113, 499-507.
13. A. Toledano, L. Serrano, J. Labidi. Enhancement of lignin production from olive tree pruning integrated in a green biorefinery. *Industrial & Engineering Chemistry Research*, (2011), *50*(11), 6573-6579.
14. M.M. Ibrahim, S.B. Chuah, W.W. Rosli. Characterization of lignin precipitated from the soda black liquor of oil palm empty fruit bunch fibers by various mineral acids. *Asian journal on science and technology for development*, (2004), *21*, 57-68.
15. S. Dapía, V. Santos, J.C. Parajó. Study of formic acid as an agent for biomass fractionation. *Biomass and bioenergy*, (2002), *22*(3), 213-221.
16. P. Ligero, J.J. Villaverde, A. de Vega, M. Bao. Delignification of Eucalyptus globulus saplings in two organosolv systems (formic and acetic acid): Preliminary analysis of dissolved lignins. *Industrial crops and products*, (2008), *27*(1), 110-117.

17. F. Xu, J.X. Sun, R. Sun, P. Fowler, M.S. Baird. Comparative study of organosolv lignins from wheat straw. *Industrial crops and products*, (2006), *23*(2), 180-193.
18. H.Q. Lam, Y. Le Bigot, M. Delmas, G. Avignon. A new procedure for the destructuring of vegetable matter at atmospheric pressure by a catalyst/solvent system of formic acid/acetic acid. Applied to the pulping of triticale straw. *Industrial Crops and Products*, (2001), 14(2), 139-144.
19. S.I. Mussatto, M. Fernandes, I.C. Roberto. Lignin recovery from brewer's spent grain black liquor. *Carbohydrate Polymers*, (2007), *70*(2), 218-223.
20. N.E. El Mansour, J. Salvadó. Structural characterization of technical lignins for the production of adhesives: Application to lignosulfonate, kraft, soda-anthraquinone, organosolv and ethanol process lignins. *Industrial Crops and Products*, (2006), *24*(1), 8-16.
21. J. Zhang, H. Deng, L. Lin, Y. Sun, C. Pan, S. Liu. Isolation and characterization of wheat straw lignin with a formic acid process. *Bioresource technology*, (2010), *101*(7), 2311-2316.
22. A. García, M.G. Alriols, G. Spigno, J. Labidi. Lignin as natural radical scavenger. Effect of the obtaining and purification processes on the antioxidant behavior of lignin. *Biochemical Engineering Journal*, (2012), *67*, 173-185.
23. A. Toledano, X. Erdocia, L. Serrano, J. Labidi. Influence of extraction treatment on olive tree (Olea europaea) pruning lignin structure. *Environmental Progress & Sustainable Energy*, (2013), *32*(4), 1187-1194.
24. R. Sun, J.M. Lawther, W.B. Banks. Fractional and structural characterization of wheat straw hemicelluloses. *Carbohydrate polymers*, (1996), *29*(4), 325-331.

25. X.F. Sun, R. Sun, P. Fowler, M.S. Baird. Extraction and characterization of original lignin and hemicelluloses from wheat straw. *Journal of agricultural and food chemistry*, (2005), *53*(4), 860-870.
26. C. Vanderghem, A. Richel, N. Jacquet, C. Blecker, M. Paquot. Impact of formic/acetic acid and ammonia pre-treatments on chemical structure and physico-chemical properties of Miscanthus x giganteus lignins. *Polymer Degradation and Stability*, (2011), *96*(10), 1761-1770.
27. J. Li, G. Henriksson, G. Gellerstedt. Lignin depolymerization/repolymerization and its critical role for delignification of aspen wood by steam explosion. *Bioresource technology*, (2007), *98*(16), 3061-3068.
28. X.F. Sun, Z. Jing, P. Fowler, Y. Wu, M. Rajaratnam. Structural characterization and isolation of lignin and hemicelluloses from barley straw. *Industrial Crops and Products*, (2011), *33*(3), 588-598.

Chapter 3

Determination of S/G ratio by Py/GC-MS

3.1. Pyrolysis

The word “pyrolysis” is of Greek origin and means “to decompose by heat”, yet it would be wrong to associate pyrolysis with burning. Burning decomposes a molecule in the presence of oxygen to water, carbon dioxide and heteroatom oxides, with no analytical information on the original molecule. By contrast, pyrolysis is the thermal fission of a sample in the absence of oxygen into molecules of lower mass, low enough to be suitable for GC or MS, yet large enough to provide analytical information on the original sample. This is usually done by rapid heating in an inert atmosphere or in a vacuum. In essence, analytical pyrolysis refers to the decomposition of the macromolecule to the greatest possible extend whilst maintaining the size of the fragments as large as possible, the limit being the upper mass limit of the instrumental employed [1].

Pyrolysis is the transformation of nonvolatile compounds into a volatile degradation mixture by heat in the absence of oxygen. A rate of heating to the final temperature in the millisecond range is typical for analytical pyrolysis, in contrast to the slow heating rates employed for other thermal characterization techniques, e.g., thermogravimetric (TG) and differential scanning calorimetry (DSC) that are in the range of minutes or hours. Simple sample preparation (drying and milling), rapid analysis times (from minutes up to 1.5 hours) and small sample size (1 to 100 μg) are the key features of analytical pyrolysis [2].

There are basically different ways to pyrolyze a sample which can be divided into continuous or pulse modes. In the continuous mode, the sample is introduced rapidly into the hot furnace and kept at a fixed temperature during the pyrolysis. In the pulse mode, the sample is placed on a cold pyrolysis probe, which is rapidly (typically in the

milliseconds range) heated to a predetermined pyrolysis temperature and maintained at that temperature for the time required to complete the pyrolysis of the sample (typically a few seconds).

Techniques for pulse mode pyrolysis include electric discharge, laser, radiation induced heated filament and Curie-point pyrolysis. Heated filament and Curie-point are the systems most widely employed for analytical purposes. The two methods differ in the control of the pyrolysis temperature and in the design of the apparatus.

Curie-point pyrolyzers (Figure 3.22) rely upon high-frequency inductive heating of a ferromagnetic wire (< 1 mm diameter) to its Curie-point, temperature that is a temperature at which a transition from ferromagnetism to paramagnetism occurs. At appropriate values of wire dimensions and field strength, the wire temperature reaches an equilibrium close to the Curie-point temperature. Selected and precise temperatures (up to 1128 ºC) can be set in less than 200 miliseconds by using appropriate alloys of ferromagnetic materials. For instance, the Curie-point temperatures of pure nickel, iron and cobalt are 358, 770 and 1128 ºC, respectively. However, it should be mentioned that the temperature-rise profile depends on various operating parameters such as wire diameter and strength of the inductive field frequency. The main advantage of Curie-point pyrolyzers is the rigorously controlled pyrolysis temperature. However, the pyrolysis temperature can be varied only at discrete intervals and depends on careful manufacturing and cleaning procedures of the employed wires.

Figure 3.22 Curie point pyrolyzer

Heated filament pyrolyzers consist of a resistance element made from platinum coil or ribbon. The temperature and time of pyrolysis are electronically controlled. Sample solution can be syringed on the ribbon and pyrolyzed after solvent evaporation by drying in or by pre-heating the ribbon at a suitable temperature. Coil pyrolyzers are commonly used for lignin pyrolysis. Finely ground lignin samples are usually placed in a quartz sample tube, which in turn are loosely plugged with glass wool to prevent the sample from being blown out of the tube by the carrier gas. The main advantage of heated filament versus Curie-point systems is that the temperature of pyrolysis can be varied continuously. Moreover, relatively large amounts of sample can be loaded compared to Curie-point systems. This enables a higher degree of reproducibility for the analysis of dishomogeneous materials, such as natural samples of lignocellulose [1].

Figure 3.23 Heated filament pyrolyzer

3.2. Different methods to measure the S/G ratio

In this chapter the syringyl/guaiacyl (S/G) ratio of different agricultural and industrial lignins were measured in order to determine the lignin with the highest syringyl and guaiacyl groups for further depolymerization.

There are several techniques that have been used to determine the lignin S/G ratio. In this paragraph, a brief summary of each method with their advantages and disadvantages is exposed.

Several chemical degradative methods have been used for determining the lignin S/G ratio in lignin. Permanganate and alkaline nitrobenzene oxidation [3], as well as acidolysis [4] and thioacidolysis [5] or CuO oxidation [6] have been utilized to determine the S/G ratio. However, these methods are often labor-intensive, require the usage of toxic reagents and are bond-specific, and therefore, may not provide a "true" measurement of lignin monomers. Spectroscopic methods, such as Fourier-Transformed Infrared Spectroscopy (FTIR) [7], or solid-state Carbon Nuclear Magnetic Resonance (^{13}C NMR) [3,8,9] have been used to determine the S/G ratio in various hardwoods. However, it is often difficult to determine the precise S/G ratio in lignin owing to both insufficient sensitivity and poor resolution in the spectra, and lignin extraction is always required. On the other hand, pyrolysis- gas chromatography/mass spectroscopy (Py-GC/MS) is rapid and highly sensitive for characterizing the chemical structure of lignin, which allows the analysis of very small amounts of sample without prior manipulation and/or isolation [10,11].

Py–GC/MS is an analytical technique which is able to provide useful information concerning the structure of lignin components, assuming that pyrolysis products represent, to a greater or lesser degree, the structural units forming the

macromolecule. Py–GC/MS is based on depolymerization of the macromolecules by heat followed by identification of the fragments by mass spectrometry [12]. Characteristic features in terms of H, G and S units, have been established based on this analytical method.

3.3. Objective

This chapter is focused on the full analysis of different agricultural residues (olive tree pruning, almond shell and apple tree pruning) and industrial residues (kraft liquor) and the analysis of the lignins obtained from those raw materials using Py-GC/MS, gel permeation chromatography (GPC) and FTIR to get a better inside of the chemical composition for future applications. In this case, the interest centers on the S and G content of the analyzed lignins to choose the one with the highest syringyl and guaiacyl units to be depolymerized.

3.4. Materials and methods

3.4.1. Raw materials and lignin extraction process

The kraft liquor resulting from Eucalyptus wood pulping was kindly supplied by the company Iberpapel. Apple tree (Malus domestica) pruning was kindly supplied by local farmers; almond shell was kindly supplied by the local farmer and originated from an almond tree (Prununs amygdalus) cultivated in La Rioja (Spain) belonging to the varieties called Marcona and Larqueta; olive tree pruning was supplied by an independent producer and originated from an olive tree (Olea europea) cultivated in Navarra belonging to the variety called Arróniz. The raw materials were milled by a Retsch 2000 hammer mill to produce chips of 4 mm free of dust and soil. The raw materials were characterized according to standard methods (TAPPI) described in the **Appendix I**.

Olive tree pruning was treated by an organosolv process based on previous works [13]. Organosolv treatment consisted in the fractionation of the raw material with an ethanol/water mixture (70:30, v/v) with a solid/liquid ratio of 1:6, in a 4 L pressure stainless steel batch reactor (ELO723 Iberfluid) controlled by Adkir software at 180ºC for 90 min under constant stirring.

Almond shell was treated with another organosolv process. In this case the raw material was fractionated with mixture of acetic acid/ formic acid/water (60:30:10, v/v/v) and with 0.2% of catalyst (HCl) with a solid/liquid ratio of 1:10. The reaction was carried out in the same 4 L pressure reactor at 130ºC, for 90 min under constant stirring [14].

Apple tree was fractionated with acetosolv process. This treatment consisted in the fractionation with acetic acid/water (60:40, v/v) with a solid/liquid ratio of 1:10, using the 4 L pressurized reactor (180°C, 90 min) under constant stirring [15].

3.4.2. Lignin recovery from the black liquor

Organosolv ethanol liquor volume was measured and was diluted with two volumes of acidified water (pH 2), and the precipitated lignin was recovered by centrifugation and then vacuum dried at 50 ºC until constant weight [16]. The acidified water was prepared adding sulphuric acid (96% v/v) dropwise to a disitilled water volume until pH value changed to two. Organosolv acid liquors (acetosolv and acetosolv-formosolv) were both precipitated by adding five times their volumes of distilled water, and the precipitated lignin was recovered by filtration and then vacuum dried at 50 ºC until constant weight [17]. The filtration was done with a filter paper with a diameter of 110 mm placed into a number 3 sintered glass Buchner funnel.

Kraft liquor was acidified to pH 2 with sulphuric acid (96% w/w) and the precipitated lignin was separated by filtration with a 110 mm of diameter filter paper placed into a number 3 sintered glass Buchner funnel, washed several times with acidified water (pH 2) to remove impurities and then vacuum dried at 50 ºC until constant weight.

3.4.3. Liquid fraction characterization and lignin characterization

The liquid fractions recovered from each of the extraction processes were characterized according to the TAPPI methodology described in the **Appendix II.**

The four different lignins were characterized by different techniques described in the **Appendix II** and **Appendix IV**.

Lignin from different raw materials was analyzed with gel permeation chromatography in order to determine average molecular weight M_w. lignin samples were examined using Jasco system equipped with an interface (CLC-NETII/ACD) and a refractive detector (RI-2031Plus). Two serial columns were used PolarGel 2x (300 x 7.5 mm). Dimethylformamid with 0.1 % (wt) of lithium bromide was the mobile phase as well as the eluent of the samples. The calibration was done with polystyrene standards.

Different lignin samples were characterized by PerkinElmer two FTIR Spectrometer equipped by a Universal Attenuated Total Reflectance (ATR) accessory with DiCompTM crystal (2.4 refractive index; 1.66 depth of penetration).

Four different lignin samples were analyzed by Py-GC/MS, where each sample was thermally degraded in an inert atmosphere, and its macromolecules were break down to relatively simple aromatic compounds that provide structural information about the lignin.

The Py-GC/MS was carried out using a commercial pyrolyzer (Pyroprobe model 5150, CDS, Analytical Inc., Oxford, PA) coupled to a GC-MS apparatus (Agilent Techs. Inc. 6890 GC/5973 MSD) using a fused silica capillary column (HP-5MS, 30m x 0.25 x 0.25 μm). Small sample (in the range of 100μg range) was pyrolyzed in a quartz boat at 500 °C for 10s with a heating rate of 2°C/ms with the interface kept at 250 °C. the GC oven program, with helium (<99.999%) as carrier gas with 0.7 mL/min flow, started at 50 °C and was held for 2 min. then it was raised to 120 °C at 10 °C/min, was help for 5 min and after that the temperature was raised to 280 °C at 10 °C/min, was held for 8 min and finally raised to 300 °C at 10 °C/min and was held for 10 min.

The identification of the pyrolysis products was accomplished using a GC/MS instrument. The obtained mass spectra were compared to the mass spectra of pure compounds, National Institute of Standards Library (NIST) and with those compounds reported in literature [11, 18].

The absence of a normalized quantitave method made it difficult to calculate the S/G ratio. There are reported quantitative methods in literature in which the amount of each degradation product is calculated using the corresponding pure compound for calibration [Izumi 1995]. It is quite complicated method and in addition, not all the lignin degradation products are commercially available. There is another method in which the calibration was done with one monomeric internal standard and calibration curves only with some of the pyrolysis products. This method underestimates the lignin content [20].

In this chapter the S/G ratio was calculated by integrating the peak areas of each pyrolysis degradation product to the weight of the sample and normalizing the products to 100%. The S/G ratio was finally calculated by dividing the sum of the peak areas from syringyl units by the sum from the peak

areas of guaiacyl units and the data for two repetitive pyrolysis experiments were averaged.

The value of the S/G ratio was obtained by considering the relative areas of all lignin derivatives and dividing them as syringyl type (S), guaiacyl type (G) and p-hydroxyphenyl type (H). The first group included syringol, 3,4-dimethoxyphenol, 4-methylsyringol, 3-ethylsyringol, 4-ethylsyringol, 4-vynylsyringol, 4-allylsyringol, 4-propylsyringol, 4-propenylsyringol, syringaldehyde, syringyl acetone and propiosyringone for the syringyl type lignin; guaiacol, 4-methylguaiacol, 3-methoxycatechol, 4-ethylguaiacol, 4-vinylguaiacol, eugenol, 4-propylguiacol, vanillin, *cis*-isoeugenol, *trans*-isoeugenol, propenylguaiacol, acetoguaiacone, guaiacyl acetone, propioguaiacone for the guaiacyl type of lignin and phenol, 2-methylphenol, 4-methylphenol, 4-ethylphenol, 4-vinylphenol for the *p*-hydroxyphenyl type of lignin.

3.5. Different raw material and treatment results

3.5.1. Raw materials

The raw materials were characterized in order to obtain some characteristics and the results are shown in Table 3.7.

Table 3.7 Chemical composition of raw materials on dry basis (wt, %)

Samples	Apple pruning	Olive pruning	Almond shell
Moisture	7.99 ± 0.10	10.62± 3.47	10.77 ± 0.10
Extractives	8.06 ± 0.41	12.19 ± 0.48	0.07 ± 0.01
Lignin	31.21 ± 2.69	24.44 ± 2.28	52.59 ± 3.71
α-cellulose	32.50 ± 1.40	29.34 ± 0.25	41.29 ± 2.19
Hemicellulloses	28.24 ± 1.53	22.45 ± 1.27	8.57 ± 0.80
Ashes	2.24 ± 0.07	1.43 ± 0.46	0.89 ± 0.01

The humidity results were similar for all the analyzed raw materials varying between an 8 and 11%. As far as the value of the ash content is concerned, the low inorganic value (0.89%) obtained by the almond shell should be emphasize. These values are related to the mineral components such as the sodium, potassium or iron that conform the raw materials. The extractives include a large variety of compounds grouped into general classes including terpenoids, fats and waxes and their components, and phenolics as well as other minor components not formally classified into these three groups, such as carbohydrates, peptides and inorganic compounds [21]. In the analyzed raw materials there was not big result variation, with the exception of the almond shell which in accordance with other authors [22] had low percentage of extractives (0.07%). According to the theory of Vassilev et al. [23], biomass could be classified into six groups (CHL, CLH; HCL, LCH, HLC and LHC) based on the proportions of cellulose, hemicelluloses and lignin. As demonstrated in the Figure 3.24 these results were as follows: (1) CLH type: apple tree pruning and olive tree pruning; (2) LCH type: almond shell.

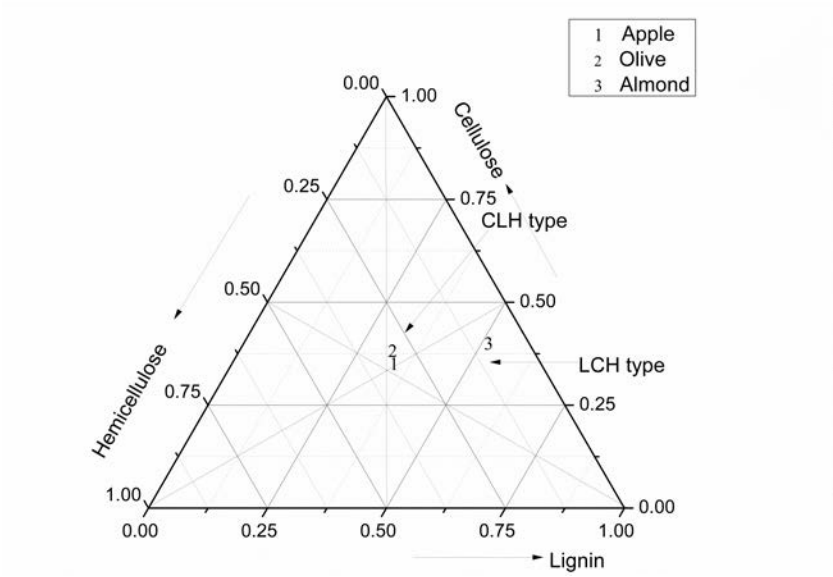

Figure 3.24 The structural compositions of the raw materials

3.5.2. Characterization of the liquid fraction and lignin purity analysis

The liquid fractions resulted from the pretreatment of different raw materials were characterized to determine several parameters and the results are summed up in Table 3.8.

Table 3.8 Physicochemical properties of olive tree organosolv (OO) kraft (KL), Apple tree acetosolv (AA) and almond Shell acetosolv formosolv (ASAF) liquid fractions.

Samples	OO	KL	AA	ASAF
pH	4.54	12.9	1.10	1.00
Density (g/mL)	0.90 ± 0.00	1.05 ± 0.00	1.06 ± 0.00	1.10 ± 0.00
TDS (wt, %)	7.39 ± 0.10	15.80 ± 1.83	5.03 ± 0.43	5.24 ± 0.02
IM (wt, %)	0.04 ± 0.02	10.20 ± 0.06	0.24 ± 0.02	0.17 ± 0.02
OM (wt, %)	7.36 ±	5.60 ± 1.89	4.78 ±	5.08 ±

	0.11		0.42	0.02
Lignin (wt, %)	2.91 ± 0.17	6.39 ± 0.49	1.92 ± 0.06	2.00 ± 0.12

As expected the pH is highly affected by the fractionation solvents that were used. Very low pH values were obtained for the OO and ASAF liquid fractions (from 1-1.10) whereas the liquor from the alkaline treatment showed higher pH values (12.9). The slightly acid condition (4.54) of the liquor obtained from the neutral OO conditions was related to the release of the acetyl group during the solubilization of the hemicellulosic fraction of the raw material [24]. Table 3.8 results showed that all applied pretreatments showed high lignin solubilization rates (from 1.92 to 6.39%) and as the inorganic loading is high for the kraft process, so it is the IM content for the kraft liquid fraction.

The chemical composition of the obtained four different lignins after precipitation, which are organosolv olive tree lignin (OOL), kraft lignin (KL), apple tree acetosolv lignin (AAL) and almond shell acetosolv-formosolv lignin (ASAFL), is shown in Table 3.9.

Table 3.9 Chemical composition of of the four different lignins in dry basis (wt, %)

Samples	**OOL**	**KL**	**AAL**	**ASAFL**
IL (%)	80.32 ± 2.61	84.75 ± 4.45	80.53 ± 3.08	71.13 ± 0.93
ASL (%)	3.13 ± 0.16	13.65 ± 0.83	2.49 ± 0.23	2.10 ± 0.27
TLC (%)	83.45 ± 2.46	98.39 ± 3.63	83.02 ± 2.92	73.24 ± 0.66
Total sugar (%)	0.69 ± 0.03	2.45 ± 0.28	20.41 ± 5.74	2.25 ± 0.13
Glucose (%)	0.23 ± 0.03	0.29 ± 0.02	5.37 ± 0.75	0.25 ± 0.01
Arabinose (%)	-	0.11 ± 0.01	0.05 ± 0.02	0.09 ± 0.01
Xylose (%)	0.47 ± 0.01	2.05 ± 0.24	0.38 ± 0.05	1.91 ± 0.13
Maltose (%)	-	-	14.60 ± 5.33	-
Ash (%)	2.61	4.55	4.89	3.18

The purity of the lignin resulted from the sum of the acid insoluble lignin and the acid soluble lignin, was quite similar for all the extracted lignins being the highest for the kraft lignin (98.39%). This high purity was achieved by cleaning the liquid fraction several times with acidified water as the inorganic matter content was high in the liquid fraction analysis (see Table 3.8). Also all the lignin-carbohydrate complexes that could have been dissolved during the alkaline extraction have disappeared due to the cleaning step. As conclusion, all the lignins showed a sugar content below 6% expect for the AAL which had a high percentage of maltose. Furthermore, the analyze lignin showed an ash content below the 6%.

3.5.3. Lignin structure and molecular weight

Molecular weight distribution of the obtained lignins and weight average (M_w), number average (M_n) molecular weight and polydispersity (M_w/M_n) of the different extracted lignin are shown in Table 3.10.

Table 3.10 Weight average (M_w) molecular weight, number average (M_n) molecular weight and polydispersity (M_w/M_n) of the different lignins

	OOL	**KL**	**AAL**	**ASAFL**
M_w	4209	2418	6082	12500
M_n	1116	753	1255	2850
M_w/M_n	3.77	3.21	4.85	4.40

Lignin molecular weight depends on both the nature of the raw material and the method use for the extraction. In relation with the extraction process, the almond shell and the apple tree pruning with the severe extraction conditions suffered from the repolymerisation/self-condensation mechanisms because of the formation of highly reactive and

unstable carbocations, resulting in an increase in the molecular weight [25]. This fact could explain the higher M_w observed for the acetosolv and acetosolv-formosolv samples when compared with the ethanol-organosolv ones. Kraft lignin gave similar results as the acetilated kraft lignin [26].

The polydispersity indicates the fraction of high or low molecular weight molecules present in the samples. However in this case there were not significant variations between the polydispersity results obtained for the different extraction methods.

In Figure 3.25 the molecular weight distribution of the extracted lignin could be observed. It can be seen that the peaks were quite wide which indicated a high heterogeneity on lignin molecular weight and therefore a high polydispersity. Moreover, some shoulders were identified at higher retention times which indicate the presence of low molecular weight fractions of lignin as it can seen in the case of the kraft lignin [17].

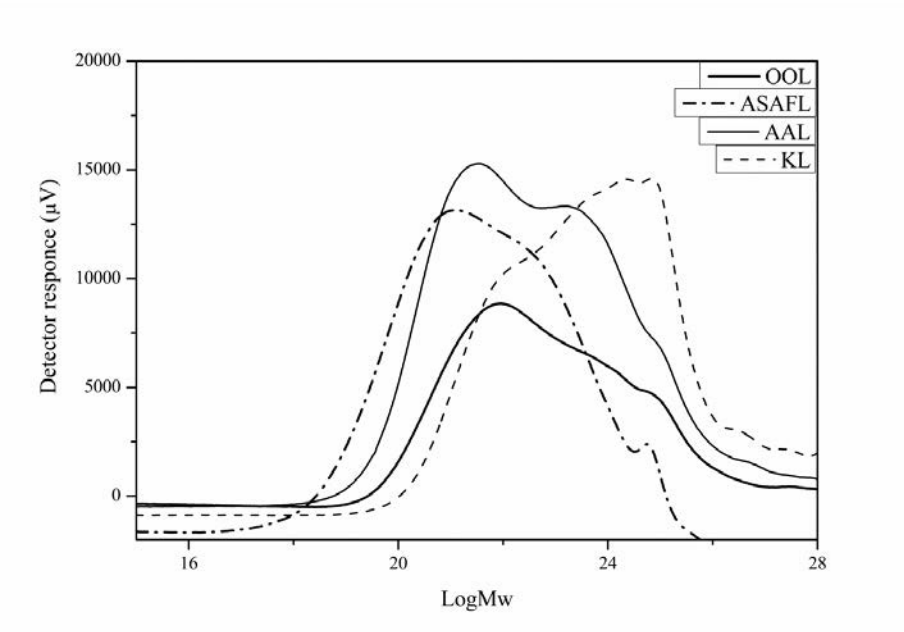

Figure 3.25 Molecular weight distribution of different lignins

FTIR spectra of different extracted lignin samples (Figure 3.26) showed some changes in the peak intensity and form. The band observed around 3400 cm^{-1} (1) represented the stretching of OH and hydrogen bonding. The peak at 2950 cm^{-1} (2) and 2840 cm^{-1}(3) were assigned to –CH stretching of methyl and methylene groups. The band at 1715 cm^{-1} (4) represented the unconjugated and conjugated carbonyl group in ketones. The bands at 1600 (5), 1510 (6) and 1422 cm^{-1} (8) were assigned to aromatic skeletal vibration. The peak 1365 cm^{-1} attributed to aliphatic –CH stretching in $–CH_3$ was of the same intensity in the case of AAL, OOL and ASAFL, but did not appear in the case of KL [28] The peak at 1460 cm^{-1} (7) represented the anti-symmetric deformation of the –CH group. The band at 1325 (9) cm^{-1} was assigned to syringyl breathing with CO stretching, band at 1218 (10) cm^{-1} was assigned to guaiacyl ring breathing with CO stretching, band from 1110 to 1117 cm^{-1} (11) was assigned to –CH in plane deformation in syringyl and the band at 909 cm^{-1} (13) was assigned to –CH in plane deformation of guaiacyl. The band at 1273 cm^{-1} only appeared in the OOL and KL spectrum and was associated to guaiacyl ring breathing and CO stretching [28]. Other difference between the spectra was located at 1153 cm^{-1} that was attributed to CO stretch in ester group. This peak is attributed to the HGS type of lignin and all lignin showed this peak to a greater or lesser degree [22].

a)

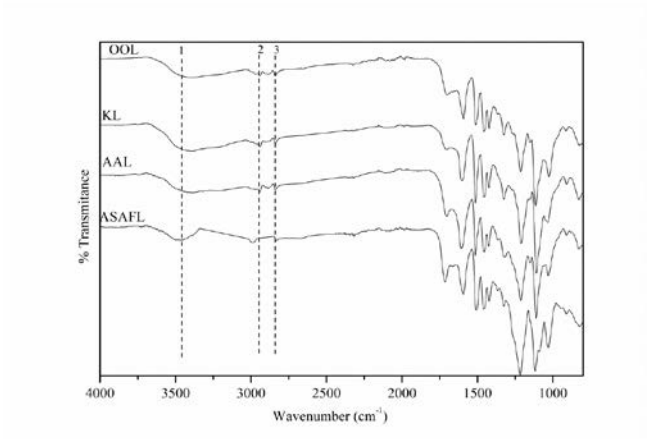

b)

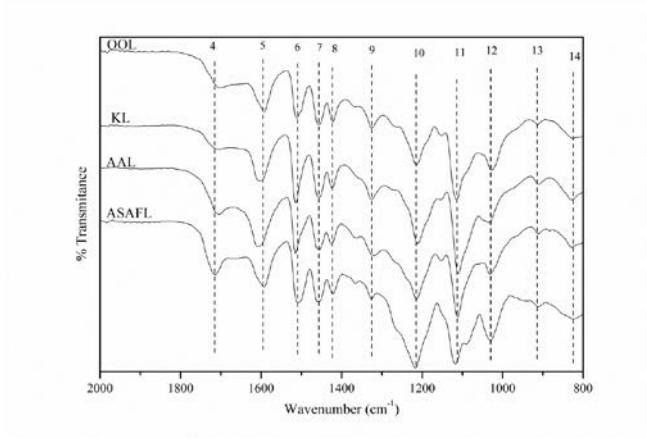

Figure 3.26 FTIR spectra of the obtained lignins. (a) wave number from 4000 to 700 cm^{-1} and (b) magnification of 2000-700 cm^{-1} region.

3.5.4. Lignin chemical composition by Py/GC-MS

The measurement of S, G and H lignin monomers enables classification of plants as gymnosperm or softwood (G-lignin), angiosperm or hardwood (S-G lignin), or herbaceous

(S-G-H lignin), with some exceptions, such as eucalyptus, which are classified as angiosperms, but are known to contain H lignin [29].The majority of the analyzed lignins are of hardwood origin (olive tree pruning, apple tree pruning, and eucalyptus globulus).

The pyrolytic behavior of different raw materials lignin is shown in the pyrograms of Figure 3.27. The identities and the relative areas of the 32 compounds are exposed in Table 3.11

Table 3.11 and their chemical structure divided in their group of origin (H, G or S) is shown in Figure 3.28.

a)

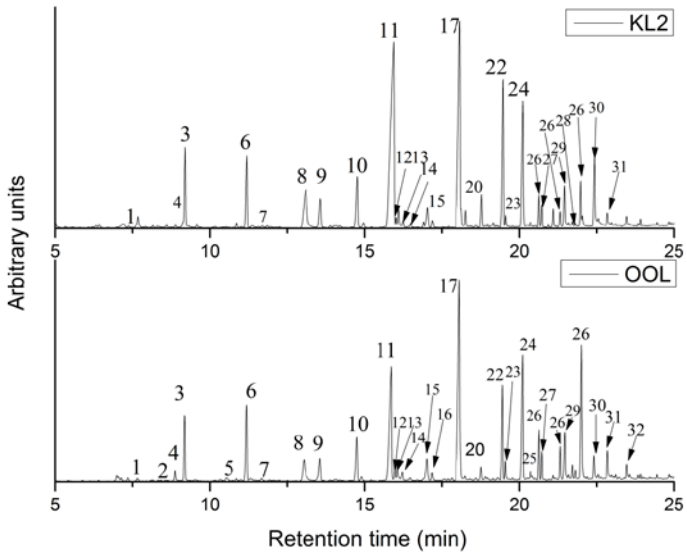

b)

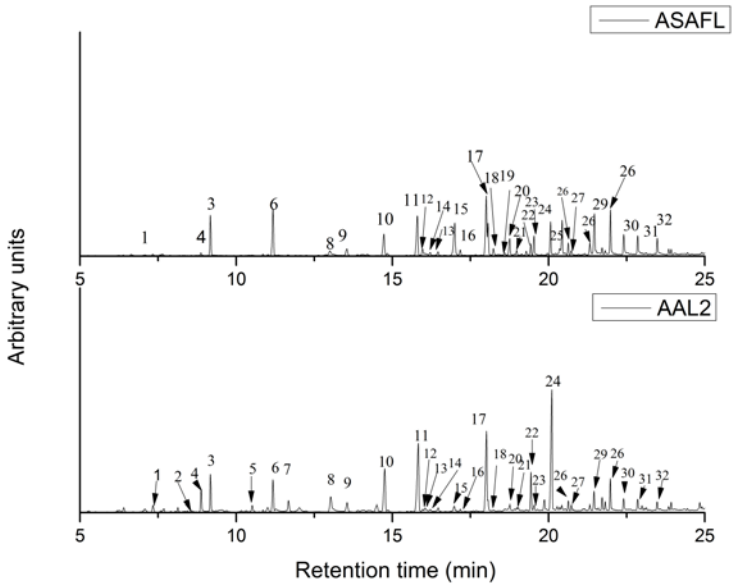

Figure 3.27 Py-GC/MS chromatograms of KL, OOL, AAL and ASAFL. The numbers refer to the compounds listed in **Table 3.11**

Table 3.11 Peak assignments for the different pyrograms obtained by Py-GC/MS with their retention times (RT).

Peak n.	RT[a] (min)	Compound	Monomer assignment	m/z	Area (%)			
					OOL	KL	AAL	ASAFL
1	7.33	Phenol	H	94/66/65	0.34±0.00	0.20±0.00	1.08±0.05	0.35±0.06
2	8.87	*o*-cresol	H	85/108/107	0.11±0.16	-	0.42±0.03	-
3	9.18	Guaiacol	G	109/124/81	4.11±0.12	3.74±1.02	4.08±0.42	6.03±0.88
4	11.18	*p*-cresol	H	107/108/77	0.81±0.00	0.23±0.06	2.83±0.24	0.48±0.05
5	10.54	4-ethyl-phenol	H	107/122/77	0.51±0.06	-	1.07±0.20	-
6	11.21	4-methyl-guaiacol	G	138/123/95	5.59±0.29	3.49±0.64	4.02±0.38	8.73±1.02
7	11.69	4-vinylphenol	H	120/91/119	0.20±0.22	0.06±0.09	1.85±0.33	-
8	13.00	3-methoxycatechol	G	140/125/97	3.21±0.16	4.42±1.12	3.61±0.60	1.97±0.54
9	13.55	4-ethyl-guaiacol	G	137/152/122	2.54±0.20	2.13±0.12	1.77±0.28	2.02±0.30
10	14.73	4-vinylguaiacol	G	135/150/107	3.75±0.05	3.36±0.25	8.16±0.80	4.66±0.27
11	15.80	Syringol	S	154/139/96	13.57±0.46	23.52±3.61	12.76±0.59	8.98±1.29
12	15.97	Eugenol	G	164/149/77	0.78±0.00	0.49±0.00	0.46±0.04	1.33±0.09
13	16.04	3,4-dimethoxyphenol	S	154/139/111	0.96±0.06	0.93±0.27	0.86±0.11	0.59±0.07
14	16.21	4-propyl-guaiacol	G	137/166/122	0.86±0.01	1.44±0.15	0.65±0.02	0.85±0.13
15	16.99	Vanillin	G	151/152/81	2.19±0.22	1.63±0.12	1.38±0.08	6.82±0.80

16	17.17	Isoeugenol (cis)	G	164/149/131	0.69±0.02	-	0.37±0.01	0.95±0.02
17	17.99	4-methyl-syringol	S	168/153/125	20.18±0.17	17.86±2.32	12.86±1.70	11.95±0.82
18	18.07	Isoeugenol (trans)	G	164/149/77	-	-	0.77±1.09	4.63±0.21
19	18.60	propenylguaiacol	G	162/147/91	-	-	-	0.59±0.02
20	18.76	Acetoguaiacone	G	151/166/123	0.88±0.12	2.14±0.64	1.54±0.05	2.77±0.10
21	18.98	3-ethyl-syringol	S	182/167/139			0.49±0.02	0.80±0.04
22	19.41	4-ethyl-syringol	S	167/182/77	5.83±0.38	7.97±0.41	3.91±0.62	1.57±0.07
23	19.54	Guaiacyl acetone	G	137/180/122	1.01±0.32	0.96±0.41	0.91±0.05	2.88±0.23
24	20.07	4-vinyl-syringol	S	180/165/137	8.10±1.41	8.38±1.33	20.47±2.73	4.60±0.14
25	20.37	propioguaiacone	G	151/180/123	3.76±4.42	-	-	1.21±0.13
26	20.63	4-allyl-syringol	S	194/91/119	11.69±2.64	5.77±1.84	5.33±0.98	9.80±0.40
27	20.73	4-propyl-syringol	S	167/196/123	1.43±0.03	0.97±0.13	0.66±0.03	1.36±0.81
28	21.32	4-propenyl-syringol	S	194/91/179	-	0.50±0.21	0.45±0.64	-
29	21.47	Syringaldehyde	S	182/181/167	2.93±0.46	3.16±1.37	2.72±0.19	5.64±2.09
30	22.41	Acetosyringone	S	181/196/153	1.39±0.35	5.41±2.22	1.69±0.14	2.99±0.49
31	22.86	Syringyl acetone	S	167/210	1.72±0.35	1.24±0.48	1.77±0.15	3.06±0.22
32	23.48	Propiosyringone	S	181/182/210	0.86±0.06	-	1.04±0.10	2.40±0.75
				H	5.26	0.49	7.25	0.83
				G	26.07	23.80	27.72	45.43
				S	68.67	75.70	64.54	53.74
				S/G	2.63	3.18	2.33	1.18

H structures

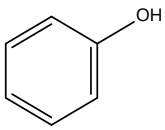

phenol

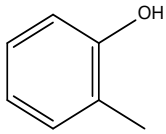

o-cresol

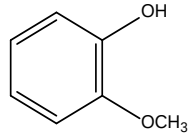

2-methoxyphenol

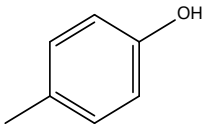

p-cresol

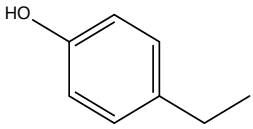

4-ethylphenol

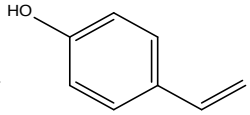

4-vinylphenol

G structures

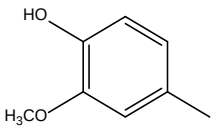

4-methylguaiacol

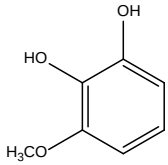

3-methoxycatechol

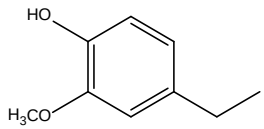

4-ethylguaiacol

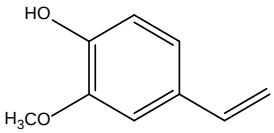

4-vinylguaiacol

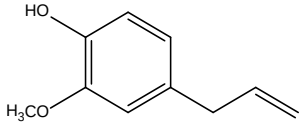

Eugenol

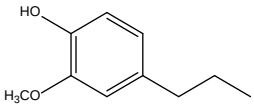

4-propylguaiacol

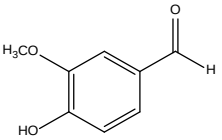

vanillin

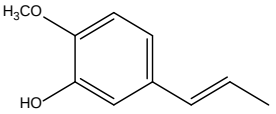

isoeugenol(*cis*)

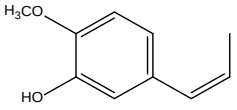

isoeugenol(*trans*)

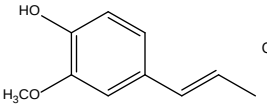

4-propenylguaiacol

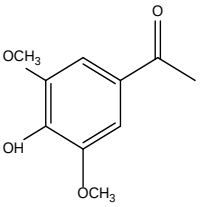

Acetoguaiacone

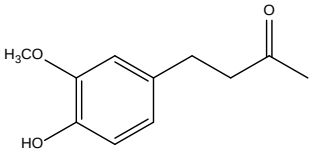

guaiacyl acetone

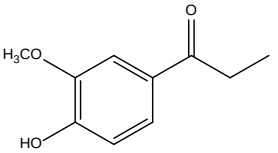

propioguaiacone

S structures

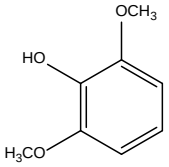

syringol

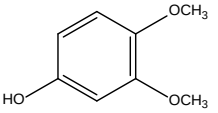

3,4-dimethoxyphenol

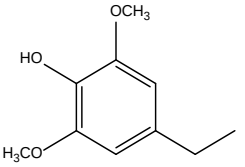

4-ethylsyringol

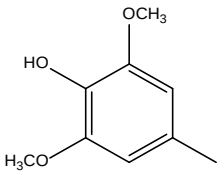

4-methylsyringol

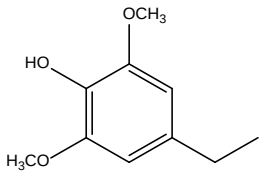

4-ethylsyringol

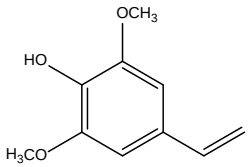

4-vinylsyringol

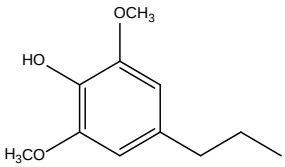

4-propylsyringol

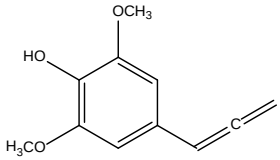

4-allylsyringol

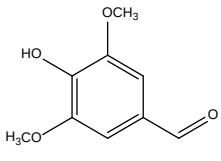

syringaldehyde

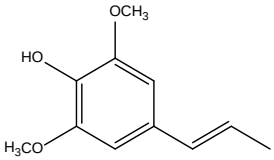

4-propenylsyringol

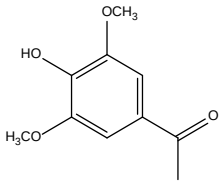

acetosyringone

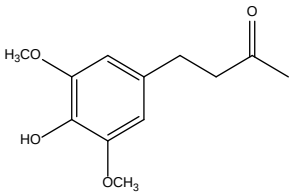

syringyl acetone

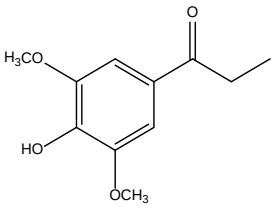

propiosyringone

Figure 3.28 Chemical structures of the 32 compounds found after the pyrolysis on the different lignins

Olive tree pruning, *Eucalyptus globulus* and apple pruning lignin released predominantly syringyl type of compounds. S/G ratios and composition in terms of total S, G and H values of different raw materials are shown in Table 3.11.

The pyrolytic behavior of the recovered lignins is shown in the pyrograms of Figure 4. The identities and the relative abundances of the 31 compounds are exposed in Table 6. As the main products of the pyrolisis process of olive tree pruning, *Eucalyptus globulus* and apple tree pruning 10 syringyl-type of compounds were detected. The peaks of largest proportions in each case were 4-methylsyringol, 4-allylsyringol; syringol, (peak 17, 26 and 11) in the case of olive tree pruning; syringol, 4-methylsyringol, 4-ethylsyringol (peak 11, 17 and 22) in the case of *Eucalyptus globulus* and 4-methylsyringol, syringol, 4-vinylguaiacol (peak 17, 11 and 10) in the case of apple tree pruning. In contrast, almond shell lignin released predominantly a mix of syringyl and guaiacyl structures, being 4-methylsyringol, 4-methylguaiacol and 4-allylsyringol (peak 17, 6 and 26). All samples except for ASAFL lignin, revealed lignin derived S-type of phenols were present in higher abundances than the respective G-type of phenols. Furthermore, as it could be seen in the FTIR results all lignin showed a relative abundance of the H units been the almond shell the raw material with the highest abundance.

Olive tree pruning lignin showed an S/G ratio of 2.63. This value was in concordance with the values (acetosolv lignin 2.05; formosolv lignin 1.96 and acetosolv-formosolv lignin 2.01) obtained by Erdocia et al [17] for olive tree pruning where the technique of alkaline nitrobenzene oxidation was used to determine the pheolic composition. Although lignin was extracted by three different organosolv methods there was not significant variation on the S/G ratio results showing that the extraction method did not affect lignin nature. Continuously, eucalyptus lignin had a value of 3.19 a similar value to the one shown by Rencoret et al [28] who obtained a value of 2.9 S/G by HSQC-NMR. The S/G value obtained for almond shell lignin was 1.18 of and for apple tree pruning lignin was 2.33.

The release of the most abundant compounds during the pyrolysis of the lignin is going to be discussed in the following paragraphs. The first thing that needs to be address is the relationship that was found between the lignin isolation procedure and the volatile phenolic composition. Monolignols (*p*-coumaril, coniferyl and sinapyl alcohols) were predominant in native or milled wood lignins, while guaiacol, syringol and lighter phenols were important in more severe lignin isolation methods (e.g. kraft, organosolv lignins) [30]. So it is worth to notice that the results of these experiments are in agreement with this finding.

One possible route for the formation of guaiacol and syringol is the cleavage of the aryl-alkyl-aryl ether bond (ß-O-4 bond) in the lignin during the pyrolysis, in parallel to the H-abstraction for phenoxy to form the corresponding phenolic hydroxyl. The syringol and guaiacol derives with the saturated alkyl side-chain structure, such as 4-methylguaiacol and 4-methylsyringol, are possibly formed by the cleavage of the C-C linkage on the side-chain [30, 29]. The higher content of syringol and its derivates it is due to firstly that the ß-O-4 linkage between syringyl units are easier to split than those between guaiacyl units. Secondly, because Py-GC/MS on G and GS lignin as well as on different model compounds at different temperatures corroborate: syringol and syringaldehyde and other S phenolics are found in higher quantities among pyrolysis products that the corresponding degradation products from guaiacylpropanes. Guaiacol type phenols easily undergo ionic condensation and under pyrolytic conditions mainly radical coupling reaction on the aromatic ring in *ortho* or *meta* position to the phenolic OH groups. Such condensation products remain in the high boiling tar fraction or in the solid coal residue [32].

Interestingly, allylbenzene formation from cinnamyl alcohol can probably serve as a model for the production of allyl syringol and eugenol in wood and lignin pyrolysis. It can be therefore assumed that the terminal OH-groups in the propanoid chain of the lignin monomer units yield allyl syringol and eugenol upon pyrolysis, while OH-funtionalities in the ß-position yield *cis*- and *trans*-1-propenylsyringol and *cis*-and *trans*-isoeugenol. Dehydration of OH-groups in the alkyl chain of different species of wood and lignin samples leading to similar unsaturated compounds has also been reported by [32, 33 and 34].

In general the aim of this work was to establish the raw material with the highest syringyl and guaiacyl units to be depolymerized afterwards. The raw materials with the highest and most equal syringyl and guaiacyl units were the olive tree pruning lignin with S 68.67% and G 26.07% and almond shell lignin with S 53.74% and G 45.43%.

3.6. Conclusions

The objective of this work was to analyze lignin from different agricultural and industrial residues to choose the proper lignin to be depolymerized.

The lignin purity analysis revealed high content being the KL, after a cleaning stage, the purest one. Moreover, all lignins showed a carbohydrate content below 6%, except for the AAL that had high percentage of maltose. Furthermore, the ash content was below 6% in all cases. With these analyses the proper lignin for depolymerization would be the olive tree pruning and the almond shell as there is no need for a cleaning stage.

Finally, the Py-GC/MS was used to measure the guaiacyl and syringyl units. The results showed that the raw materials with the highest and most equal syringyl and

guaiacyl units were olive tree pruning with S 68.68% and G 26.07% and almond shell lignin with S 53.74% and G 45.43%.

3.7. References

1. G.C. Galletti, P. Bocchini. Pyrolysis/gas chromatography/mass spectrometry of lignocellulose. *Rapid communications in mass spectrometry*, (1995), 9 (9), 815-826.
2. D.Meier, O. Faix, *Pyrolysis-Gas Chromatography-Mass Spectroscopy,* In: S.Y. Lin, C.W. Dence editors, Methods in lignin chemistry Springer-Verlag Berlin, Heidelberg, (1992), pp. 177-196.
3. Y.M. Xie, Difference of condensed lignin structures in eucalyptus species, *Nordic Pulp Paper Res*earch, (2004), 19, 18-21.
4. K. Lundquist, *Acidolysis*, in: S.Y. Lin, C.W. Dence (Eds.), Methods in Lignin Chemistry, Springer-Verlang, Berlin, (1992), pp. 289-300.
5. C. Lapierre, B. Monties, C. Rolando, Thioacidolysis of poplar lignins: identification of monomeric syringyl products and characterization of guaiacyl-syringyl lignin fractions, *Holzforschung*, (1986), 40, 113-118.
6. A.T. Martínez, A.E. González, A. Prieto, F.J. González-Vila, R. Fründ, p-Hydroxyphenyl: guaiacyl: syringyl ratio of lignin in some austral hardwoods estimated by CuO-oxidation and solid-state NMR, *Holzforschung*, (1991), 45, 279-284.
7. O. Faix, Classification of lignins from different botanical origins by FT-IR spectroscopy, *Holzforschung*, (1991), 45, 21-28.
8. H.H. Nimz, H.D. Robert, O. Faix, M. Nemr, Carbon-13 NMR spectra of lignins, 8. Structural differences between lignins of hardwoods, softwoods, grasses and compression wood, *Holzforschung*, (1981), 35, 16-26.
9. W.F. Manders, Solid-state 13C NMR determination of the syringyl/guaiacyl ratio in hardwoods, *Holzforschung*, (1987), 41, 13-18.
10. J. Ralph, R.D. Hatfield, Pyrolysis-GC-MS characterization of forage materials, *Journal of*

*Agricultural and Food Chem*istry, (1991) 39, 1426-1437.

11. O. Faix, D. Meier, I. Fortmann, Thermal degradation products of wood, *Holz Roh Werkst*. (1990), 48, 281-285.
12. K.L. Kuroda, T. Ozawa, T. Ueno, Characterization of sago palm (Metroxylon sagu) lignin by analytical pyrolysis, *Journal of Agricultural and Food Chemistry,* (2001), 49, 1840-1847.
13. A. Toledano, L. Serrano, J. Labidi, Enhancement of lignin production from olive tree pruning integrated in a green Biorefinery, *Industrial and Engineering Chemical Research*, (2011), 50, 6573-6579.
14. F. Xu, J.X. Sun, R. Sun, P. Fowler, M.S. Baird, Comparative study of organosolv lignins from wheat straw, *Industrial Crops and Prod*ucts, (2006), 23, 180-193.
15. L. Serrano, G. Spigno, A. García, D. Amendola, J. Labidi. Properties of Soda and Organosolv Lignins from Apple Tree Pruning. *Journal of Biobased Materials and Bioenergy*, (2012), *6*(3), 329-335.
16. M.N.M. Ibrahim, S.B. Chuah, W.D.W. Roski, Characterization of lignin precipitated from the soda black liquor of oil palm empty fruit bunch fibers by various mineral acids, *Journal of Science and Technology Development*, (2004), 21, 57–67.
17. X. Erdocia, R. Prado, M.A. Corcuera, J. Labidi, Effect of different organosolv treatments on the structure and properties of olive tree pruning lignin, *Journal of Industrial and Engineering Chemistry*, (2014), 20, 1103-1108.
18. J.S. Lupoi, S. Singh, R. Parthasarathi, B.A. Simmons, R.J. Henry, Recent innovations in analytical methods for the qualitative and quantitative assessment of lignin, *Renewable and Sustainable Energy Review*s, (2015), 49, 871-906.
19. A. Izumi, K.I. Kuroda, H. Ohi, A. Yamaguchi. Structural Analysis of Lignin by Pyrolysis-Gas

Chromatography (III)-Comparative studies of pyrolysis-gas chromatography and nitrobenzene oxidation for the determination method of lignin composition in hardwood. *Japan TAPPI Journal*, (1995), *49*, 61-68.

20. P. Bocchini, G.C. Galletti, S. Camarero, A.T. Martinez. Absolute quantitation of lignin pyrolysis products using an internal standard. *Journal of Chromatography A*, (1997), *773*(1), 227-232.
21. M.P. Fernandez, P.A. Watson, C. Breuil, Gas chromatography–mass spectrometry method for the simultaneous determination of wood extractive compounds in quaking aspen. *Journal of Chromatography A*, (2001), 922, 225-233.
22. L. Chen, X. Wang, H. Yang, Q. Lu, D. Li, Q. Yang, H. Chen, Study on pyrolysis behaviors of non-woody lignins with TG-FTIR and Py-GC/MS, *Journal of Analytical Applied Pyrol*ysis, (2015), 113, 499-507.
23. S.V. Vassilev, D. Baxter, L.K. Andersen, C.G. Vassileva, T.J. Morgan, An overview of the organic and inorganic phase composition of biomass. *Fuel*, (2012), 94, 1-33.
24. I. Egüés, C. Sanchez, I. Mondragon, J. Labidi, Effect of alkaline and autohydrolysis processes on the purity of obtained hemicelluloses from corn stalks, *Bioresource and Technol*ogy, (2012), 103, 239-248.
25. .A. Sequeiros, D.A. Gatto, J. Labidi, L. Serrano. Different Extraction Methods to Obtain Lignin from Almond Shell. *Journal of Biobased Materials and Bioenergy*, (2014), *8*(3), 370-376.
26. X.F. Zhou, Conversion of kraft lignin under hydrothermal conditions. *Bioresource and Technol*ogy, (2014), 170, 583-586.
27. R. El Hage, N. Brosse, L. Chrusciel, C. Sanchez, P. Sannigrahi, A. Ragauskas, Characterization of milled wood lignin and ethanol organosolv lignin from miscanthus, *Polymer Degradation and Stab*ility, (2009), 94, 1632-1638.

28. M.G. Alriols, A. García, R. Llano-Ponte, J. Labidi, Combined organosolv and ultrafiltration lignocellulosic biorefinery process, *Chemical Engineering Journal,* (2010), 157, 113-120.
29. J. Rencoret, G. Marques, A. Gutiérrez, L. Nieto, J. I. Santos, J. Jiménez-Barbero, A.T. Mantínez , J.C. del Río, HSQC-NMR analysis of lignin in woody (Eucalyptus globulus and Picea abies) and non-woody (Agave sisalana) ball-milled plant materials at the gel state, *Holzforschung*, (2009), 63, 691-698.
30. C. Amen-Chen, H. Pakdel, C. Roy. Production of monomeric phenols by thermochemical conversion of biomass: a review. *Bioresource Technology*, (2001), *79*(3), 277-299.
31. D.K. Shen, S. Gu, K.H. Luo, S.R. Wang, M.X. Fang. The pyrolytic degradation of wood-derived lignin from pulping process. *Bioresource technology*, (2010), *101*(15), 6136-6146.
32. O. Faix, E. Jakab, F. Till, T. Székely. Study on low mass thermal degradation products of milled wood lignins by thermogravimetry-mass-spectrometry. *Wood science and technology*, (1988), *22*(4), 323-334.
33. R.A. Fenner, J.O. Lephardt. Examination of the thermal decomposition of Kraft pine lignin by Fourier transformed infrared evolved gas analysis. *Journal of Agriculture and Food Chemistry*, (1981), 29, 846-849.
34. J.F. Haw, T.P. Schultz. C^{13} CP/MAS NMR and FTIR study of low temperature lignin pyrolysis. *Holzforchung*, (1985), 39, 289-296

Chapter 4

Polyol production from lignin by microwave heating

4.1. Introduction

4.1.1. Microwave heating

Microwave radiation is an electromagnetic radiation that ranges in a frequency from 0.3 to 300 GHz, corresponding to the wavelength from 1 mm to 1 m (

Figure 4.29). The microwave region, in the electromagnetic effect, is comprised between the infrared and radio frequencies. The most common use of the microwave is for the information transmissions (telecommunications) or for the energy transmission [1].

Organic chemistry synthesis is carried out at frequencies of 2.45 GHz, though this frequency is not enough to induce chemical reactions directly, microwave radiation benefits come from the efficient heat of materials by dielectric heating. Typical microwave reactor is shown in Figure 4.30 [1].

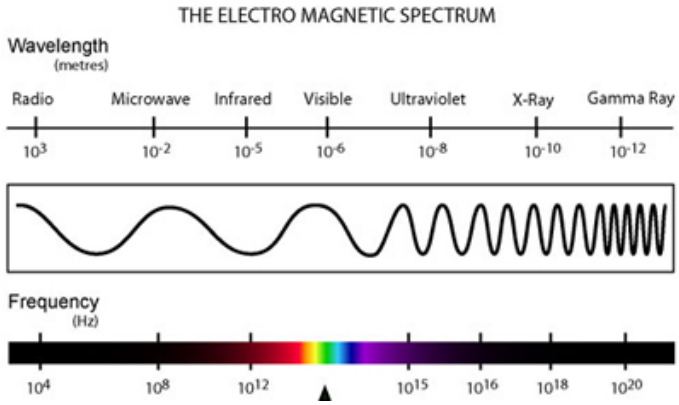

Figure 4.29 Electromagnetic spectrum

The chemistry of the microwave is based on heating efficiency of the material by the effect of the dielectric

heating of the microwave. Dielectric heating depends on the ability of the material to absorb microwave energy and transform it into heat. Microwaves are electromagnetic waves composed by electric and magnetic field. The electric component causes heating by two main mechanisms: dipolar polarization and ionic conduction.

The first mechanism is the dipolar polarization. In order to transform microwave radiation in heat, incident substances must possess dipole moment. When exposed to microwave radiation the dipoles tend to align in the electric field. The heat generated by this process is directly proportional to the ability of the dipoles to align itself with the electric field.

The second mayor mechanism of heating is the ionic conduction. During the ionic conduction, as the dissolved charged particles oscillate forward and backwards under the influence of microwave field, they collide with their neighbor molecules or atoms, causing movement that creates heat.

Material (solvent) heating characteristics under the microwave heating depend on the dielectric properties of the material. The ability to convert dielectric energy into energy in a given frequency and temperature is defined by the loss tangent, tan δ which is express as:

$$\tan \delta = \frac{\varepsilon''}{\varepsilon'}$$

Ɛ´´= dielectric loss which indicates the efficiency with which the electromagnetic radiation is converted into heat.

Ɛ´= dielectric constant that describes the molecule polarizability in the electric field.

For efficient absorption and as consequence, a fast heating a reaction medium with high tanδ is needed. In general the solvent are classified into high (tanδ >0.5), medium (tanδ 0.1-0.5), and low microwave absorbance (tanδ <0.1) (Table 4.12) [1].

Table 4.12 Loss tangent (tanδ) of different solvents

Solvent	**tanδ**	**Solvent**	**tanδ**
Ethylene glycol	1.350	*N,N*-dimethylformamide	0.161
Ethanol	0.941	1.2-dichoroethane	0.127
Dimethylsulfoxide	0.825	Water	0.123
2-propanol	0.799	Chlorobenzene	0.101
Formic acid	0.722	Chloroform	0.091
Methanol	0.659	Acetonitrile	0.062
Nitrobenzene	0.589	Ethyl acetate	0.059
1-butanol	0.571	Acetone	0.054
2-butanol	0.447	Tetrahydrofuran	0.047
1.2-dichlorobenzene	0.280	Dichloromethane	0.042
1-methyl-2-pyrrolidone	0.275	Toluene	0.040
Acetic acid	0.174	Hexane	0.020

4.1.2. Microwave versus conventional thermal heating

The traditional heating depends on convection heat and conduction phenomena, so generally the reaction vessel temperature is higher than the bulk reaction mixture. Microwave radiation, therefore, raises the temperature of the whole volume simultaneously, since the reaction vessels are made out of transparent materials to microwaves, like borosilicate glass, quartz or Teflon. If the microwave cavity is well designed, the temperature will be uniform throughout the sample, because of the direct coupling of microwave energy with the molecules that are present in the reaction mixture [1].

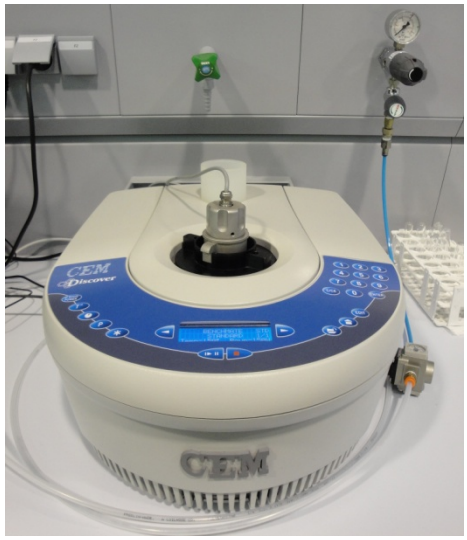

Figure 4.30 Microwave reactor

4.1.3. Lignin liquefaction

Liquefaction process is regarded as an efficient way to convert lignin into liquid polyols with high content of reactive hydroxyl groups. Liquid polyols have been used in polyurethane foam preparation [2] and as components of adhesives [3-5].

This process is usually carried out at high temperatures with the use of reagents and catalysts with sufficient reactivity towards biomass components. In most reported researches, liquefaction reagent such as phenol [6] and various glycols [7-9] are used in conjunction with strong acid as catalysts.

The liquefaction with organic solvents is usually carried out with conventional external heating systems such as water, oil, salt bath, fluidized sand bath, and electrical furnaces [10-13]. These heating systems are relatively slow and heat is not transfer efficiently due to the dependence on the conductivity. The use of microwave systems is emerging as an alternative heating mode allowing to achieve fast heating in the bulk material [14]. With an appropriate choice of reagents that absorb microwaves, a rapid heating throughout the entire reactor volume can be achieved. This generally has the effect of speeding up reactions compared to reactions using conventional heating. [15].

In this work a mixture of polyethyneglycol (PEG 400) (Figure 4.31 left) and glycerol (G) (Figure 4.31 right) with sulphuric acid (AS) as catalyst were used for lignin liquefaction. The molecular weight of the PEG was chosen based on a studied

done by Jin et al where PEG of different molecular weights (400, 600, and 1000) was used. They found out that the smaller the molecular weight of PEG, the more beneficial it was for the liquefaction under the same condition, and the liquefaction yield reached the highest of 97%. The hydroxyl number of liquefaction products was 410 mgKOH/g with PEG400, higher than with PEG600 and PEG1000 [16].

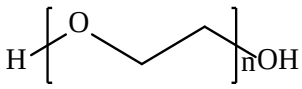

n=8, PEG400

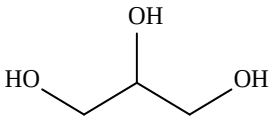

Glycerol

Figure 4.31 PEG400 structure (left) and glycerol structure (right)

Glycerol has three hydrophilic hydroxyl groups that are responsible for its solubility in water and its hygroscopic nature. The huge amount of glycerol as side product is produced from the transesterification of oil with methanol in the biodiesel production. Considering that glycerol is a commodity chemical widely used by pharmaceutical industry, the availability of glycerol has leaded to excessive supply and devaluation in the market price [17,18]. Therefore, the use of glycerol as secondary reagent in organosolv lignin liquefaction would open the door for a new market of glycerol.

4.2. Objective

In this work, lignin obtained from olive tree pruning by organosolv (ethanol/water 70:30, 180ºC, 90 min) process was subjected to liquefaction under microwave heating and

experimental conditions (time, temperature and catalyst concentration) were modified with the aim to obtain the highest reaction yields and hydroxyl number. Lignin extracted by organosolv process and the resulted polyols were characterized to assess the differences between them by Fourier transformed infrared spectroscopy (FTIR), thermogravimetric analysis (TGA), gel permeation chromatography (GPC), and another parameters such as the hydroxyl number (I_{OH}).

4.3. Material and methods

4.3.1. Olive tree pruning and lignin extraction process

Olive tree pruning (*Olea europea)* was kindly supplied by an independent producer and originated from an olive tree cultivated in Navarra belonging to the variety called Arróniz. It was locally collected and then dried at room temperature. The olive tree prunings were milled in a Retsch 2000 hammer mill to produce 4-6 cm chips free of small stones, dust and soil. Obtained wood chips were then characterized.

The raw material was characterized according to the standard methods detailed in the **Appendix I**. Moisture content (10.62 ± 3.47%) was determined after drying the sample at 105 ºC for 24 h (TAPPI T264 cm-97). Chemical composition, given on an oven dry weight basis, was the following: 1.4 ± 0.5% ash (TAPPI T211 om-93), 12.2 ± 0.5% ethanol-toluene extractives (TAPPI T204 cm-97), acid insoluble lignin 24.4 ± 2.3% (TAPPI T222 om-98)

holocellulose 51.8 ± 1.0%, α-cellulose 29.3 ± 0.2% and hemicelluloses 22.4 ± 1.3%.

Olive tree pruning was treated by the organosolv fractionation process. Organosolv treatment consisted in the fractionation of olive tree pruning with an ethanol/water mixture (70:30, v/v) with a solid/liquid ratio of 1:6, in a 4 L pressurized reactor (180 ºC, 90 min) under constant stirring. This reaction conditions were selected in the basis of previous experiences for ensuring high quality lignin. After the reaction time, the solid fraction was separated from the liquid by filtration and washed to remove residual liquor.

The solid fraction was recovered after the organosolv process and was characterized according to TAPPI standard. The characterization is summed up in Table 4.13. The main physic-chemical properties of obtained liquid fraction were determined according to standard methods detailed in **Appendix II**. pH 4.53 was measured with a digital CRISON GLP 22 pH-meter. Density (0.9 g/mL) was determined measuring the weight of the black liquor in a known volume previously weighed and moisture free. Total dissolved solids (7.39 ± 0.10%) were measured after keeping a weighed sample at 100 ºC until constant weight. Inorganic matter (0.04 ± 0.02%) was determined after combustion of the sample at 525 ºC (TAPPI T211 om-93). Organic matter (7.36 ± 0.11%) was defined as the difference between total dissolved solid and inorganic matter. Lignin content of liquor (2.91 ± 0.17%) was determined by weighting the mass of the precipitated lignin from the liquid fraction. Lignin was isolated from organosolv liquor by precipitation by adding two volumes of acidified water [19] after that the solid was centrifuged and oven dried at 50 ºC.

Table 4.13 Chemical composition (% in dry basis) of the solid fraction.

	Solid fraction
Ashes	1.17 ± 0.38
Humidity	1.46 ± 0.13
Extractives	3.89 ± 0.17
Lignin	21.58 ± 0.30
Cellulose	70.34 ± 0.35
Hemicelluloses	1.24 0.61

4.3.2. Liquefaction under microwave heating

In the liquefaction reaction PEG #400 and glycerol (80/20 w/w) were used as solvents and sulphuric acid 98% (AS) as catalyst with different temperatures, times and catalyst concentrations. The liquefaction reactions were carried out in CEM Microwave Discover System Model (Figure 4.30). The microwave system was a temperature-controlled instrument with an internal temperature sensor.

Microwave power was applied in order to heat the reaction mixture until reaching the desired temperature, residence time, and cooling time was defined using the microwave system software. There was constant stirring during the time of the microwave activation. A typical workout procedure for the experiments was as follows: organosolv lignin, with a solvent ratio of 15/85 w/w which contained a percentage of AS as catalyst; were loaded into the reaction vessel. After the liquefaction time, the pressurized vessel was immersed in cold water and could safely be opened after 15 min.

After cooling the liquefaction product was diluted with dioxane/water (80/20 v/v) and filtered to remove remaining solids which were dried to constant mass. The liquefaction yield (η) was calculated as the weight percent based on the starting sample material by the equation 1:

$$\eta = \left[1 - \frac{M}{M_0}\right] \times 100$$

(Eq.1)

where M_0 is the mass of initial organosolv lignin

M is the mass of the residue insoluble in dioxane/water obtained after the liquefaction process.

4.3.3. Experimental design

The applied model uses a series of points (experiments) around central one and several additional points to estimate the first and second order interaction terms of a polynomial. The design meets the general requirement that it allowed all parameters in the mathematical model to be estimated with a relatively small number of experiments [20].

Experimental data were fitted to the following second order polynomial model:

$$Y = a_0 + \sum_{i=1}^{n} b_i \, X_{ni} + \sum_{i=1}^{n} c_i \, X_{ni}^2 + \sum_{i=1;j=1}^{n} d_{ij} \, X_{ni} \, X_{nj} \qquad (i < j)$$

(Eq.2)

where

$$X_n = 2\,\frac{X - \bar{X}}{X_{max} - X_{min}}$$

(Eq.3)

Y is the dependent variables (liquefaction yield and OH number), X_n are the independent variables (X_T temperature, X_t time and X_C catalyst concentration) normalized from -1 to +1 using Eq.3 and a_0, b_i, c_i, and d_{ij} are constants. X is the experimental value of the variable concerned; $\bar{X}$ is the middle point of the variation range value for the variable in question; and X_{max} and X_{min} are the maximum and minimum values of such a variable.

The X_n were normalized between -1 and +1 using Eq.3 in order to facilitate direct comparison of the coefficients and visualization of the effects of the individual independent variables on the response variable.

Experimental results were subjected to regression analysis using the STATGRAPHIC software. The normalized values of independent variables, for the 27 experiments of the experimental design plus 2 repetitions of the central experiment to measure the method error, are shown in Table 4.14.

4.3.4. Hydroxyl number

The hydroxyl numbers [21] of the liquefied organosolv lignin were determined as follows: 0.5 to 1.0 g of sample was dissolved in 25 mL of a phthalation reagent and heated at 115 ºC, for 1h under reflux. This was followed by an addition of 50 mL of pyridine through the condenser. The mixture was backtitrated with 0.5 M sodium hydroxide solution. The

indicator was 1 % phenolphthalein solution in pyridine. The phtalation reagent consisted of 115 g of phthalic anhydride dissolved in 700 mL of pyridine.

The hydroxyl number, defined as mg KOH/g of sample, was calculated as follows:

$$\text{Hydroxyl number} = \frac{(B - A) \cdot M \cdot 56.1}{w} + \text{acid number} \quad \text{(Eq.4)}$$

Here, A is the volume of the 0.5 M sodium hydroxide solution required for the titration of sample (mL). B is the volume of the sodium hydroxide solution required for the titration of the blank solution (mL). M is the molarity of the sodium hydroxide solution and w is the amount of the sample (g) to be analysed.

If the sample is acidic, the acid uses the phthalation reagent during the analysis and the hydroxyl number must be corrected accordingly. The acid number was determined as follows. 0.4 g of sample was weight into a 400 mL Erlenmeyer flask and dissolved in 50 mL of the solvent mixture. The solvent mixture consisted of dioxane and water (4:1 v/v). 0.5 mL of phenolphathalein indicator solution (1 % in ethanol), was added and titrated with 0.1M KOH solution in ethanol, to the equivalent point. The acid number (mg KOH/g of sample) was calculated using the equation 5:

$$\text{Acid number} = \frac{(C - B) \cdot M \cdot 56.1}{w} \quad \text{(Eq. 5)}$$

Here, C is the titration volume of the potassium hydroxide solution (ml). B is the titration volume of blank solution (mL). M is the molarity of the potassium hydroxide solution and w is the amount of the sample (g) being analysed.

Lignin and the optimized polyols were characterized by FTIR, TGA and GPC that are summed up in the Appendix II.

4.4. Analysis of the polyols

4.4.1. Olive tree pruning lignin characterization

Organosolv olive tree pruning lignin was characterized according to standard methods (**Appendix II**) and presented the following composition: acid insoluble lignin 80.32 ± 2.61% acid soluble lignin, 3.13 ± 0.16%, total dissolved sugars 0.69 ± 0.03% with 0.23 ± 0.03% and xylose 0.47 ± 0.01%, ash content 2.61%.

4.4.2. Liquefaction experimental design

The experimental conditions that were applied to the organosolv lignin are shown in Table 4.14.

Table 4.14 Experimental conditions applied to the organosolv lignin

Experiment	X_T[a]	X_t[b]	X_C[c]	Experiment	X_T[a]	X_t[c]	X_C[c]
1	-1	-1	-1	16	+1	+1	+1
2	+1	0	+1	17	-1	-1	0
3	0	-1	0	18	+1	+1	0
4	-1	+1	-1	19	-1	-1	+1
5	-1	+1	0	20	+1	0	0
6	0	0	+1	21	0	+1	-1
7	+1	0	-1	22	+1	-1	+1
8	+1	-1	0	23	-1	0	+1
9	+1	-1	-1	24	0	-1	-1
10	0	-1	+1	25	+1	+1	-1
11	-1	0	0	26	0	+1	0
12	0	0	-1	27	0	0	0
13	-1	0	-1	28	0	0	0
14	-1	+1	+1	29	0	0	0
15	0	+1	+1				

[a]X_T: normalized temperature

[b]X_t: normalized time

[c]X_C: normalized concentration of catalyst

Ranges: temperature 130-155-180 °C (normalized -1; 0; +1); time 5-10-15 min (normalized -1; 0; +1); concentration of catalyst 1-2-3% (normalized -1; 0; +1).

Two dependant variables were considered to follow the liquefaction process, liquefaction yield (%) and OH number (I_{OH}). Three independent variables were varied during the liquefaction process under microwave heating: temperature (*T*), time (*t*) and concentration of sulphuric acid as catalyst (*C*). Temperature and catalyst concentration was established empirically on the bases of previous studies of liquefaction,

and time was established given the fact that microwave chemistry is claimed to need shorter times than conventional reactions. All the experiments were carried out with a solvent ratio of 15/85 w/v in base of previous liquefaction works [13, 16]. The results of 29 experiments are shown in Table 4.15.

Table 4.15 Yield and the Hydroxyl Number of the experiments of the experimental design

Experiment	Yield (%)	I_{OH} (mg KOH/g)	Experiment	Yield (%)	I_{OH} (mg KOH/g)
	96.7	264.2	16	98.3	380.4
2	97.1	443.8	17	96.8	749.6
3	97.2	351.3	18	96.8	757.5
4	98.0	415.9	19	96.7	700.6
5	96.0	432.2	20	96.6	273.4
6	99.7	667.2	21	97.1	318.3
7	99.9	464.4	22	98.8	737.4
8	99.9	278.6	23	97.4	493.5
9	97.3	746.7	24	99.1	811.8
10	99.3	261.3	25	97.8	502.8
11	98.8	263.7	26	97.3	457.9
12	97.2	441.9	27	97.6	610.8
13	96.9	507.5	28	96.7	612.5
14	94.9	314.8	29	95.6	821.0
15	96.8	175.6			

Applying the software STATGRAPHICS Centurion to the data in the Table 4.15, the following equations that predict the behaviour of the dependant variables were obtained:

$$I_{OH} = 411.158 - 16.6056X_C + 0.462107X_T - 0.478329X_t + 0.410008X_C^2$$

$$- 0.637006X_T^2 \quad - 0.321671X_t^2 + 0.15X_CX_T - 0.38333X_CX_t + 0.0151735X_TX_t \quad \text{(Eq.6)}$$

$$Yield = 97.9513 - 0.0555556X_C + 0.462107X_T - 0.478329X_t + 0.410008X_C^2 - 0.637006X_T^2 - 0.321671X_t^2 + 0.15X_CX_T - 0.383333X_CX_t + 0.0151735X_TX_t \quad \text{(Eq.7)}$$

Table shows the statistical values (Snedecor's F, $R^2$and R^2-adjusted) for the different terms in the equation (6) and (7).

Table 4.16 Snedecor's F Value for the obtained equation in the experimental design. R^2 and R^2-adjusted values obtained from the adjusted model eqs. (6) and (7)

Equation	**Snedecor's F**	**R^2**	**R^2-adjusted**
I_{OH}	0.43	18.59	-
Yield	1.02	35.15	0.82

According to the Table 4.16 the dependant variable of the hydroxyl number was not taken into account for the experimental design for presenting bad regression values; it was adequate for the OH number to be between 300 and 800 mgKOH/g in view to future applications.

Table 4. 17 t Student value for each of the eq. (6) and (7) values

Equation	Variables	Student t
	X_C	-0.34
	X_T	0.85
	X_t	-1.41
I_{OH}	X_c^2	0.05
	X_T^2	0.87
	X_t^2	0.28
	X_C*X_T	-0.66
	X_T*X_t	0.12
	X_C*X_t	-0.34
	X_C	-0.19
	X_T	1.51
	X_t	-1.61
Yield	X_c^2	0.79
	X_T^2	-1.26
	X_t^2	-0.63
	X_C*X_T	0.42
	X_C*X_t	-1.07
	X_T*X_t	0.04

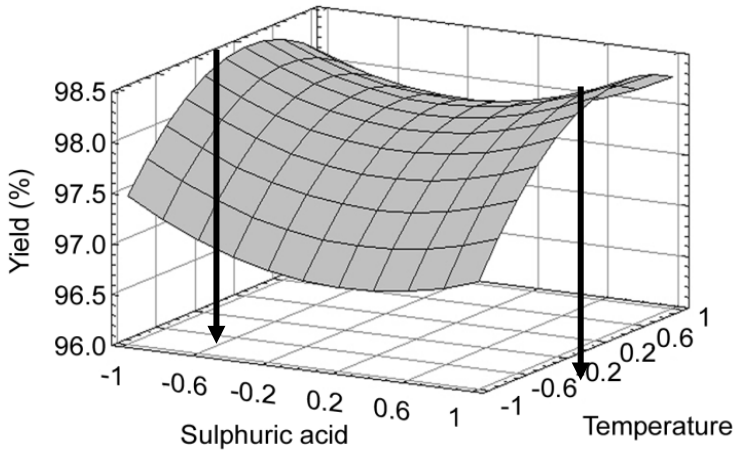

Figure 4.32 Variation of the yield (%) with the normalized catalyst concentration and normalized temperature

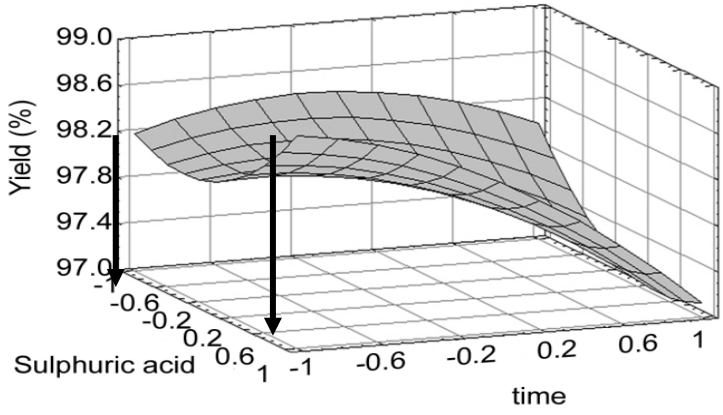

Figure 4.33 Variation of the yield (%) with the normalized catalyst concentration and normalized time.

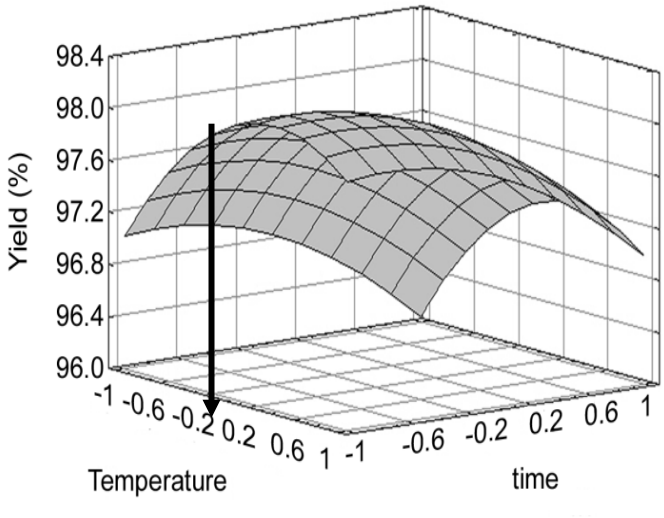

Figure 4.34 Variation of the yield (%) with the normalized temperature and time

From the equation 7 that predict the behaviour of the yield (%) with the time, temperature and catalyst concentration Figure 4.32, Figure 4.33 and Figure 4.34 were obtained. In these figures the optimal conditions for the polyol production are shown. In Figure 4.32 it could be said that the maximum yield is obtained when minimum and maximum concentration of catalyst was applied (normalized -1 and 1). In the case of the temperature the yield rose to the maximum when the temperature was 155 ºC (normalized 0). In Figure 4.33 it could be observed that the yield rose when the time went towards the minimum 5 min (normalized -1). The reduction of reaction time is an important factor while using the microwave technology. The catalyst concentration had the same behaviour as in Figure 4.32 reaching its maximum with the minimum and maximum values (normalized -1 and1). Figure 4.34 results were in concordance with Figure 4.32 and Figure 4.33 where the yield reached its maximum when the temperature was 155 ºC (normalized 0) and the time was 10 min (normalized 0).

In conclusion, for the highest yield two optimal conditions were obtained. The first one with temperature of 155 ºC (normalized 0), time of 5 minutes (normalized -1) and catalyst concentration of 1% (normalized -1) (polyol 10). The second with temperature of 155 ºC (normalized 0), time of 5 minutes (normalized -1) and catalyst concentration of 3% (normalized 1) (polyol 24) (Figure 4.35). Bearing in mind that for future application the hydroxyl number had to be between 300 and 800 mgKOH/g polyol 24 was selected presenting the highest liquefaction yield and hydroxyl number. (99.1%; 811.8 mgKOH/g).

Figure 4.35 Optimal condition polyols. Polyol 10 (left) and polyol 24 (right).

4.4.3. Fourier transformed infrared spectroscopy (FTIR)

FTIR was used to study the structural changes on the lignin before and after the liquefaction reaction. Figure 4.36 showed the spectra of organosolv lignin and the optimized products of the liquefaction.

3390 cm^{-1} band was assigned to the OH stretching. This band increased remarkably in the spectra of polyol due to the presence of PEG and glycerol. The band 2929 and 2830 cm^{-1} were assigned to C-H stretching of the methyl and methylene groups and in the polyol spectra they were sharper because of the structure of PEG and glycerol and they even overlapped [16].

In lignin spectra there were some peaks that did not appear in the polyol spectra the band at 1590 and 1510 cm^{-1} attributed to the C=C stretching of aromatic skeletal vibration and the 1419 cm^{-1} assigned to aromatic skeletal vibration, maybe due to the degradation of lignin. The band 1545 cm^{-1} was present in all spectra and was attributed to the anti symmetric deformation of C-H. In the polyol spectra the bands around 1600-1424cm^{-1} associated in many cases with the linkage C-C of the aromatic skeleton decreased the intensity because in the first stage of the liquefaction lignin was degraded to lower molecular weight structures [16, 22] The signal at 1330 cm^{-1} was assigned the syringyl (S) ring breathing and C-O stretching and the band 1219 cm^{-1} was attributed to the guaiacyl (G) ring breathing with C-O stretching. The peak at 1113 $cm^{-1}$was assigned to C-H in plane deformation in syringyl (S). The bands at 1110 cm^{-1} and 940 cm^{-1} were due to the C-O-C stretching vibration. The peak at 840 $cm^{-1}$was assigned to the β-glucosidic linkage.

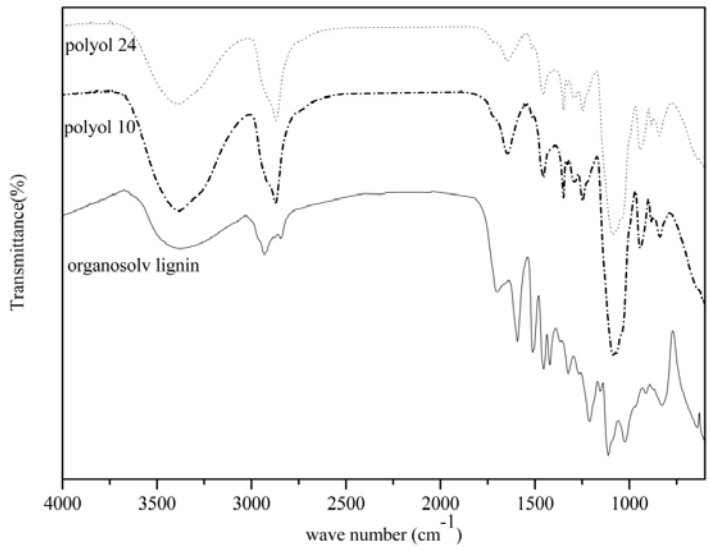

Figure 4.36 FTIR spectra of polyol 24, polyol 10 and organosolv lignin.

4.4.4. Gel permeation chromatography (GPC)

Table 4.18 Average molecular weight (M_w), average number molecular weight (M_n) and polydispersity (M_w/M_n) of organosolv lignin (OL) and optimal polyols.

	OL	**Polyol 10**	**Polyol 24**
M_w	4209	2117	1812
M_n	1116	598	593
M_w/M_n	3.77	3.54	3.06

Average molecular weight (M_w), average number molecular weight (M_n) and polydispersity (M_w/M_n) results of the analyzed organosolv lignin and the optimal polyols (polyol 10, 24) are shown in Table 4.18 and Figure 4.37.

Comparing the molecular weight of the starting material and the product it could be seen that during the liquefaction lignin was degraded to lower molecular weight fractions [23]. Also, the low variation in the polydispersity between the lignin and polyols showed the presence of high and low molecular weight fractions. The molecular weight of the two analyzed polyols was similar as the applied conditions during the liquefaction process were nearly the same. Furthermore, it may be due to higher catalyst concentration in the polyol 24 that enhanced the decomposition of the lignin resulting in lower molecular weight fractions.

In Figure 4.37 it could be observed the molecular weight distribution. Lignin presented a wide peak which indicated high heterogeneity and therefore a high polydispersity. In the case of the polyols the distribution area was wide so was the polydispersity. The main shoulder was identified at higher retention times and was quite narrow indicating lower molecular weight [24].

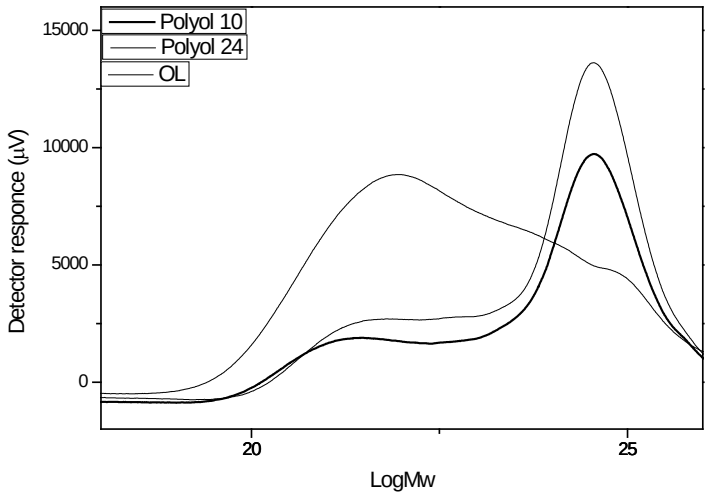

Figure 4.37 Molecular weight distributions of organosolv lignin and optimal polyols

4.4.5. Thermogravimetric analysis (TGA)

Organosolv lignin and the optimized polyol were analyzed by thermo-gravimetric analysis and the obtained curves are shown in Figure 4.38.

Organosolv lignin showed a low weight loss around 70 ºC that was associated with the moisture presented in the lignin sample. The high quality of the lignin could be seen in the low contamination produced by hemicelluloses presented between 185 and 260 ºC. This results was in agreement with the composition analysis were the lignin showed a sugar content of 0.69 ± 0.03%. Finally, lignin degradation took place slowly in a wide range of temperatures with a maximumn mass los rate between 300 and 400 ºC, this fact was associated with the complex structure of lignin with phenolic hydroxyl, carbonyl groups, and benzylic hydroxyl, which are connected by straight links [25].

Secondly, according to Briones et al., [26], DTG analysis of pure PEG:Glycerol presented a glycerol decomposition from 153 to 267 ºC and PEG decomposition from 267 and 392 ºC. DTG curves of optimized polyols presented similar patterns with peaks ranging from 155 to 287 ºC and from 287 to 489 ºC (polyol 24); from 154 to 310 ºC and from 310 to 464 ºC (polyol 10). So, it could be assubed that the peaks presented in the polyols curves are due to the presence of glycerol and PEG in the final product. These results confirm the combination of the lignin and the liquefaction solvents. However the introduction of the chemical reactant retarded the degradation temperature of the liquefaction product.

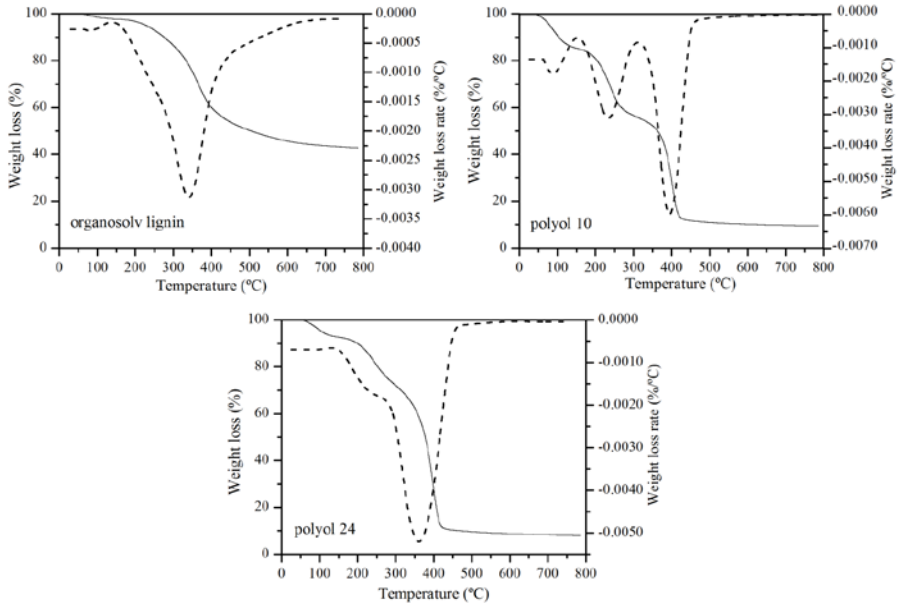

Figure 4.38 TGA and DTG curves of organosolv lignin and optimized polyol 10 and 24.

4.5. Conclusion

In this work a process was developed for the revalorization of the olive tree pruning, a common agricultural residue from Spain. Lignin was extracted from this residue by an organosolv process achieving high purity lignin.

An experimental design was produce varying temperature, time and catalyst concentration for the production of liquid polyols ensuring high yield and high hydroxyl number. As the statistic analysis of the hydroxyl number equation gave bad regression values that equation was not taken into account. For the experimental design based on literature the hydroxyl number had to be between 300-800 mgKOH/g. Applying these limitations two optimal conditions were

obtained (polyol 10 and polyol 24), being the polyol 24 the one with highest hydroxyl number and yield.

The FTIR analysis of the starting material and the products showed some differences on the spectra mainly due to the presence of PEG and G on the resulted polyols and also to the degradation of lignin structure.

The GPC results showed that both lignin and polyols presented a wide molecular weight distribution area and therefore high polydispersity with low and high molecular weight fractions. The molecular weight of the polyols was lower due to the degradation of the lignin during the liquefaction reaction and the insertion of PEG and G.

The TGA results showed the PEG and G presence in the polyols as they retarded their thermal degradation.

4.6. References

1. C.O. Kappe, D. Dallinger, S.S Murphree. *Practical microwave synthesis for organic chemists*. Wiley-VCH Verlag GmbH &Co. KGaA, Weinhem, (2009), pp.11-20.
2. Y. Wei, F. Cheng, H. Li, J. Yu. Synthesis and properties of polyurethane resins based on liquefied wood. *Journal of applied polymer science*, (2004), *92*(1), 351-356.
3. S.H. Imam, S.H. Gordon, L. Mao, L. Chen. Environmentally friendly wood adhesive from a renewable plant polymer: characteristics and optimization. *Polymer Degradation and Stability*, (2001) *73*(3), 529-533.
4. S.I. Tohmura, G.Y. Li, T.F. Qin. Preparation and characterization of wood polyalcohol-based isocyanate adhesives. *Journal of applied polymer science*, (2005), *98*(2), 791-795.
5. M. Kunaver, S. Medved, N. Čuk, E. Jasiukaitytė, I. Poljanšek, T. Strnad. Application of liquefied wood as a new particle board adhesive system. *Bioresource Technology*, (2010) *101*(4), 1361-1368.
6. D. Maldas, N. Shiraishi. Liquefaction of biomass in the presence of phenol and H_2O using alkalies and salts as the catalyst. *Biomass and Bioenergy*, (1997) *12* (4), 273-279.
7. M. Kobayashi, T. Asano, M. Kajiyama, B. Tomita. Analysis on residue formation during wood liquefaction with polyhydric alcohol. *Journal of wood science*, (2004) *50*(5), 407-414.
8. A. Kržan, M. Kunaver, V. Tišler. Wood liquefaction using dibasic organic acids and glycols. *Acta Chim. Slov*, (2005) 52, 253-258.
9. T. Zhang, Y. Zhou, D. Liu, L. Petrus. Qualitative analysis of products formed during the acid catalyzed

liquefaction of bagasse in ethylene glycol. *Bioresource technology*, (2007) 98(7), 1454-1459.

10. S.H. Lee, M. Yoshioka, N. Shiraishi. Liquefaction and product identification of corn bran (CB) in phenol. Journal of applied polymer science, (2000) 78(2), 311-318.
11. Y. Kurimoto, M. Takeda, A. Koizumi, S. Yamauchi, S. Doi, Y. Tamura. Mechanical properties of polyurethane films prepared from liquefied wood with polymeric MDI. *Bioresource technology*, (2000), 74(2), 151-157.
12. J. Ge, W. Zhong, Z. Guo, W. Li, K. Sakai. Biodegradable polyurethane materials from bark and starch. I. Highly resilient foams. *Journal of Applied Polymer Science*, (2000), 77(12), 2575-2580.
13. M.H. El-barbary, N. Shukry. Polyhydric alcohol liquefaction of some lignocellulosic agricultural residues. *Industrial Crops and Products*, (2008), 27(1), 33-38.
14. Z. Zheng, H. Pan, Y. Huang, Y. Chung, X. Zhang, H. Feng. Rapid liquefaction of wood in polyhydric alcohols under microwave heating and its liquefied products for preparation of rigid polyurethane foam. *Open Materials Science Journal*, (2011), 5, 1-8.
15. A. Kržan, M. Kunaver. Microwave heating in wood liquefaction. *Journal of applied polymer science*, (2006), 101(2), 1051-1056.
16. Y. Jin, X. Ruan, X. Cheng, Q. Lü. Liquefaction of lignin by polyethyleneglycol and glycerol. *Bioresource technology*, (2011), 102(3), 3581-3583.
17. T. Werpy, G. Petersen. Top value added chemicals from biomass. Volume 1-Results of screening for potential candidates from sugars and synthesis gas. U.S. Department of Energy; Pacific Northwest National Laboratory (PNNL) and National Renewable Energy Laboratory (NREL); Golden, CO Washington DC, (2004).

18. R. Briones, L. Serrano, R. Llano-Ponte, J. Labidi. Polyols obtained from solvolysis liquefaction of biodiesel production solid residues. *Chemical Engineering Journal,* (2011), 175, 169-175.
19. M.M. Ibrahim, S.B. Chuah, W.W. Rosli. Characterization of lignin precipitated from the soda black liquor of oil palm empty fruit bunch fibers by various mineral acids. *Asean journal on science and technology for development.*, (2004), *21*, 57-68.
20. D.C. Montgomery. Design and analysis of experiments; Iberoamericana, Eds.; Mexico. (1991), pp.303-313.
21. American Society for Testing Materials (ASTM). Standard Test Method for Testing Polyurethane Raw Materials: Determination of Hydroxyl Numbers of Polyos; *ASTM, Pennsylvania, D4274, (2005).*
22. A. García, A. Toledano, M.Á. Andrés, J. Labidi. Study of the antioxidant capacity of Miscanthus sinensis lignins. *Process Biochemistry,* (2010), 45(6), 935-940.
23. W. Xiao, L. Han, Y. Zhao. Comparative study of conventional and microwave-assisted liquefaction of corn stover in ethylene glycol. *Industrial Crops and Products*, (2011), *34*(3), 1602-1606.
24. X. Erdocia, R. Prado, M.A. Corcuera, J. Labidi. Effect of different organosolv treatments on the structure and properties of olive tree pruning lignin, J. Ind. Eng. Chem. (2014), 20, 1103-1108
25. J.C. Domínguez, M. Oliet, M.V. Alonso, M.A. Gilarranz, F. Rodríguez. Thermal stability and pyrolysis kinetics of organosolv lignins obtained from Eucalyptus globulus. *Industrial crops and products,* (2008), 27(2), 150-156.
26. R. Briones, L. Serrano, J. Labidi. Valorization of some lignocellulosic agro-industrial residues to obtain biopolyols. *Journal of Chemical Technology and Biotechnology,* (2012), 87(2), 244-249.

Chapter 5

Aromatic acids from lignin monomers

5.1 Introduction

5.1.1. Commodities from lignin

Due to its chemical structure, lignin is a very promising source of renewable products and chemicals. One of the most important aromatic monomer derived from lignin is vanillin. Vanillin (4-hydroxy-3-methoxybenzaldehyde) is widely used as flavoring and fragrance ingredient in food, cosmetic and as intermediate for the synthesis of several second generation fine chemicals (as veratraldehyde, photocatechualdehyde, and respective acids) and pharmaceuticals (as papaverine, levodopa and cyclovalone) [1].

Today there are two commercial types of vanillin: synthetic vanillin, derived from petrochemical guaiacol and glyoxylic acid or lignosulfonates and vanilla extract obtained from the cured beans, or pods, of tropical *Vanilla* orchids. The raw material costs turned natural vanillin more expensive than the synthetic counterpart. Hence, synthetic vanillin became competitive and widely used. Nowadays the synthesis of vanillin from petrochemical guaiacol accounts for the 85% of the word supply, with the remaining 15% being produced from lignin [2].

Another lignin derived compound is catechol, which is used in a variety of applications. It is used as reagent for photography, in rubber and plastic production, to produce food additive agents, hair dyes, antioxidants, and in the pharmaceutical industry [3, 4].

Other important lignin derived compounds are aromatic acids. For example benzoic acid, benzyl alcohol and

benzaldehyde are all important fine chemicals. They are widely used in the field of pharmaceutical, perfumery, dyestuffs and agrochemicals and so on [5]. Salicylic acid (SA), 2-hydroxy benzoic acid, is a phenolic compound named after the Latin name of the willow tree (*Salix*). Historically, willow bark has been used against fever and pain. A major breakthrough occurred in 1899, when the chemist Felix Hoffman, working for the Bayer company in Germany, synthetically made a derivate of SA, acetylsalicylic acid, also known as aspirin, that has become the most used medical drug in the World [6].

As it could be seen in Figure 5.39 all the above mentioned products are “value-added” chemicals derived from lignin. Vanillin to set an example has one of the highest market prices compare to the rest of the products.

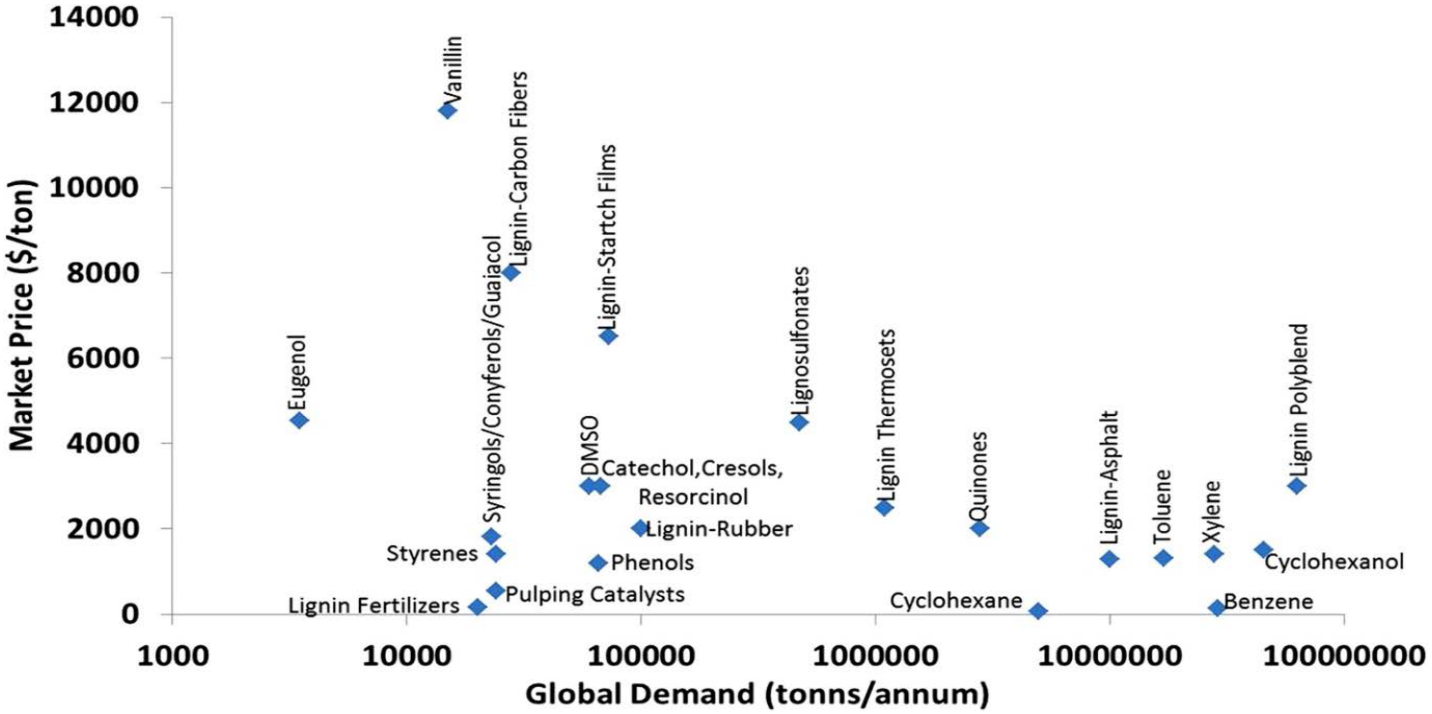

Figure 5.39 Market price vs. demand for lignin derived products

5.1.2 Lignin to monomers

Several studies have been done to convert lignin to value added products. One of the most important routes to achieve this goal is the thermochemical methods of lignin depolymerisation, which include the thermal treatment of lignin in the presence, or absence of solvent, chemical additives and catalysts.

Fragmentation reactions of lignin can be principally divided into, cracking or hydrolysis reactions, reduction reactions and oxidation reactions [8].

For lignin reductions, typical reactions involve removal of extensive functionality of lignin subunits to form simpler monomeric compounds such as phenols, benzene, toluene, or xylene. Lignin reduction can be achieved by hydrogenation or by hydrogen donating solvents such as tetralin, formic acid or 2-propanol [9]. Usually applied temperatures are between 300 and 600 °C. The product mixture consists of volatile hydrocarbons together with phenol and methyl-, ethyl-, and propyl-substituted phenol catechols and guaiacols. Guaiacols are formed at the lowest temperatures together with small amounts of aldehydes. At higher temperatures (600 °C) only the more stable phenols remain, the amount of char increases, and also benzene, toluene, and xylene emerge [10].

Whereas reductive reactions tend to disrupt and remove functionality in lignin to produce simpler phenols, oxidation reactions tend to form more complex aromatic compounds with additional functionality. Many of these chemicals

whether serve as platform chemicals used for subsequent organic synthesis, or they serve as target fine chemicals themselves.

Heterogeneous oxidative catalysts have played an important role in pulp and paper industry as a means to remove lignin and other compounds from wood pulps to increase the quality of the final paper product. The first examples include photocatalytic oxidation catalysts, which were designed to remove lignin from paper industry wastewater streams. The most common catalysts involve TiO_2 or supported precious metals, such as Pt/TiO_2 which were found to efficiently degrade lignin using ultraviolet light. The use of UV light was necessary to displace the valence-band electrons in the TiO_2, which was necessary to initiate the oxidation.

Oxidation of lignin by homogeneous catalysts represents one of the most promising approaches toward the production of fine chemicals from lignin and lignin pulp streams. Several homogeneous catalysts that are capable of performing selective oxidation of lignin have been reported in literature. Homogeneous catalysts offer several advantageous properties that make them particularly suitable for lignin oxidation, especially the ability to use a wide range of ligands, electronic and steric properties of which drastically influence the activity, stability, and solubility of the catalyst [8].

The second most important part of a homogeneous catalyst is the ligand, which steers fundamentally the selectivity of the reaction. Ligand could be an ion or a molecule or a radical that is within a bonding distance from the metal [10]. Finding the right ligand for a certain problem is not easy and even today often trial-and-error principle is applied.

However, there are some important criteria which should be observed:

The first decision is whether monodentate or chelating ligands are used. *Monodentate ligands* coordinate to transition metal through a single donor atom (e.g., P, O, N or C). Such ligands are relative flexible: they can rotate and, depending on their donor properties, they also can dissociate. On the contrary, *chelating ligands* coordinate through two, three, or more donor atoms to the metal. Often they are very strongly bound and have only limited freedom to move.

Some important properties to take into account while choosing a ligand are their basicity, steric demand and asymmetry [12].

In the last two decades, the key to successful developments of homogeneous catalysts has undoubtedly been the exploitation of the effects that ligands exert on the properties of metal complexes: by tuning electronic and steric properties of a catalytically active complex, selectivity's and rates can be dramatically altered. There are many examples for each metal in the periodic table which show how one and the same metal can catalyze totally different reactions, depending on the surrounding ligands. Ligands that have been utilized to induce changes in the outcome of catalytic reactions include phosphine, amines and imines, alkoxides, and cyclopentadienyl anions [13].

One of the most studied cracking treatments of lignin is pyrolysis. Pyrolysis represents the thermal treatment of biomass or lignin in absence of oxygen, with or without any catalyst [14]. The major pyrolysis products of lignin can be divided into gaseous mixture (gaseous hydrocarbons, carbon monoxide and carbon dioxide), volatile liquids (water, methanol, acetone, and acetaldehyde), monolignols,

monophenols (phenol, guaiacol, syringol, and catechol), and other polysubstituted phenols [10]. Pyrolysis of lignin is highly complex and is affected by several factors, such as its feedstock type, heating rate, reaction temperature and additives.

Hydrolysis (often also referred to as solvolysis) is the process where water is used to break down lignin. Hydrolysis process of lignin has many advantages as it is performed at lower temperatures than all other methods studied. The employed reactives are cheap and favors higher yields of liquid including monomeric phenols. In lignin hydrolysis to enhance the production of monomeric phenols basic compounds, such hydroxides are used as catalyst [15, 16, 17].

Alkaline hydrolysis (or base-catalyzed depolymerization BCD) is more applicable and yields a broad mixture of monomers, amongst others, catechol, syringol, guaiacol and vanillin. The reported yields of phenolic products in mixture, however, do usually not exceed 10%.

Hydrolysis in supercritical water has been reported as an alternative approach for lignin fragmentation. Supercritical water offers several advantages, such as the occurrence of oxidation and hydrolysis reactions without a catalyst, its thermal stability as well as the miscibility with gases, hydrocarbons and aromatic substances. Reactions with model compounds (guaiacol and catechol) have shown the ability to produce phenol under supercritical conditions. Gasification of lignin into carbon dioxide and hydrogen with suppression of char formation was also reported under supercritical conditions [18].

5.2 Formation of aromatic acids via Pd catalysed alkoxy carbonylation

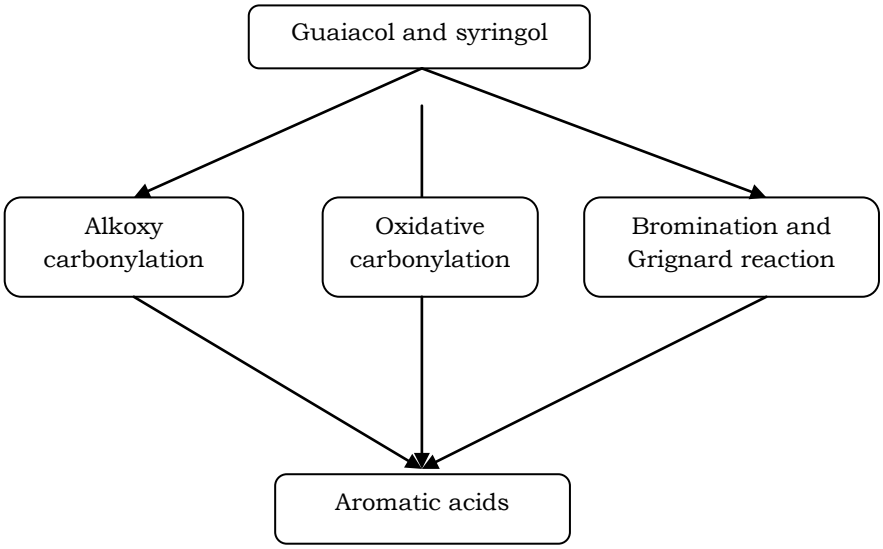

Scheme 5.1 General scheme of the three main pathways towards aromatic acids.

In this chapter carbonylation chemistry was used for formation of methoxy substituted phenols to corresponding acids. Aromatic hydroxyl group will have to be activated via mesylation or tosylation. Metal catalyzed carbonylation reactions are well known and have been reviewed extensively [19, 20, 21]. Commonly, palladium (Pd) is used as catalytically active transition metal and a number of ligands have been identified to form active Pd complexes. In this study palladium sources of choice was the palladium (II) acetate ($Pd(OAc)_2$) and tris(dibenzylideneacetone) dipalladium ($Pd_2(dba)_3$). Regarding the choice of ligands, the influence of the ligand on the Pd-CO interaction is crucial. CO is a strong π-acceptor; hence, it lowers the electron density at the metal centre slowing down the oxidative addition step. Ligands with strong σ-donor properties increase the electron density at palladium but strengthen

the Pd-CO bond at the same time. In order to balance the rate of the oxidative addition and the ability of CO to insert ligands with strong σ-donor properties as well as bulkiness are required. An additional challenge is the sterically hindered carbonylation position in the substrate in close proximity to electron donating methoxy groups.

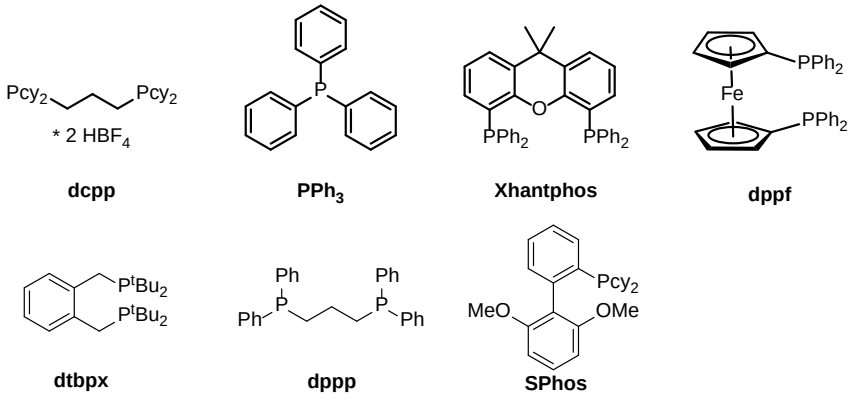

Figure 5.40 Carbonylation ligands

Figure 5.40 depicts lead structures of promising ligands, chosen to be tested in a screening within this chapter. The first alkoxycarbonylation of tosylates was reported in 1998 by Sugi et al. utilizing $PdCl_2$ with the bidentate phosphine ligand dcpp [22]. Later on, Buchwald et al. presented a protocol starting general reaction conditions 80-100 °C, 2 equiv. K_2CO_3, atmospheric CO pressure and molecular sieves [23]. Mesylates are more atom economic due to their lower molecular weight. Additionally, a broader substrate scope was reported. Again, substrates as challenging as the lignin model substrates guaiacol and syringol, were not subjected to the protocol. The Buchwald type biaryl monophosohine ligands (eg. SPhos) are known to be excellent ligands for Pd-catalysed coupling reactions [23]. Due to their electronic and steric properties-electronic rich and bulky-it is expected that these ligands will also show activity in the carbonylation of the lignin model compounds.

Ligands dppf and dtbpx are known to be active ligands for carbonylation reaction with more challenging arylchlorides. Therefore, they are also suitable candidates for the screen. Finally, the monodentate phosphine ligand PPh_3 will be included to put the screening results in a context. Apart from Pd precursor and ligands, the influence of a base will be investigated regarding its necessity and type (eg. K_2CO_3, NaOAc, NR_3, DABCO).

In general, alkoxycarbonylation of mesylated and tosylated arenes proceed by the following mechanism (Scheme 5.2) (1) involves the oxidative addition and (2) CO insertion in the Pd-arene bond to form acyl species, which reacts with the nucleophile. The reductive elimination (3) releases the product. Regeneration of the Pd(0) (4) closes the catalytic cycle.

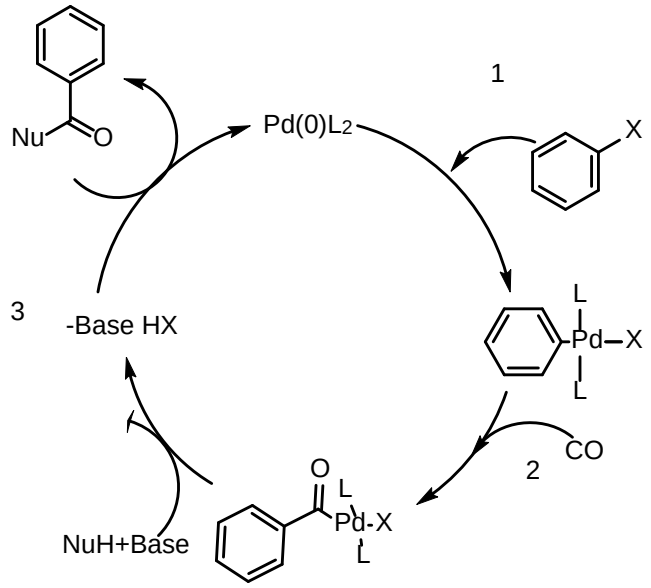

Scheme 5.2 Alkoxy carbonylation mechanism for Ms and Ts arenes

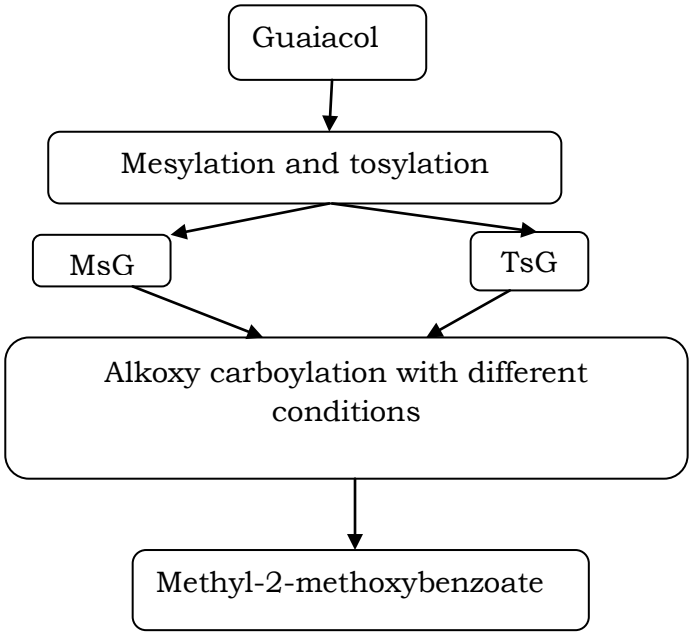

Scheme 5.3. Process scheme

5.2.1. Mesylation and tosylation of the starting material

Mesylation of guaiacol:

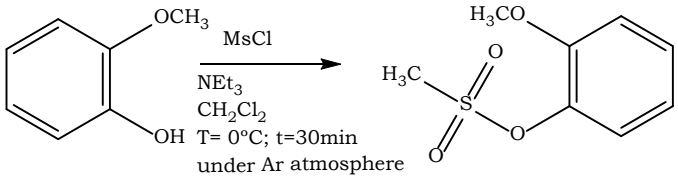

Figure5.41 Guaiacol mesylation

Under argon atmosphere, 12 mL methanesulfonyl choride were added to a neat liquid solution of 10 g of guaiacol and 17 mL of triethylamine in 50 mL of dichoromethane at 0°C (see Figure5.41). After the reaction was completed the product was extracted first with dichloromethane (CH_2Cl_2) and then washed with brine and water and dried over with sodium sulphate (Na_2SO_4). The solvent was rotavaporated to eliminate any trace of solvent from the product. The reaction was done following literature procedure [24].The product

was distilled by a kugelrohr to eliminate impurities and the product was characterized by ^{1}H NMR and ^{13}C NMR. Data for ^{1}H are reported as follows: chemical shift (δ, ppm), multiplicity s(singlet), d(doublet), t(triplet), q(quartet) and m(multiplet). Data for ^{13}C are reported in terms of chemical shift (δ, ppm).

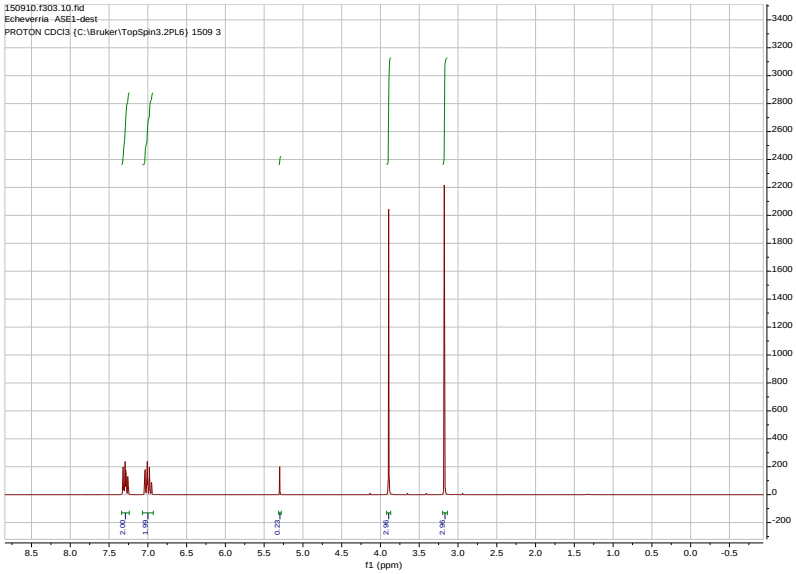

Figure5. 42 ^{1}H NMR of the mesylated guaiacol

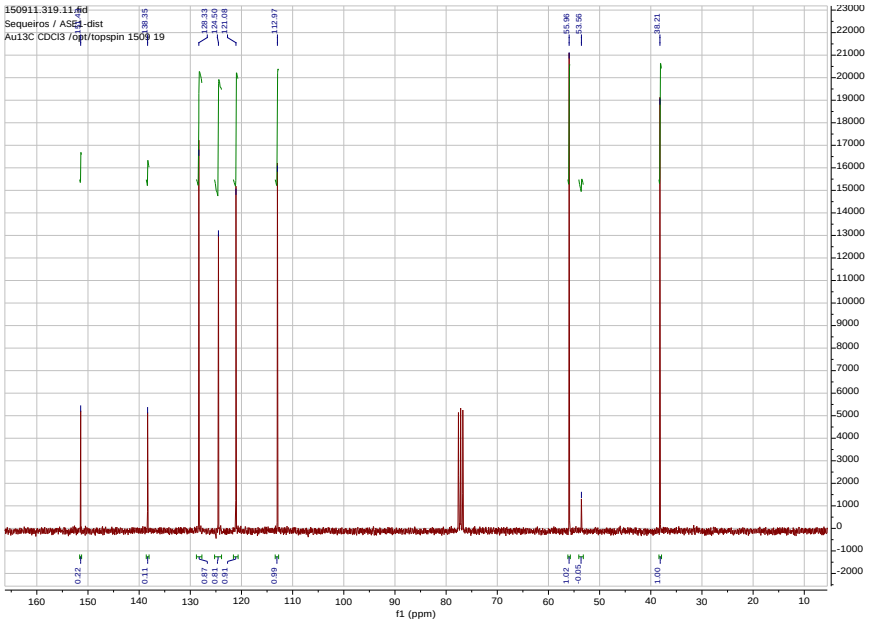

Figure5.43 ^{13}C NMR of mesylated guaiacol

^{1}H NMR (300 MHz, $CDCl_3$): δ 3.16 (s, 3H), 3.98 (s, 3H), 6.95-7.04 (m, 2H), 7.25-7.33 (m, 2H).

The first singlet is due to the methyl group in mesylated guaiacol, the second singlet is due to the methoxy group in the aromatic rign and the two multiplets are due to the aromatic ring.

^{13}C NMR (75 MHz, $CDCl_3$): 38.21, 55.96, 112.97, 121.08, 124.50, 128.33, 138.35, 151.43.

The results showed that the reaction after recrystallitation was successful with no trace of impurities.

Tosylation of guaiacol

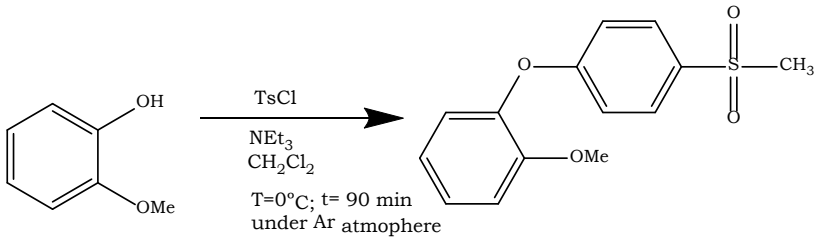

Figure 5.44 Tosylation reaction of guaiacol

In a flask with magnetic stirring 10g of guaiacol were dissolved in 50 mL of dichloromethane (see Figure 5.44.). The solution was brought to 0°C and 19.9 mL of trimethylamine was added. Then 13.6 g (1.1 eq.) of *p*-toluenesulfonyl chloride was sequentially added. Reaction mixture was stirred for 90 min and then, the mixture was washed with two portions of 1M aq. HCl and one portion of brine. The organic layer was dried with Na_2SO_4 and concentrated with a rotavaporator. The products (white crystals) were recrystallized to remove any trace of impurities. Recrystallization was done by dissolving crystals in ethanol and heating the solution in an oil bath at 80°C. After the solubilization of crystals, the solution was cooled down slowly and then filtered. This reaction was done following literature procedure [24]. Tosylated guaiacol was characterized by ^{1}H NMR and ^{13}C NMR.

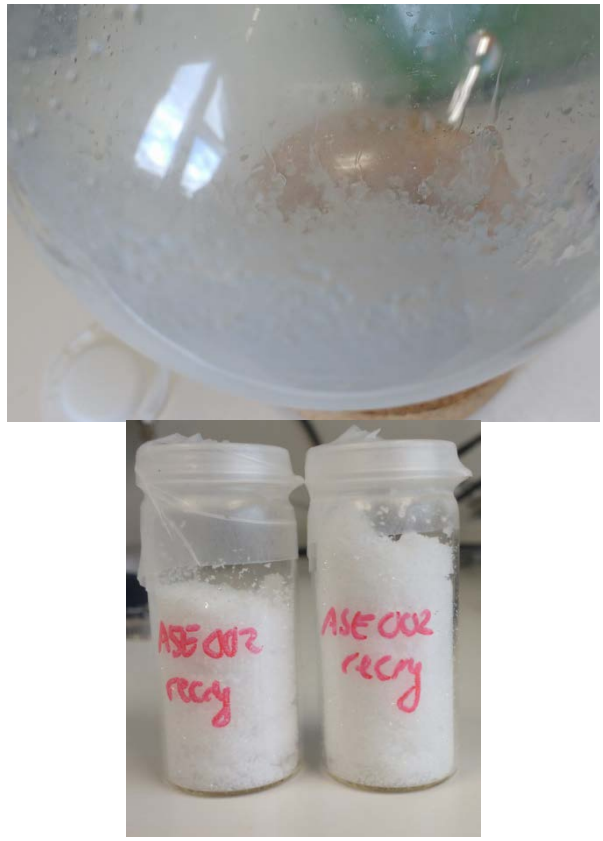

Figure 5.45 Tosylated guaiacol (ASE2) before and after recrystalization

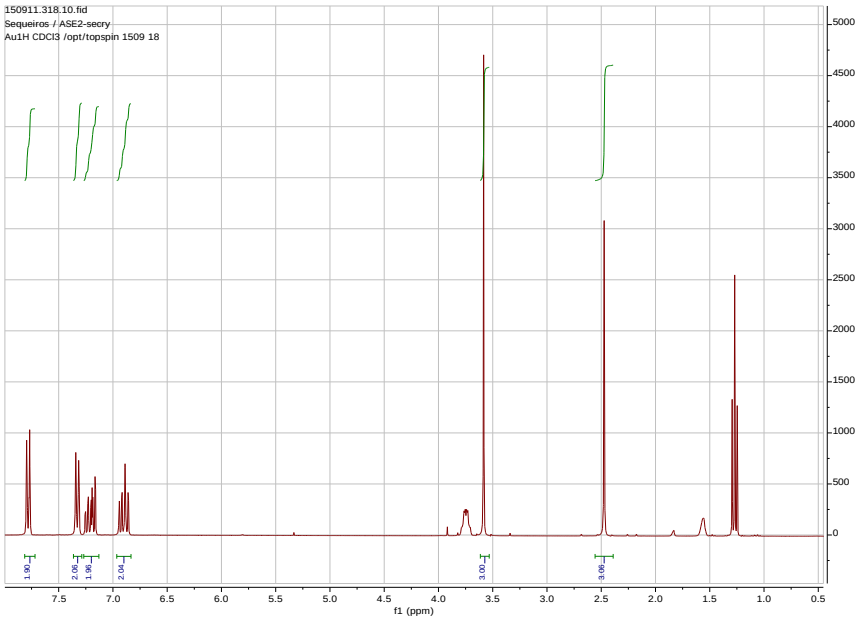

Figure 5.46 ^{1}H NMR of the tosylated guaiacol

^{1}H NMR results (300 MHz, $CDCl_3$): δ 7.78-7.77 (d, 2H), 7.34-7.32 (d, 2H), 7.25-7.16 (m, 2H), 6.95-6.86 (m, 2H), 3.58 (s, 3H), 2.47 (s, 3H).

The first two duplets are due to the resognance of aromatic ring. The next to multiplets are due to the aromatic ring of the tosylated group; the next singlet is due to the presence of the methoxy group in the guaiacyl ring and the last singlet is due to the methyl group in the tosylated group.

^{13}C NMR results (75MHz, $CDCl_3$): 151.88, 145.07, 138.48, 133.30, 129.40, 128.68, 128.11, 124.10, 120.68, 112.75, 55.58, 21.75. Impurities: ethanol: 58.48, 18.49.

The results showed that the reaction of tosylation was successful with small traces of ethanol in the final product and could be used in the following steps.

5.2.2. Alkoxy carbonylation of MsG using different conditions, ligands, bases and catalysts

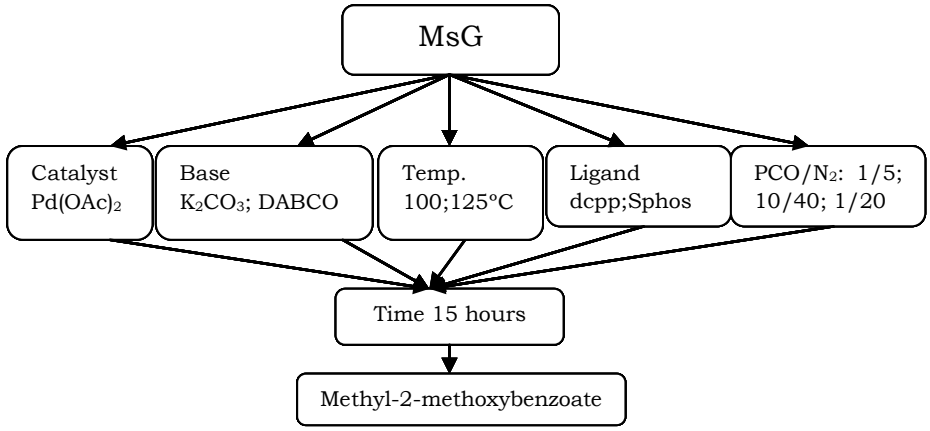

Scheme 5.4 Process scheme of alkoxy carbonylation with MsG

Alkoxycarbonylation with mesylguaiacol and tosylguaiacol were carried out in batch autoclave reactor-5500 Parr reactor-with 4848 Reactor controller and with small vials that can be seen in Figure 5.47, where all the compounds were added in the order presented in the following tables: catalyst, ligand, base and substrate.

Figure 5.47 Autoclave and reaction vials

As the reaction substrates were viscous, stock solution in ethanol and toluene were prepared. From one side, the stock solution of ethanol was prepared in a dry schlenk mixing 0.78 mL of MsG with 20 mL of ethanol. From the other side, stock solution of toluene was done by mixing 0.8 mL of MsG with, three equivalents of ethanol, 0.9 mL of ethanol and with 10 mL of toluene.

The autoclave was sealed and purged three times with nitrogen to remove any trace of air and reach an inert atmosphere. Once it was purged the autoclave was charged with the chosen ratio of pressure. Afterwards, autoclave was cooled down in an ice bath before degassing the CO/N_2 gas mixture and purging it three times with nitrogen. Samples for the GC were prepared by adding 100 µL of the standard, and then 50µL of the mixture were taken to dilute it with 1mL of ethanol.

Alkoxy carbonylation with mesylated guaiacol

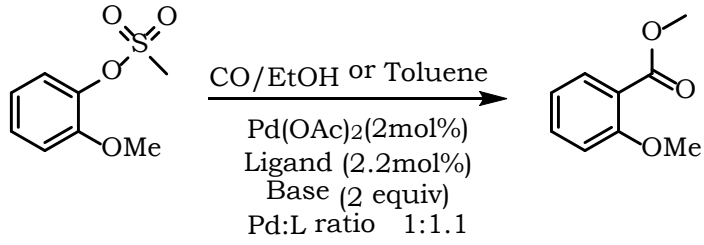

Figure 5.48 Alkoxycarbonylation of mesylated guaiacol

All reaction conditions that were tried for alkoxy carbonylation with mesylated guaiacol are summed up in the following tables.

Table 5.19 Alkoxy carbonylation reaction conditions

Exp.	Catalyst 1% mol	Ligand 1.1%mol	Base	Subs.	T (°C)	PCO/N_2 (bars)	Conversion (%)	Yield (%)
ASE5	$Pd(OAc)_2$	Xantphos	K_2CO_3	2 mL EtOH	100	10/40	61	-
ASE6	$Pd(OAc)_2$	dtbpx	K_2CO_3	2 mL EtOH	100	10/40	82	-
ASE7	$Pd(OAc)_2$	PPh_3	K_2CO_3	2 mL EtOH	100	10/40	83	-
ASE8	$Pd(OAc)_2$	dppf	K_2CO_3	2 mL EtOH	100	10/40	65	1
ASE9	$Pd(OAc)_2$	SPhos	K_2CO_3	2 mL EtOH	100	10/40	81	-
ASE10	$Pd(OAc)_2$	dppp	K_2CO_3	2 mL EtOH	100	10/40	77	-

Table 5.20 Alkoxy carbonylation reaction conditions

Exp.	Catalyst 2%mol	Ligand 2.2% mol	Base	Subs.	T (°C)	PCO/N_2 (bars)	Conversion (%)	Yield (%)
ASE12	$Pd(OAc)_2$	dcpp	K_2CO_3	MsG	100	1/5	97	1
ASE13	$Pd(OAc)_2$	PPh_3	K_2CO_3	MsG	100	1/5	91	-
ASE14	$Pd(OAc)_2$	PPh_3	DABCO	MsG	100	1/5	91	-
ASE15	$Pd(OAc)_2$	dppf	K_2CO_3	MsG	100	1/5	91	-
ASE16	$Pd(OAc)_2$	dppf	DABCO	MsG	100	1/5	91	-
ASE17	$Pd(OAc)_2$	Xantphos	DABCO	MsG	100	1/5	91	-

Table 5.21 Alkoxy carbonylation reaction conditions

Exp.	Catalyst 2% mol	Ligand 2.2% mol	Base	Subs.	T (°C)	PCO/N_2 (bars)	Conversion (%)	Yield (%)
ASE18	$Pd(OAc)_2$	dcpp	K_2CO_3	1mL tol	100	5/20	21	11
ASE19	$Pd(OAc)_2$	PPh_3	K_2CO_3	1mL tol	100	5/20	26	-
ASE20	$Pd(OAc)_2$	PPh_3	DABCO	1mL Tol	100	5/20	15	-
ASE21	$Pd(OAc)_2$	dppf	K_2CO_3	1mL Tol	100	5/20	21	-
ASE22	$Pd(OAc)_2$	dppf	DABCO	1mL Tol	100	5/20	32	-
ASE23	$Pd(OAc)_2$	Xantphos	DABCO	1mL Tol	100	5/20	13	-

Table 5.22 Alkoxy carbonylation reaction conditions

Exp.	Catalyst 2%mol	Ligand 2.2% mol	Base	Subs.	T (°C)	PCO/N_2 (bars)	Conversion (%)	Yield (%)
ASE24	$Pd(OAc)_2$	dcpp	K_2CO_3	1 mL tol	125	10/40	53	6
ASE25	$Pd(OAc)_2$	PPh_3	K_2CO_3	1 mL tol	125	10/40	76	-
ASE26	$Pd(OAc)_2$	PPh_3	NaOAc	2 mL EtOH	125	10/40	0	-
ASE27	$Pd(OAc)_2$	dppf	K_2CO_3	1 mL tol	125	10/40	0	-
ASE28	$Pd(OAc)_2$	dppf	NaOAc	2 mL EtOH	125	10/40	12	3
ASE29	$Pd(OAc)_2$	Xantphos	NaOAc	2 mL EtOH	125	10/40	0	-

The reaction time for all the experiments was of 15 hours. Experiments from the Table 5.19 showed mainly instead of carbonylation reaction hydrogenation and direct coupling. Conversion results were high, but they did not give any yield of desired product. For the next experiment (Table 5.20) conditions that were applied were the once that Buchwald et al. applied in their work applying higher catalyst and ligand loading and lower pressure ratio. Results showed higher conversions than before, but no trace of desired products due to direct coupling. In the following experiments (Table 5.21) catalyst and ligand loading was maintained and pressure ratio was raised. Results showed low conversion, but 11% of yield in the first experiment. In the following experiments (Table 5.22) catalyst and ligand loading was also maintained, but temperature and pressure ratio were raised. Results showed higher conversions, but lower yields.

In experiments of alkoxy carbonylation done with MsG the best results were obtained with ligand dcpp with a yield of 11% and 6% respectively. These two experiments were done with the same amount of substrate, catalyst and ligand, but changing temperature and pressure. Higher temperature conditions (125°C) and higher pressure conditions (CO/N_2, 10/40) highered conversion of the reaction 53%, but lowered the yields of the reactions 6%. Lowering temperature to 100°C and pressure to 5/20 lowered the conversion 21%, but higher the yield 11%. Maintaining temperature conditions at 100°C and lowering the pressure 1/20 gave higher conversion 92% but no yield.

5.2.3. Alkoxy carbonylation of TsG using different conditions, ligands and catalysts

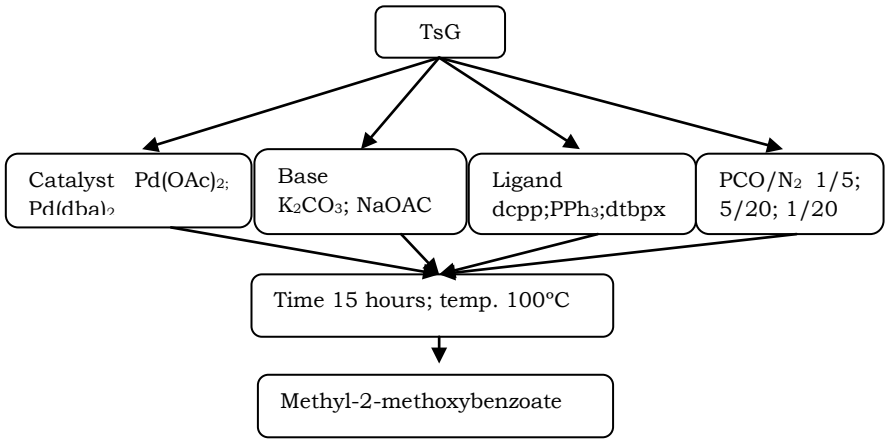

Scheme 5.5 Scheme of alkoxy carbonylation reactions with TsG

Alkoxy carbonylation with tosylated guaiacol was carried out in batch autoclave reactor-5500 Parr reactor-with 4848 Reactor controller and with small vials that can be seen in Figure 5.47, where all the compounds were added in the order presented in the following tables: catalyst, ligand, base and substrate.

In the case of TsG stock solutions were done following the same procedure. Stock solution of ethanol was done by mixing 1g TsG with 20 mL of ethanol and the stock solution of toluene was done mixing 1g TsG with, three equivalents of ethanol, 0.6 mL ethanol and with 10 mL of toluene. Before the addition of the stock solution molecular sieves and a stirrer were added. The stock solution was added to the reaction vials under argon atmosphere.

The autoclave was sealed and purged three times with nitrogen to remove any trace of air and reach an inert atmosphere. Once it was purged the autoclave was charged with the chosen ratio of pressure. Afterwards, the autoclave was cooled down in an ice bath before degassing the CO/N_2 gas mixture and purging it three times with nitrogen.Samples for the GC were prepared by adding 100 μL of the standard, and then 50μL of the mixture were taken to dilute it with 1mL of ethanol.

Alkoxy carbonylation reaction with tosylated guaiacol

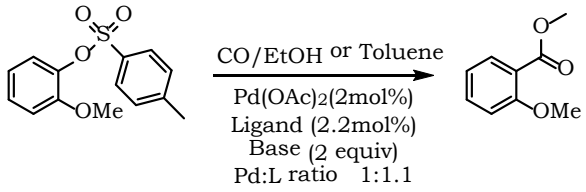

Figure 5.49 Alkoxy carbonylation of tosylated guaiacol

Table 5.23 Alkoxy carbonylation reaction conditions

Exp.	Catalyst 2%mol	Ligand 2.2%	Base	Substrate	T (°C)	PCO/N_2 (bars)	Conversion (%)	Yield (%)
ASE30	$Pd(OAc)_2$	dcpp	K_2CO_3	1 mL Tolu	100	1/5	14	8
ASE31	$Pd(OAc)_2$	PPh3	K_2CO_3	1 mL Tolu	100	1/5	13	-
ASE32	$Pd(OAc)_2$	PPh3	K_2CO_3	2 mL EtOH	100	1/5	33	-
ASE33	$Pd(OAc)_2$	dppf	K_2CO_3	1 mL Tolu	100	1/5	17	-
ASE34	$Pd(OAc)_2$	dppf	K_2CO_3	2 mL EtOH	100	1/5	35	2
ASE35	$Pd(OAc)_2$	Xhantpos	K_2CO_3	2 mL EtOH	100	1/5	24	-

Table 5.24 Alkoxy carbonylation reaction conditions

Exp.	Catalyst 2%mol	Ligand 2.2%	Base	Substrate	T (°C)	PCO/N_2 (bars)	Conversion (%)	Yield (%)
ASE36	$Pd(OAc)_2$	dcpp	K_2CO_3	1 mL Tolu	100	5/20	45	7
ASE37	$Pd(OAc)_2$	PPh3	K_2CO_3	1 mL Tolu	100	5/20	42	-
ASE38	$Pd(OAc)_2$	PPh3	K_2CO_3	2 mL EtOH	100	5/20	78	-
ASE39	$Pd(OAc)_2$	Dppf	K_2CO_3	1 mL Tolu	100	5/20	38	-
ASE40	$Pd(OAc)_2$	dppf	K_2CO_3	2 mL EtOH	100	5/20	79	-
ASE41	$Pd(OAc)_2$	Xhantpos	K_2CO_3	2 mL EtOH	100	5/20	67	-

Table5.25 Alkoxy carbonylation reaction conditions

Exp.	Catalyst 2%mol	Ligand 2.2% mol	Base	Substrate	T (°C)	PCO/N_2 (bars)	Conversion (%)	Yield (%)
ASE60	$Pd(OAc)_2$	dtbpx	K_2CO_3	1 mL Tolu	100	1/5	13	7
ASE61	$Pd(OAc)_2$	PEPPSI	K_2CO_3	1 mL Tolu	100	1/5	19	-
ASE62	$Pd(OAc)_2$	$BuP(Ad)_2$	NaOAc	1 mL Tolu	100	1/5	19	-
ASE63	$Pd(OAc)_2$	SPhos	K_2CO_3	1 mL Tolu	100	1/5	18	-
ASE64	$Pd(OAc)_2$	Xantphos	NaOAc	1 mL Tolu	100	1/5	6	-
ASE65	$Pd(OAc)_2$	Johnphos	NaOAc	1 mL Tolu	100	1/5	11	

Table 5.26 Alkoxy carbonylation reaction conditions

Exp.	Catalyst 2%mol	Ligand 2.2%mol	Base	Substrate	T (°C)	PCO/N_2 (bar)	Conversion (%)	Yield (%)
ASE66	$Pd(OAc)_2$	dcpp	K_2CO_3	1 mL Tolu	100	1/20	42	7
ASE67	$Pd(OAc)_2$	dcpp	NaOAc	1 mL Tolu	100	1/20	28	-
ASE68	$Pd(OAc)_2$	PCy3	K_2CO_3	1 mL Tolu	100	1/20	15	-
ASE69	$Pd(OAc)_2$	PCy3	K_2CO_3	1 mL Tolu	100	1/20	10	-
ASE70	$Pd(OAc)_2$	PCy3	NaOAc	MsG+Tolu	100	1/20	92	-

Table 5.27 Alkoxy carbonylation reaction conditions

Exp.	Catalyst 2%mol	Ligand 2.2%mol	Base	Substrate	T (°C)	PCO/N_2 (bar)	Conversion (%)	Yield (%)
ASE84	$Pd(dba)_2$	dtbpx	K_2CO_3	1 mL Tolu	100	1/20	22	-
ASE85	$Pd(dba)_2$	PEPPSI	K_2CO_3	1 mL Tolu	100	1/20	12	-
ASE86	$Pd(dba)_2$	BuP(Ad)$_2$	K_2CO_3	1 mL Tolu	100	1/20	21	-
ASE87	$Pd(dba)_2$	SPhos	K_2CO_3	1 mL Tolu	100	1/20	20	-
ASE88	$Pd(dba)_2$	dcpp	K_2CO_3	1 mL Tolu	100	1/20	0	-
ASE89	$Pd(dba)_2$	PCy3	K_2CO_3	1 mL Tolu	100	1/20	18	-

Reaction time for all experiments (Table 5.23-Table 5.26) was of 15 hours and in all cases catalyst and ligand loading was the same as in the Buchwald et al. experiments. Experimental conditions that were varied in these set of experiments were ratio of pressure, base and in Table 5.27 source of palladium.

In the experiments of alcoxycarbonylation done with TsG the best results were again obtained with ligand dcpp. In these three (ASE 30, 36, 66) experiments the charge of substrate, ligand, base, catalyst were the same, as well as temperature used in the experiments (100°C). In these experiments, the increasing of the pressure ratio affected the conversion with higher results. However, the yield did not showed any positive effect. As conclusion, the results of the ASE 30 with pressure ratio of 1/5 were considered as the best.

As general conclusion, it could be said that the alkoxy carbonylation reactions with MsG and TsG gave low yield of the desired products due to sterically hindered substrates.

5.3 Formation of aromatic acids via oxidative carbonylation

Development of environmentally more benign and efficient synthetic methods relies to a significant extent on progress in catalysis and organometallic chemistry. The carbonylation chemistry constitutes an industrial key technology, which produces many products for our daily life. More specifically, carbonylative cross-coupling reactions based on the refinement of arenes, olefins which comprise the basic raw materials for the chemical industry, provide access to valuable products such as aldehydes, alcohols and carboxylic acid derivates. Among the different types of carbonylation reactions, palladium-catalyzed oxidative carbonylation apply different organic nucleophiles or electrophiles in the presence of CO and oxidation reagents to prepare various carbonyl-containing compounds [26]. Pd catalyzed oxidative carbonylation reactions are well established and belong to the broad research field of C-H activation.

Scheme **5.6** shows the general reaction mechanism for the direct carbonylation of arenes. It is assumed that the C-H activation, which is the rate determining step, involves the electrophilic attack of Pd^{II} on the arene (1). Then, CO will insert in the Pd-arene bond (2) to form an acyl species, which reacts with the nucleophile. Reductive elimination (3) releases the product. Reoxidation of Pd(0) closes the catalytic cycle (4). Commonly used oxidants are $K_2S_2O_8$ or peroxides [27], benzoquinone (BQ) [28, 29], Cu(II)[30, 31]- or Ag(I)-salts [32], and O_2 [33, 34, 35].

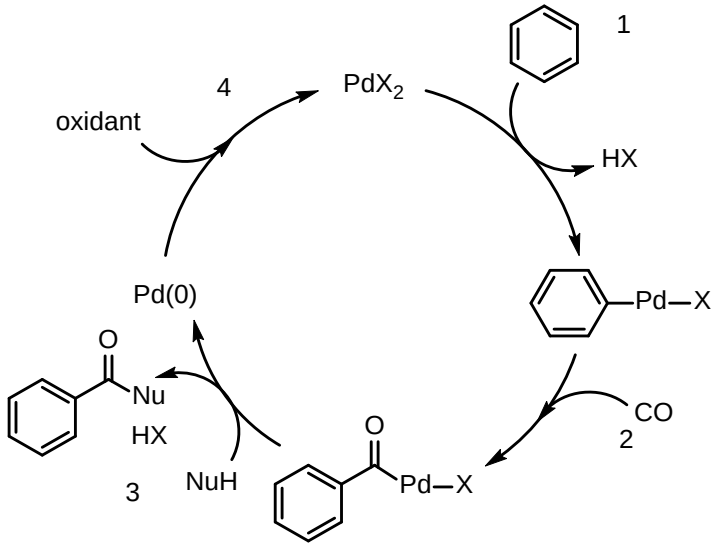

Scheme 5.6 Oxidative carbonylation mechanism of arenes

Direct oxidative carbonylation of arenes was pioneered by Fujiwara et al. [36] The direct carbonylations of benzene, toluene, anisole, chlorobenzene, furan and thiophene were performed under CO in the presence of $Pd(OAc)_2$. 2-43% of the corresponding benzoic acids were formed as the terminal products. Later on, the selectivity of arenes was investigated by Ishii et al. who reported on the oxidative carbonylation of anisole in the presence of catalytic amounts of $Pd(OAc)_2$ and molybdocanadophosphoric acid (HPMoV) utilizing acetic acid as solvent in an CO/O_2 atmosphere [37]. An isomeric mixture of *p*- and *o*-anisic acid (ratio approx. 3/1) was obtained. Further carbonylation experiments with *o*-, *m*-, *p*-methylanisole revealed a decreasing reactivity of *p*>*m*>*o*. The carbonylation selectivity was explained by electronic effects of the methoxy group. The same was found to be true for the oxidative carbonylation of phenol. Furthermore, to improve the reaction efficiency, Fujiwara et al. developed a more powerful catalytic system. A series of simple arenes such as toluene, chlorobenzene, anisole and naphthalene were oxidatively carbonylated by $Pd(OAc)_2$ in the presence of potassium peroxodisulfate ($K_2S_2O_8$) as the oxidant in

trifluoroacetic acid (TFA) at room temperature under an atmosphere of CO. The aromatic carboxylic acids were formed in good yields. The author proposed that $Pd(OAc)_2$ reacted with TFA first to generate $Pd(OTFA)_2$ having a more electron-deficient palladium center. As mentioned above, the mechanism of C-H activation in this kind of reaction involves electrophilic attack of aromatic ring by the Pd^{II} species. Therefore, the more electron-poor Pd^{II} species, $Pd(OTFA)_2$, would facilitate this process and make it possible to react under mild reaction conditions (room temperature). [38, 39]

To summarize, major challenges in the Pd catalysed oxidative carbonylation are the reported such as reduction of Pd(II) by CO, the regioselectivity -*ortho*-carbonylation in the presence of directing groups, rather low regioselectivity without directing groups, long reaction times up to 48 hours and the electrophilic attack of Pd^{II} on the arene.

5.3.1. Oxidative carbonylation using different substrates, oxidants and reaction conditions

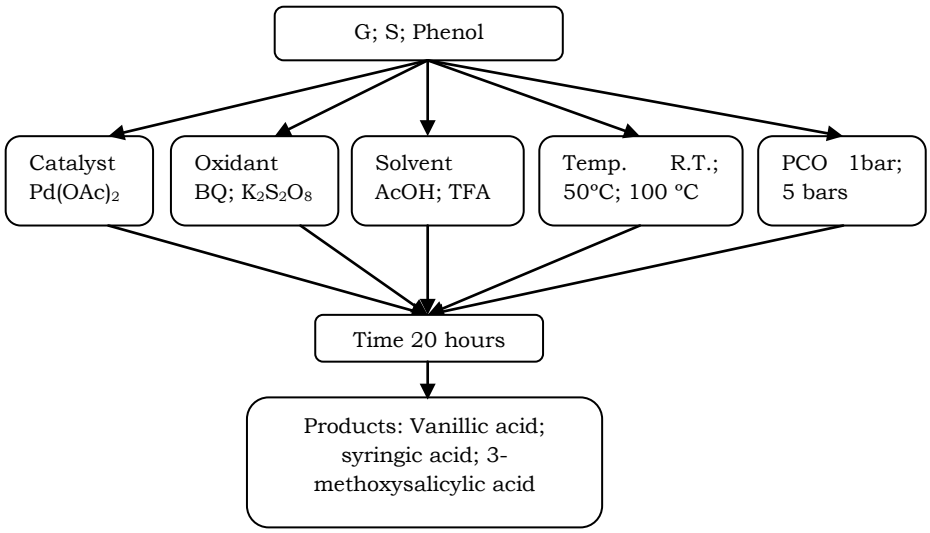

Scheme 5.7 Scheme of oxidative carbonylation with different substrates

Oxidative carbonylation was done with three different substrates (guaiacol (G), syringol (S) and phenol (P)) in a batch autoclave reactor-5500 Parr reactor- with a 4848 Reactor controller that was shown in Figure 5.47 in the presence of carbon monoxide as it can be seen in the reaction shown in Figure 5.50. Vials were filled in the order that the compounds are named in the table below, reactive, oxidant, catalyst and solvent. The solvent was added once vials were under argon atmosphere. Then the autoclave was sealed and fluxed with nitrogen three times to remove any reactive air and reach an inert atmosphere. Afterwards, desired pressure of CO was inserted in the autoclave and the reaction was run for 20 hour. Once the reaction was over, the autoclave was cooled down in an ice bath and was degassed and fluxed three times with nitrogen to remove any trace of CO that was not released to the atmosphere. Samples were prepared to be analyzed by HPLC by adding 50 μL of biphenyl (standard) and diluting them with 1mL of ethanol. The calibration curve in the HPLC was done with guaiacol, syringol, phenol and purified vanillic acid, 3-methoxysalicylic acid and syringic acid.

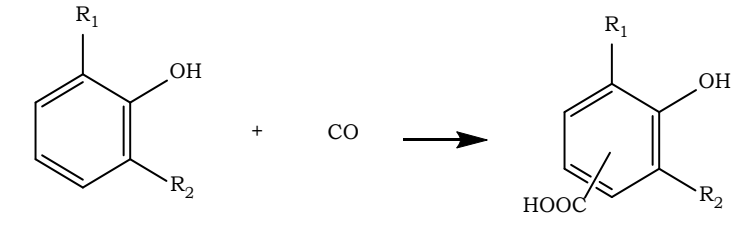

R_1=H, R_2=H 1a phenol
R_1=H, R_2= OMe 1b guaiacol
R_1=OMe, R_2= OMe 1c syringol

Figure 5.50 Oxidative carbonylation reaction of different substrates

In the following tables all experimental conditions that were applied to three substrates and the HPLC results are shown.

In the case of guaiacol two isomers of the acid were obtained that it is why two yields are shown in the tables.

Table 5.28 Oxidative carbonylation reaction conditions

	Reactive	Oxidant 2 equiv.	Catalyst %5 mol	Solvent	PCO (bar)	Temp. (°C)	Yield VA (%)	Yield MSA (%)	Conv (%)
ASE42	G	BQ	$Pd(OAc)_2$	AcOH	1	R.T.			
ASE43	**G**	**$K_2S_2O_8$**	**$Pd(OAc)_2$**	**TFA**	**1**	**R.T.**	**46**	**5**	**100**
ASE44	S	BQ	$Pd(OAc)_2$	AcOH	1	R.T.	-		39
ASE45	S	$K_2S_2O_8$	$Pd(OAc)_2$	TFA	1	R.T.	13		100
ASE46	P	BQ	$Pd(OAc)_2$	AcOH	1	R.T.			17
ASE47	P	$K_2S_2O_8$	$Pd(OAc)_2$	TFA	1	R.T.			100

Table 5.29 Oxidative carbonylation reaction conditions

	Reactive	Oxidant 2 equiv.	Catalyst %5 mol	Solvent	PCO (bar)	Temp. (°C)	Yield VA (%)	Yield MSA (%)	Conv (%)
ASE48	G	BQ	$Pd(OAc)_2$	AcOH	1	50	-	-	15
ASE49	**G**	**$K_2S_2O_8$**	**$Pd(OAc)_2$**	**TFA**	**1**	**50**	**36**	**5**	**86**
ASE50	S	BQ	$Pd(OAc)_2$	AcOH	1	50	-		40
ASE51	S	$K_2S_2O_8$	$Pd(OAc)_2$	TFA	1	50	8		100
ASE52	P	BQ	$Pd(OAc)_2$	AcOH	1	50			97
ASE53	P	$K_2S_2O_8$	$Pd(OAc)_2$	TFA	1	50			96

Table 5.30 Oxidative carbonylation reaction condition

	React.	Oxidant 2equiv.	Catalyst %5 mol	Solvent	PCO (bar)	Temp. (°C)	Yield VA (%)	Yield MSA (%)	Conv (%)
ASE54	G	BQ	$Pd(OAc)_2$	AcOH	1	100	-	-	28
ASE55	**G**	**$K_2S_2O_8$**	**$Pd(OAc)_2$**	**TFA**	**1**	**100**	**30**	**4**	**97**
ASE56	S	BQ	$Pd(OAc)_2$	AcOH	1	100	1		42
ASE57	S	$K_2S_2O_8$	$Pd(OAc)_2$	TFA	1	100	9		100
ASE58	P	BQ	$Pd(OAc)_2$	AcOH	1	100	-		96
ASE59	P	$K_2S_2O_8$	$Pd(OAc)_2$	TFA	1	100	-		99

Table 5.31 Oxidative carbonylation reaction conditions

	React.	Oxidant 2 equiv.	Catalyst %5 mol	Solvent	Water µL	PCO (bar)	Temp (°C)	Yield (%)	Conv (%)
ASE72	S	$K_2S_2O_8$	$Pd(OAc)_2$	TFA		5	50	36	100
ASE73	S	$K_2S_2O_8$	$Pd(OAc)_2$	TFA		5	50	35	100
ASE74	S	$K_2S_2O_8$	$Pd(OAc)_2$	AcOH		5	50	-	0
ASE75	S	$K_2S_2O_8$	$Pd(OAc)_2$	AcOH		5	50	-	1
ASE76	**S**	**$K_2S_2O_8$**	**$Pd(OAc)_2$**	**TFA**	**100**	**5**	**50**	**39**	**63**
ASE77	S	$K_2S_2O_8$	$Pd(OAc)_2$	AcOH	100	5	50	-	0

Table 5.32 Oxidative carbonylation reaction conditions

	React.	Oxidant 2 equiv.	Catalyst %5 mol	Solvent	Water µL	PCO (bar)	Temp (°C)	Yield (%)	Conv (%)
ASE51R	S	$K_2S_2O_8$	$Pd(OAc)_2$	TFA		1	50	34	100
ASE79	S	$K_2S_2O_8$	$Pd(OAc)_2$	AcOH		1	50	-	3
ASE80R	S	$K_2S_2O_8$	$Pd(OAc)_2$	AcOH		1	50	-	3
ASE81	**S**	**$K_2S_2O_8$**	**$Pd(OAc)_2$**	**TFA**	**100**	**1**	**50**	**54**	**100**
ASE82	S	$K_2S_2O_8$	$Pd(OAc)_2$	AcOH	100	1	50	-	1
ASE82R	S	$K_2S_2O_8$	$Pd(OAc)_2$	AcOH	100	1	50	-	17

Table 5.33 Oxidative carbonylation reaction conditions

	React.	Oxidant 2 equiv.	Catalyst %5 mol	Solvent	Water µL	PCO (bar)	Temp (°C)	Yield (%)	Conv (%)
ASE81R	S	$K_2S_2O_8$	$Pd(OAc)_2$	TFA	100	1	50	37	100
ASE91	S	$K_2S_2O_8$	$Pd(OAc)_2$	AcOH	200	1	50	39	100
ASE91R	S	$K_2S_2O_8$	$Pd(OAc)_2$	AcOH	200	1	50	20	100
ASE93	S	$K_2S_2O_8$	$Pd(OAc)_2$	TFA	500	1	50	17	100
ASE93R	S	$K_2S_2O_8$	$Pd(OAc)_2$	TFA	500	1	50	4	100
ASE95	S	BQ	$Pd(OAc)_2$	AcOH	100	1	50	1	100

Table 5.34 Oxidative carbonylation reaction conditions

	React.	Oxidant 2 equiv.	Catalyst %5 mol	Solvent	Water µL	PCO (bar)	Temp (°C)	Yield (%)	Conv (%)
ASE95R	S	BQ	$Pd(OAc)_2$	AcOH	100	1	50	2	100
ASE97	S	BQ	$Pd(OAc)_2$	AcOH	200	1	50	0	100
ASE97R	S	BQ	$Pd(OAc)_2$	AcOH	200	1	50	2	100
ASE99	S	BQ	$Pd(OAc)_2$	TFA	500	1	50	2	100
ASE99R	S	BQ	$Pd(OAc)_2$	TFA	500	1	50	3	100

The first oxidative carbonylations done with guaiacol revealed that the C-H activation done in combination with the oxidant benzoquinone (BQ) in presence of acetic acid resulted in really low conversions, being the maximum conversion 28%, and no yield of the desired products. Low conversion and non measurable yield may be due to the fact that the article that these experiments were based on used a mixture of acetic acid and dioxane and *p*-TsOH as an additive [29]. This was not the case of the carbonylation of guaiacol performed with the oxidant potassium persulfate ($K_2S_2O_8$) in combination with trifluoroacetic acid (TFA) where the reaction had good conversion and yields. The best reactions conditions, conversions and yields are summed up in Table 5.35. These experiments also showed the formation of two acid isomers as it is shown in Figure 5.51.

Table 5.35 Best reaction conditions for the oxidative carbonylation of guaiacol

	React.	Oxidant 2equiv.	Catalyst %5 mol	Solvent	PCO (bar)	Temp. (°C)	Yield VA (%)	Yield MSA(%)	Conv (%)
ASE43	G	$K_2S_2O_8$	$Pd(OAc)_2$	TFA	1	R.T.	46	5	100
ASE49	G	$K_2S_2O_8$	$Pd(OAc)_2$	TFA	1	50	36	5	86
ASE55	G	$K_2S_2O_8$	$Pd(OAc)_2$	TFA	1	100	30	4	97

Note: VA stands for vanillic acid and MSA stands for 3-methoxysalicylic acid

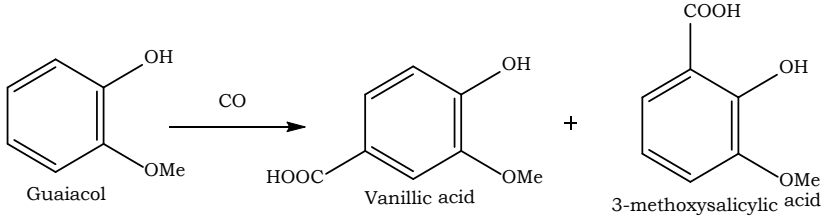

Figure 5.51 Oxidative carbonylation of guaiacol and formation of isomers

In Table 5.35 with the increment of temperature lowered the conversion and yield of desired products. The best results were obtained with the mildest conditions. Room temperature and 1 bar of carbon monoxide gave a 100% of conversion and a yield of 46% for the vanillin acid isomer and 5% 3-methoxysalicylic acid.

In the first experiments of oxidative carbonylation with syringol similar bad results were obtained with AcOH in presence of the oxidant benzoquinone, having low conversions and no yields of the desired product (syringic acid). Following the procedure applied to guaiacol, TFA and the oxidant $K_2S_2O_8$ were applied to increase the conversion and yield of the reactions. The best results were obtained at 50 °C with 100% of conversion and 20% of yield of syringic acid. As the yield was not high, carbon monoxide pressure was increased and water was introduced in the reaction media. Even if the introduction of water in the system seemed to be promising, the increment of the water amount decreased the yield of syringic acid. The best results were obtained with the addition of 100 μL of water at 50 °C at 1 bar of CO. This reaction was repeated twice with a 100% conversion and 46% yield of syringic acid.

5.4 Formation of aromatic acids via bromination and Grignard reaction

Bromination of organic substrates, particularly aromatics, is of paramount importance as building blocks in organic chemistry as well as in the manufacturing of pharmaceuticals and agrochemicals [40, 41]. Unfortunately, conventional aromatic bromination methods use toxic elemental bromine or hazardous acidic reagents, which generate toxic, corrosive and environmental pollutant wastes

[42]. Replacement of such reagents with non-toxic, inexpensive, available and more selective reagents is very interesting and still represents an important challenge in the context of clean synthesis [40]. Consequently, bromination reactions utilizing a variety of clean reagents have been extensively studied not only in conventional organic solvents, but also in ionic liquids (IL). These compounds, which are defined as materials consisting of an anion and cation that melt below 100 °C, are usually non-flammable and display no measurable vapor pressure. These properties are advantageous in a reaction medium for obvious reasons. Due to their thermal stability and ease of recycling ILs now are used on a multi-ton scale by companies such as BASF, Degussa, BP and Linde. Applications in which ILs have successfully been incorporated include, but are certainly not limited to, extraction media for metals , materials for dyes-sensitized solar cells, solvents for separation sciences and electrolytes for electrochemical storage devices [43].

Although molecular bromine is widely used for the functionalization of organic and inorganic substrates, due to its toxicity and high vapor pressure it is a hazardous chemical and cumbersome to handle. N-bromosuccinimide (NBS) is one of the most popular brominating reagents, due to its ease of handling, low price, and to the fact that the byproduct, succinimide, can be easily recovered, and reconverted back into NBS, and, as such, reused in subsequent reactions [41].

The reaction media that was explored for the aromatic bromination with NBS was the ionic liquid 1-butyl-3-methylimidazolium bromide [Bmim]Br. In recent studies, Zheng and co-workers performed bromination of activated aromatics such as phenols, naphthols, methoxynaphtalenes and anisole with 1-butyl-3-methylimidazolim tribromide

[Bmim]Br_3. The reagent of that study was prepared as a stable liquid from [Bmim]Br and bromide. The results of the reaction with phenol gave a yield of the bromophenol of 96% [44]. Another research made by Pingali et al studied the bromination reaction by mixing NBS with [Bmim]Br for phenol, aniline and their derivatives. This reaction claimed a direct and simple bromination reaction with e.g. a yield of 75% for the bromination of phenol to bromophenol [45].

5.4.1. Bromination of guaiacol and syringol with different solvents

The bromination of guaiacol and syringol started with the preparation of the bromination reagent. It is important to emphasize that the ionic liquid must be dried before its use because the presence of water substantially decreases both the conversion and the selectivity of the aromatic bromination. To eliminate this problem the ionic liquid was microwave activated. The activation process was carried out in CEM Microwave Discover System Model and the microwave system was a temperature-controller instrument with an internal temperature sensor. Into a shortly (3 min) microwave (150°C, 50W) [Bmim]Br (0.5 g) NBS (1mmol) was added to be mixed. This was immediately followed by the addition of the aromatic compounds (1mmol). In the case of the mixture of aromatic compounds an equimolecular amount of G (0.5 mmol) and S (0.5 mmol) was used. The general bromination reaction of G and S is shown in Figure 5.52.

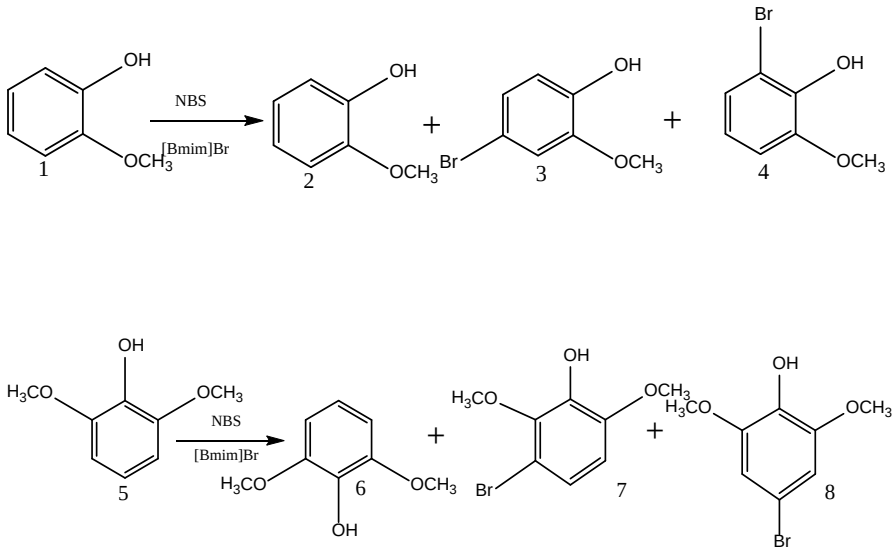

Figure 5.52. Scheme of bromination reaction of G and S and resulted *p*-BrG (3) and *o*-BrG (4) in the case of G and *m*-BrS (7) and *p*-BrS (8) in the case of S.

After the reaction was completed organic fraction was recovered from the extraction of brominated products. Liquid/liquid extraction was carried out using diethyl ether and ethyl acetate as organic fraction extractors. Combined organic extracts were washed with saturated sodium bicarbonate ($NaHCO_3$) and dried over with magnesium sulphate ($MgSO_4$). Diethyl ether and ethyl acetate were evaporated by vacuum distillation and the resulting brominated products were characterized by GC-MS and ^{13}C NMR.

Conversion of the reactants G and S were calculated using Equation 1 and the yield of products were calculated with Equation 2.

$$X_R = \left[1 - \frac{M_F}{M_I}\right] \times 100 \qquad \text{Equation 1}$$

$$Yield_P = \left[\frac{M_P}{M_R}\right] \times 100 \qquad \text{Equation 2}$$

Where M_I are the initial mol of reactants G or S. M_F are the final mol of reactants. M_P are the mol of product and M_R are the initial mol of reactant. It is worth to mention as it is shown in Figure 5.52 that the bromination with the mix of G and S is composed of two parallel reactions, G to get 4-bromo-2-methoxyphenol (*p*-BrG) and 6-bromo-2-methoxyphenol (*o*-BrG) and secondly, S to get 4-bromo-2,6-dimethoxyphenol (*p*-BrS) and 3-bromo-2,6-dimethoxyphenol (*m*-BrS). That is why the limiting reactant will vary in each case.

The first experiments that were carried out were only of guaiacol and syringol respectively because of the need to understand better the reaction media. Furthermore, bromination reactions with the mixture of G and S were also performed. All the experiments were extracted with ethyl acetate.

The GC-MS results in case of S showed firstly a peak related to succinimide. The next peak was related to the unreacted S in the final oil. After that, a peak related to desired product *p*-BrS. Bromination of G showed similar results with a peak related to the unreacted G, then, a peak related to the succinimide and finally a peak related to desired product *p*-BrG. In both chromatograms there was an unidentified peak before *p*-BrS in the case of bromination of S and after *p*-BrG in the case of G.

The mass spectrum of those unidentified peaks was analyzed as it could be seen in Figure 5.54. Results on the left side showed that the molecular ion of *p*-BrS was the same as the unidentified peak. Molecular ion peak is

observed in most of the mass spectra, which corresponds to the unfragmented molecular ions (M^+). The peak representing the molecular ion is usually the one of mayor mass in the spectrum and the m/z value of it corresponds to the molecular weight of the molecule [Wade 2006]. All this said it could be concluded that the unidentified peak with the same molecular ion as the *p*-BrS is an isomer of that compound. The same could be said about the unidentified peak in the bromination reaction of G that led to the formation of two isomers the *p*-BrG and *o*-BrG.

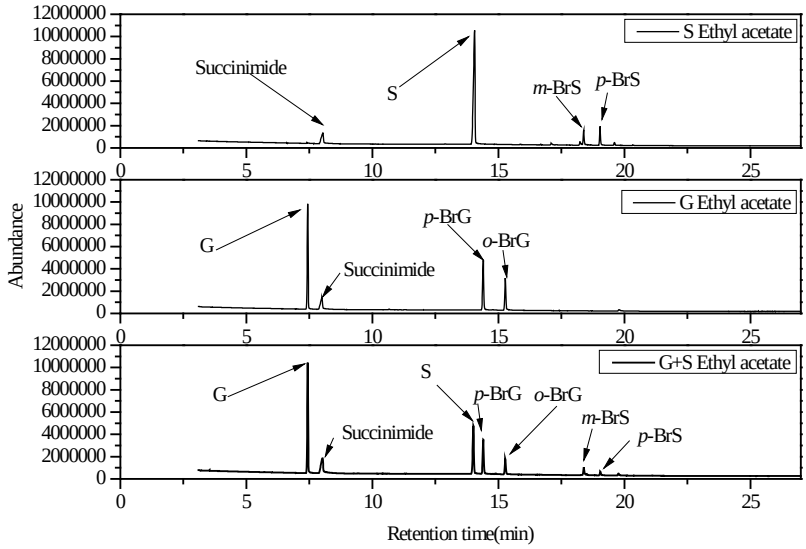

Figure 5.53. GC-MS results of the bromination with G, S and G+S.

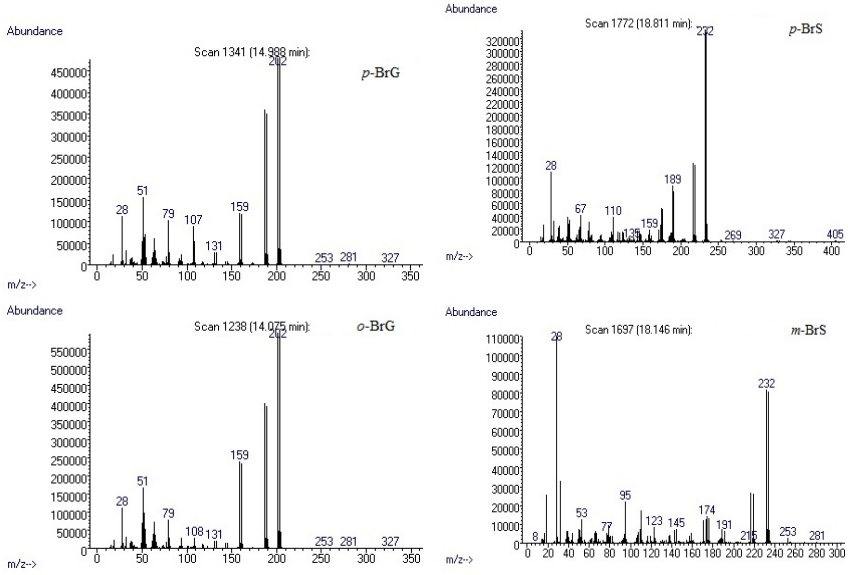

Figure 5.54 Mass spectra of (left) *p*-BrG, *o*-BrG and (right) *p*-BrS, *m*-BrS.

Table 5.36 Conversion (%) and yield (%) of the resulted products on the bromination with EtAc

	Conversion (%) and yield (%) of the resulted products					
	Ethyl acetate					
	S		**G**		**S+G**	
	Conv (%)	**Yield (%)**	**Conv (%)**	**Yield (%)**	**Conv (%)**	**Yield (%)**
G	-		57±6		50±4	
S	46±6		-		60±4	
p-BrG	-			13±3		11±0
o-BrG	-			9±2		7±1
p-BrS		13±2	-			15±1
m-BrS		5±4	-			5±1

In Table 5.36 the results of conversion and yield of each product are shown. Results showed that the mass balance of this reaction was not ideal as the sum of product yield was not the same as reactants conversion. The first reactions showed that less sterically hindered reactant, guaiacol (X_G 57%) has higher conversion than syringol (X_S 46%). However, the mix of G and S favored more conversion of X_S 60% than of X_G 50%. Accordingly, yield of BrS isomers was higher with the mix of G and S (ΣBrS 20%) than only with S (ΣBrS 18%). These results showed that the reaction with the mix of G and S favored more the reaction of S towards X_S and ΣBrS isomers than in the bromination only with S.

Once the reaction of bromination with ethyl acetate was understood, different solvents were tried to assess their effect on the reaction products. In Figure 5.16 chromatograms for the bromination with different solvent are shown. An appreciable variation between the two solvents was the presence of succinimide in the oil showing more affinity of the ethyl acetate during the liquid-liquid

extraction towards some compounds of liquid phase than diethyl ether. Both solvents showed the formation of the G isomers and S isomers.

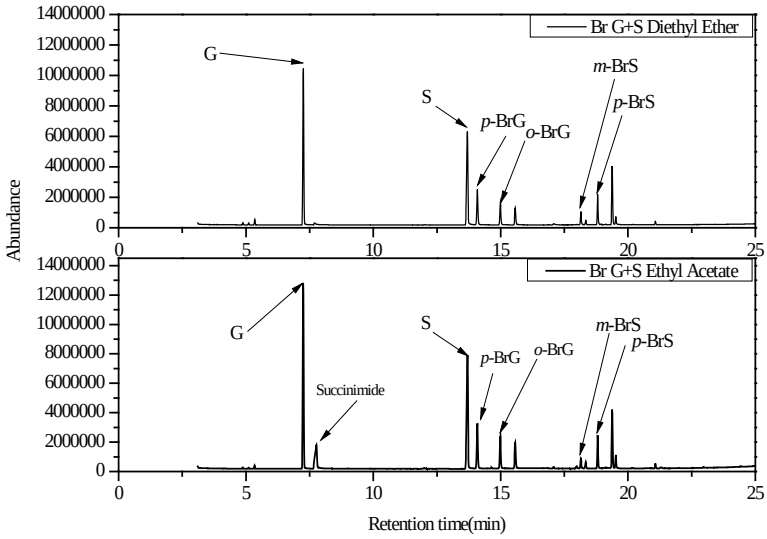

Figure 5.55 GC-MS chromatograms for the bromination products with DEE and EtAc

Table 5.37 Conversion (%) and yield (%) of bromination products and total oil (mg) of obtained products with DEE and EtAc .

	Conversion and yield resulted (%) and the total oil (mg)			
	Diethyl ether		**Ethyl acetate**	
	Conv (%)	**Yield (%)**	**Conv (%)**	**Yield (%)**
Oil	373.73±35.40		586.60±24.90	
G	57±6		50±4	
S	72±6		60±4	
***p*-BrG**		10±1		11±0
***o*-BrG**		5±0		7±1
***p*-BrS**		15±0		15±1
***m*-BrS**		8±3		5±1
ΣBrG		15		17
ΣBrS		22		20

Results of Table 5.37 showed conversion of resulted products with DEE and EtAc. As Vigneault et al. [47] reported on their work the performance of DEE and EtAc to extract monomers G and S was 100% in both cases. So it was expected that the performance of the two solvents to be similar, but high volatility of DEE made it impossible to recover it after rotavaporation and to reuse it. Accordingly, results were quite similar with slight differences. From one side, more oil was obtained with EtAc than with DEE, but these could be due to the presence of compounds from the aqueous layer in the oil of EtAc, increasing the weight of the total oil. Continuously, although the conversion of X_G and X_S was higher with DEE (X_G 57% and X_S 72%) than with EtAc (X_G 50% and X_S 60%) the results showed that in proportion EtAc (ΣBrG 17% and ΣBrS 20%) was able to extract more desired products than the DEE (ΣBrG 15% and ΣBrS 22%). These results besides the easier handling and

the possibility or reusing it made the EtAc the selected solvent for the next experiments.

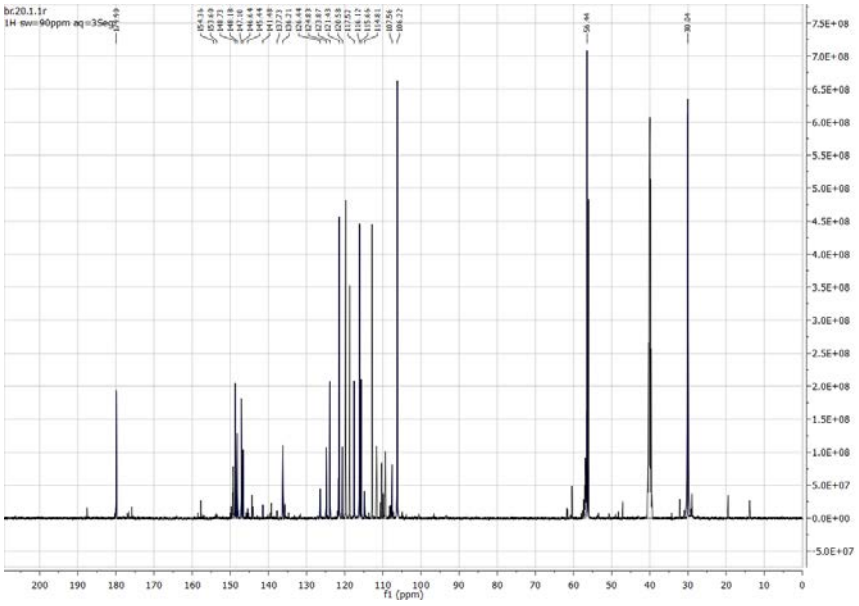

Figure 5.56 ^{13}C NMR spectra of brominated G and S with ethyl acetate

The Figure 5.56 shows the ^{13}C NMR of the product obtained from the bromination reaction of G and S with ethyl acetate. These results corroborate the presence of part of the aqueous layer, having the succinimide C-2 179.90 ppm and C-3 30.04 ppm. All the aromatic compounds showed their signals in the aromatic area (103.9-168.0 ppm). The non reacted guaiacol and syringol showed their respective signals. For the guiacol C-1 145.44 ppm, C-2 146.64 ppm, C-3 112.83 ppm, C-4, 121.61 ppm, C-5 121.61 and C-6 116.12 ppm. For the syringol C-1 137.73 ppm, C-2 148.73 ppm, C-3 107.56 ppm, C-4 123.87 ppm and for all the methoxy groups 56.04 ppm. All the brominated products showed a high peak around 154.6-153.6 ppm. For the *p*-BrS the following signals were assigned: C-1 136.21 ppm, C-2 154.36 ppm, C-3 107.56 ppm, C-4 117.52 ppm and for the

m-BrS the next signals were attributed: C-1 135.0 ppm, C-2 153.60 ppm, C-3 106.22 ppm, C-4 124.83 ppm, C-5 115.66 ppm, C-6 148.10 ppm. The following signals were attributed to the *p*-BrG: C-1 147.70 ppm, C-2 153.60 ppm, C-3 115.30 ppm, C-4 115.60 ppm, C-5 125.30 ppm and C-6 120.58 ppm and for *o*-BrG the next signals were assigned: C-1 141.76 ppm, C-2 114,81 ppm, C-3 126.44 ppm, C-4 123.87 ppm, C-5 114.81 ppm, C-6 153.6 ppm.

5.4.2. Grignard reaction

The Grignard addition reaction is one of the most important organometallic transformations for forming a carbon-carbon bond. The reaction between an organomagnesium halide and a carbonyl compound is performed under strictly anhydrous condition in an ethereal solution (usually diethyl ether or THF) [48].

Grignard reagents are usually prepared by introducing an organic halide into a stirred suspension of magnesium turning in ether (diethyl ether of THF). The reaction occurs at the surface of magnesium and for this reason is considered to be heterogeneous and has been shown to involve radical intermediates. After the Grignard reagent forms on the reactive magnesium site it dissolved away from the metal surface into the ether, exposing another fresh site for reaction. Following the initiation period, mass transfer of the alkyl halide to the reaction magnesium sites is considered to be the rate-limiting step. The magnesium of the Grignard reagent is two electron pair short if an octet but the oxygen of the ether can donate these electron pairs to the magnesium of R-Mg-X. This coordination explains the fact that ether solvents are generally required for the formation of Grignard reagents because of their ability to solubilize the Grignard reagent as it is formed. If this did not occur, the metal would eventually be covered and the

reaction would cease. The actual mechanism and specifically how the magnesium is inserted into the substrate is still not completely understood [49].

5.4.2.1. Grignard reaction for brominated guaiacol and syringol

In an three necked flask with a double surface reflux condenser, a sealed (with septum) mechanical stirrer and a separatory funnel, and place dry activated magnesium turnings (0.05 g). Add 0.7 mL of diethyl ether to the 0.395 of bromosyringol and bromoguaiacol and add them to a separatory funnel to be slowly added to the flask. If the reaction does not start immediately, heat it to reflux until it does. Continue the stirring and heating reflux for further 30 minutes. The Grignard reagent collects as heavy oil at the bottom of the flask. Once the mixture is cooled down, add it to a beaker with dry ice and mix it up until the reaction is completed.

Transfer the content of the beaker to a separatory funnel, and add 5 mL diethyl ether. Extract the aqueous layer (bottom) layer into a clean flask/beaker, and transfer the organic layer to a clean flask. Combine the two organic layers.

The organic layer is now transferred back to the separatory funnel. Add 5 mL 6M NaOH to the separatory funnel, and extract the aqueous layer, so add another 5 mL portion of 6M NaOH to the organic layer (still in the separatory funnel) and extract the product, combining this with the aqueous layer in the beaker.

Place the beaker/flask containing the basic product into an ice bath, and add 12M HCl in small portions until the product precipitates. Isolate the product via vacuum

filtration, using cold water to wash the entire product from the flask.

Aromatic acids were analyzed by HPLC JASCO instrument equipped with an interface (LC-NetII/ACD) and a photodiode array detector (MD-2018). A Teknokroma Mediterramean Sea18 column (25x0.46 cm) was used for the experiments and a mixture of acetonitrile and HPLC water (1:8, v/v) with 1% of acetic acid was used as mobile phase. The flow rate was 0.5 mL/min and the analyses were carried out at 40 ºC. Calibration was done using pure compounds standards (Sigma-Aldrich) vanillic acid, syringic acid, 3-methoxysalycilic acid.

During the first experiments the mixture of brominated guaiacol and syringol were reactioned with the magnesium tunings. Although literature procedure was followed the reaction did not start even with heat. As the starting material was a mixture and the quantities were low maybe it inhibited the reaction. That is the reason why a mixture only with the standards of bromoguaiacol and bromosyringol were tried with similar results. The starting materials did not reacted with the magnesium turnings.

5.4.2.2. Conclusions

The conclusion of these preliminaly experiments suggests that the products obtainined from the bromination should be separated in order to have a more selective media for the Grignard reaction. Also a higher concentration of the brominated guaiacol and syringol could be more effective.

5.5 References

1. E.B. da Silva, M. Zabkova, J.D. Araújo, C.A. Cateto, M.F. Barreiro, M.N. Belgacem, A.E. Rodrigues. An integrated process to produce vanillin and lignin-based polyurethanes from Kraft lignin. *Chemical Engineering Research and Design*, (2009), 87(9), 1276-1292.
2. P.C. R. Pinto, E.A.B. da Silva, A.E. Rodrigues, A. E. Lignin as source of fine chemicals: vanillin and syringaldehyde. In *Biomass Conversion*. Springer Berlin Heidelberg ,(2012), 381-420.
3. S. Cohen, P.A. Belinky, Y. Hadar,C.G. Dosoretz. Characterization of catechol derivative removal by lignin peroxidase in aqueous mixture. *Bioresource technology*, (2009), *100*(7), 2247-2253.
4. J. Huang, K. Huang, C. Yan. Application of an easily water-compatible hypercrosslinked polymeric adsorbent for efficient removal of catechol and resorcinol in aqueous solution. *Journal of hazardous materials*, (2009), 167(1), 69-74.
5. H. Wang, Q. Wang, Z. Xiong, C. Chen, B. Shen. Solubilities of benzoic acid in binary (benzyl alcohol+ benzaldehyde) solvent mixtures. *The Journal of Chemical Thermodynamics*, (2015), *83*, 61-66.
6. M. Janda, E. Ruelland. Magical mystery tour: salicylic acid signalling. *Environmental and Experimental Botany*, (2015), 114, 117-128.
7. P. Varanasi, P. Singh, M. Auer, P.D. Adams, B.A. Simmons, S. Singh, S. Survey of renewable chemicals produced from lignocellulosic biomass during ionic liquid pretreatment. *Biotechnology for biofuels*,(2013), *6*(1), 1.
8. J. Zakzeski, P.C. Bruijnincx, A.L. Jongerius, B.M. Weckhuysen. The catalytic valorization of lignin for the production of renewable chemicals.*Chemical reviews*, (2010), 110(6), 3552-3599.

9. M. Kleinert,T. Barth. Phenols from lignin. *Chemical Engineering & Technology*, (2008), 31(5), 736-745.
10. E. Dorrestijn, L.J. Laarhoven, I.W. Arends, P. Mulder. The occurrence and reactivity of phenoxyl linkages in lignin and low rank coal. *Journal of Analytical and Applied Pyrolysis*, (2000), *54*(1), 153-192.
11. B. Sumit, M. Doble. *Homogeneous catalysis: mechanisms and industrial applications* by John Wiley and Sons, Inc. (2000).
12. A. Behr. *Catalysis, Homogeneous*. Ullmann's encyclopedia of industrial chemistry. (2010), Vol.7, pp. 223-268.
13. J.A. Moulijn, P.W. van Leeuwen, R.A. van Santen (Eds.).*Catalysis: an integrated approach to homogeneous, heterogeneous and industrial catalysis*, Vol. 79, (1993), Elsevier.
14. G.W. Huber, S. Iborra, A. Corma. Synthesis of transportation fuels from biomass: chemistry, catalysts, and engineering. *Chemical reviews*, (2006), *106* (9), 4044-4098.
15. J.E. Miller, L. Evans, A. Littlewolf, D.E. Trudell. Batch microreactor studies of lignin and lignin model compound depolymerization by bases in alcohol solvents. *Fuel,* (1999), *78*(11), 1363-1366.
16. V. Roberts, V. Stein, T. Reiner, A. Lemonidou, X. Li, J.A. Lercher. Towards quantitative catalytic lignin depolymerization. *Chemistry–A European Journal*, (2011), *17*(21), 5939-5948.
17. A. Toledano, L. Serrano, J. Labidi. Organosolv lignin depolymerization with different base catalysts. *Journal of Chemical Technology and Biotechnology*, (2012), 87(11), 1593-1599.
18. T. Kanetake, M. Sasaki, M. Goto. Decomposition of a Lignin Model Compound under Hydrothermal Conditions. *Chemical Engineering & Technology* (2007), 30(8), 1113-1122.

19. T. Fukuyama, S. Maetani, I. Ryu. Carbonylation and decarbonylation reactions in Comprehensive Organic Synthesis, 2nd Ed., Ed. P. Knochel, G.A. Molander. Elsevier Amsterdam NM, Vol.3, (2014), pp. 1073-1100.
20. W. Fang, H. Zhu, Q. Deng, S. Liu, X. Li, Y. Shen, T. Tu. Design and Development of Ligands for Palladium-Catalyzed Carbonylation Reactions. *Synthesis*, (2014), *46* (13), 1689-1708.
21. R. Grigg, S.P. Mutton. Pd-catalysed carbonylations: versatile technology for discovery and process chemists. *Tetrahedron*, (2010) *66*(30), 5515-5548.
22. Y. Kubota, S. Nakada, Y. Sugi. Palladium-catalyzed alkoxycarbonylation of aryl p-toluenesulfonate. *Synlett*, (1998), (2), 183-185.
23. R.H. Munday, J.R. Martinelli, S.L. Buchwald, S. L. Palladium-catalyzed carbonylation of aryl tosylates and mesylates. *Journal of the American Chemical Society*, (2008), *130*(9), 2754-2755.
24. N. Fujikawa, T. Ohta, T. Yamaguchi, T. Fukuda, F. Ishibashi, M. Iwao. Total synthesis of lamellarins D, L, and N. *Tetrahedron*, (2006), 62(4), 594-604.
25. J.G. Morton, C. Draghici, L.D. Kwon, J.T. Njardarson. Rapid Assembly of Vinigrol's Unique Carbocyclic Skeleton. *Organic letters*, (2009), *11*(20), 4492-4495.
26. X.F. Wu, H. Neumann, M. Beller. Palladium-Catalyzed Oxidative Carbonylation Reactions. *ChemSusChem*, (2013), *6*(2), 229-241.
27. C. Jia, T. Kitamura,Y. Fujiwara. Catalytic functionalization of arenes and alkanes via CH bond activation. *Accounts of chemical research,* (2001), *34*(8), 633-639.
28. C.E. Houlden, M. Hutchby, C.D. Bailey,J.G. Ford, S.N. Tyler, M.R. Gagné, K.I. Booker-Milburn. Room-Temperature Palladium-Catalyzed C-H Activation: ortho-Carbonylation of Aniline Derivatives. *Angewandte Chemie International Edition*, (2009), *48*(10), 1830-1833.

29. R. Giri, J.K. Lam, J.Q. Yu. Synthetic applications of Pd (II)-catalyzed C− H carboxylation and mechanistic insights: expedient routes to anthranilic acids, oxazolinones, and quinazolinones. *Journal of the American Chemical Society*, (2009), *132*(2), 686-693.
30. B. Liu, B.F. Shi. Efficient Synthesis of Carboxylic Esters via Palladium (II)-Catalyzed Direct Alkoxycarbonylation of Arenes with CO and Alcohols. *Synlett*, (2013), *24*(17), 2274-2278.
31. M. Chen, Z.H. Ren, Y.Y. Wang, Z.H. Guan. Palladium-Catalyzed Oxidative Carbonylation of Aromatic C–H Bonds of N-Alkylanilines with CO and Alcohols for the Synthesis of o-Aminobenzoates. *The Journal of organic chemistry*, (2015), *80*(2), 1258-1263.
32. R. Giri, J.Q. Yu. Synthesis of 1, 2-and 1, 3-Dicarboxylic Acids via Pd (II)-Catalyzed Carboxylation of Aryl and Vinyl C− H Bonds. *Journal of the American Chemical Society*, (2008), *130*(43), 14082-14083.
33. S. Ohashi, S. Sakaguchi, Y. Ishii. Carboxylation of anisole derivatives with CO and O_2 catalyzed by $Pd(OAc)_2$ and molybdovanadophosphates. *Chemical communications*, (2005), (4), 486-488.
34. H. Zhang, D. Liu, C. Chen, C. Liu, A. Lei. Palladium-Catalyzed Regioselective Aerobic Oxidative C-H/N-H Carbonylation of Heteroarenes under Base-Free Conditions. *Chemistry–A European Journal*, (2011), *17*(35), 9581-9585.
35. L. Wang, Y. Wang, C. Liu, A. Lei. CO/C-H as an Acylating Reagent: A Palladium-Catalyzed Aerobic Oxidative Carbonylative Esterification of Alcohols. *Angewandte Chemie International Edition*, (2014), 53(22), 5657-5661.
36. Y. Fujiwara, T. Kawauchi, H. Taniguchi. Palladium-promoted one-step carboxylation of aromatic compounds with carbon monoxide. *Journal of the Chemical Society, Chemical Communications*, (1980), (5), 220-221.

37. S. Ohashi, S. Sakaguchi, Y. Ishii. Carboxylation of anisole derivates with CO and O_2 catalyzed by $Pd(OAc)_2$ and molybdovanadophosphates. *Chemical communications*, (2005), (4), 486-488.
38. Y. Taniguchi, Y. Yamaoka, K. Nakata, K. Takaki, Y. Fujiwara. Palladium(II) Catalyzed Carboxylation of Aromatic Compounds with CO under Very Mild Conditions. *Chemistry Letters*, (1995), (5), 345-346.
39. W. Lu, Y. Yamaoka, Y. Taniguchi, T. Kitamura, K. Takaki,Y. Fujiwara. Palladium (II)-catalyzed carboxylation of benzene and other aromatic compounds with carbon monoxide under very mild conditions. *Journal of organometallic chemistry*, (1999), 580(2), 290-294.
40. K. Khosravi, S. Kazemi, Green, mild and efficient bromination of aromatic compounds by HBr promoted by *trans*-3,5-dihydroperoxy-3,5-dimethyl-1,2-dioxolane in waster as solvent. *Chim Chen Lett* , (2012), 23, 387-390.
41. J. Pavlinac, M. Zupan, K.K. Laali, S. Stavber. Halogenation of organic compounds in ionic liquids. *Tetrahedron*, (2009), 65, 5625-5662.
42. U. Bora, G. Bose, M.K. Chaudhuri, S.S. Dhar, R. Gopinath, A.T. Khan, B.K. Patel. Regioselective bromination of organic substrates by tetrabutylammoium bromide promoted by V_2O_5-H_2O_2: An environmentally favorable synthetic protocol. *Org Lett*, (2000), 2, 247-249.
43. F. Atefi, M.T. Garcia, R.D. Singer, P.J. Scammells. Phosphonium ionic liquids: design, synthesis and evaluation of biodegradability. *Green Chemistry*, (2009), 11, 1595-1604.
44. Z.G. Le, Z.C. Chen, Y. Hu. (Bmim) Br3 as a New Reagent for Regioselective Monobromination of Phenols and Several Activated Aromatics under Solvent-free Conditions. *Chinese Journal of Chemistry*, (2005), *23*(11), 1537-1540.

45. S.R. Pingali, M. Madhav, B.S. Jursic. An efficient regioselective NBS aromatic bromination in the presence of an ionic liquid. *Tetrahedron Letters,* (2010), 51(10), 1383-1385.
46. LG Wade JC, in *Química Orgánica*, ed by Pérez Bonilla J T. Prentice Hall Hispanoamerica S.A., México, pp 510-511 (2006).
47. A. Vigneault, D.K. Johnson, E. Chornet. Base-Catalyzed Depolymerization of Lignin: Separation of monomers. *The Canadian Journal of Chemical Engineering*, (2007), 85, 906-916.
48. G. Osztrovszky, T. Holm, R. Madsen. Ultrafast Grignard addition reactions in the presence of water. *Organic & Biomolecular Chemistry,* (2010), 8(15), 3402-3404.
49. D.J. Ende, P.J. Clifford, D.M. Antonis, C. SantaMaria, S.J. Brenek. Preparation of Grignard reagents : FTIR and Calorimetric investigation for safe scale-up, *Organic Process Research & Development*, (1999), 3, 319-329.

Chapter 6

Conclusion

1. Conclusion

In this chapter the summary of the main conclusions drawn from the development of this research work are presented.

The study concerning lignin extraction was focused on the influence of the extraction conditions in order to enhance lignin production.

As lignin structure strongly depends on the raw material and the applied pretreatment. The relationship between them was studied. Almond shell was subjected to four different processes (alkali, ethanol organosolv, formosolv and acetosolv and formosolv) to extract the lignin. Obtained lignins (AS, OE, OF and OAF) were deeply characterized in order to evaluate which pretreatment yielded the highest quality lignin. The applied alkali pretreatment produced very impure lignin. The contamination was mainly due to carbohydrates and inorganic salts. The purity of the organosolv samples was very high (more than 70% of AIL) with low content of inorganic salts and hemicelluloses. Otherwise, all lignin samples, except for the AS lignin, had a very high antioxidant power and an average total phenolic content. Taking into account all obtained results, acid organosolv conditions were selected as the ones that yielded the highest quality lignin.

The study concerning the pyrolytic study of the different agricultural and industrial lignins was focused on the measurement of the syringyl and guaiacyl groups to know the lignin with the highest and most equal content of guaiacyl and syringil units for further depolymerization. The raw materials and the lignins extracted by different extraction methods were deeply characterized. The results showed that the raw materials with the highest and most equal syringyl and guaiacyl units were olive tree pruning and almond shell.

In the fourth chapter lignin extracted from olive tree pruning by an organosolv method was subjected to an experimental design where, the temperature, time and catalyst concentration were varied to obtain polyol under microwave heating with the highest yield and hydroxyl groups. The results revealed bad regression values for the hydroxyl number equation and for that reason this equation was not taken into account. Based on literature the hydroxyl number had to be between 300-800 mgKOH/g for further applications. Applying these limitations two optimal experiments were obtained being the polyol 24 the one with the highest hydroxyl number and yield.

In the fifth chapter guaiacol and syringol the two main monomers obtained from the depolymerization of lignin were chemically transformed to obtain aoromatic acids. The first part of this chapter deals with the alkoxy carbonylation reactions were guaiacol and syringol were activated via mesylation and tosylation. The alkoxy carbonylation reactions done with different conditions (temperature and pressure), ligands, bases and catalysts revealed that the best conversion and yields were obtained with the ligands dcpp. However, the yield was low in all cases due to sterically hindered substrates and because of secondary reactions as direct couplings were the main reactions. In the second part oxidative carbonylation using different substrates (G, S and P), oxidants and reaction conditions was performed. In the case of guaiacol the results with benzoquinone (BQ) in combination with acetic acid (AcOH) gave bad yields and the reason may be due to the lack of dioxane and *p*-TsOH in the reaction media. The best results were obtained with potassium persulfate ($K_2S_2O_8$) as oxidant and TFA as solvent with the mildest conditions with a yield of 46% for vanillic acid and 5% for 3-methoxysalicylic acid. In the case of syringol similar results were observed as the reaction with BQ and AcOH gave bad results and good results with $K_2S_2O_8$

and TFA. Although the results were better in the second case they were not as high as expected so the pressure was highered and water was introduced in the reaction media with the best results being with 100µL of water, 50ºC and 1 bar of CO aiming 46% of yield for syringic acid. In the third part of this chapter guaiacol and syringol were firstly brominated to proceed to the Grignard reaction of the mixture. The bromination was done firstly only with guaiacol and syringol and then with the mixture of them. The results showed that reaction with the mix of G and S favored more the reaction of S towards X_s and and ΣBrS isomers than in the bromination only with S. Once the reaction was understood ethyl acetate and diethyl ether were tried in the extraction stage. Although the of the X_G and X_S was higher with DEE (X_G 57% and X_S 72%) than with EtAc (X_G 50% and X_S 60%) the results showed that in proportion EtAc (ΣBrG 17% and ΣBrS 20%) was able to extract more desired products than the DEE (ΣBrG 15% and ΣBrS 22%). Lastly, Grignard reactiond were tried. During the first experiments the mixture of brominated guaiacol and syringol were reactioned with magnesium tunings. Although literature procedure was followed the reaction did not stat even when heat was applied. As the starting material was a mixture and the quantities were low it is possible they were inhibiting the reaction. As solution standards of bromoguaiacol and bromosyringol were tried with no success.

Overally, lignin extracted by different extraction methods was analyzed to obtain pure lignins. Afterwards, lignins from different raw materials and extraction methods were analyzed to determine its guaiacyl and syringyl group content by Py-GC/MS for further lignin depolymerization. Syringol and guaiacol after separation would be utilized as source for value added chemicals. In the devepolment of this thesis lignin was liquefied under microwave heating into polyols applying different conditions with the aim of high hydroxyl number and yield. Furthermore, guaiacol and syringol were used as raw materials for the conversion to

aromatic acids with three lines of research (alkoxy carbonylation, oxidative carbonylation and bromination followed by the Grignard reaction) each one with different results. Althought there was conversion in the experiment of alkoxy carbonylation low yields were obtained. In the case of the oxidative carbonylation significant yiends of the desired products such as vanillic acid, 3-methoxysalicylic acid and syringyc acid were recover. Finally, guaiacol and syringol were brominated, but as the resulting product was a mixture of products it was no possible to utilize it for the Grignard reaction.

2. Future works

To continue the work in this field, the following lines of research are proposed:

- Measure the H:G:S ratio by nitrobenzene oxidation to see if the ratios are similar. Following the same line of research, depolymerize almond shell and olive tree pruning lignin with the best possible conditions to reach high yields of guaiacyl and syringyl units.

- In the polyol production under microwave heating lower the power from 500W to 300W and analyze the polyols to see if there is any difference on the properties.

- Search for methods to separate the bromination products. Firstly, use the thin layer chromatography (TLC) to choose the adequate solvent to separate the different products.

- Search for oxidative carbonylation methods were the carbon monoxide source is not a gas.

3. Publications

1- Itziar Egües, Xabier Erdocia, Ane Sequeiros, Jalel Labidi

Chapter 31: New Advances in Biobased Resins.

Editor: Inamuddin; Green Polymer Composites Technology (2016), pp. 449-461. CRC Press.

Ane Sequeiros, Jalel Labidi

Characterization and determination of the S/G ratio via Py-GC/MS of agricultural and industrial residues

Industrial Crops and Products (sended)

Ane Sequeiros, Luis Serrano, Jalel Labidi

Bromination of guaiacol and syringol using ionic liquids to obtain bromides.

Journal of chemical technology and biotechnology. Wiley, 2015

DOI 10.1002/jctb.4773

IF: 2.349; JC: Engineering, Chemical; JR: 39/135

Ane Sequeiros; Alberto Garci Gatto; Jalel Labidi; Luis Serrano

Different extraction methods to obtain lignin from almond Shell.

Journal of biobased materials and bioenergy, (2014), 8 (3), pp. 370-376.

IF: 0.653; JC: Engineering, Chemical; JR: 53/72

Ane Sequeiros; Luis Serrano, Rodrigo Briones; Jalel Labidi

Lignin liquefaction under microwave heating.

Journal of Applied Polymer Science, (2013), 130 (5), pp. 3292-3298.

IF: 1.768; JC: Engineering, Chemical; JR: 35/82

Rodrigo Briones, Luis Serrano, Ane Sequeiros, Jalel Labidi

Influence of microwave heating on chemical properties of liquefied lignocellulosic residues.

Industrial and Engineering Chemistry Research, (2013), 52 (8), pp. 2755-2761.

IF: 2.587; JC: Engineering, Chemical; JR: 27/135

Marian Andrés; Ane Sequeiros; Rodrigo Sánchez; Ana Requejo, Luis Serrano.

Production of paper and lignin from Hesperaloe funifera.

Environmental Engineering and management journal, (2013).

IF: 1.062; JC: Engineering, Chemical.

Congress contributions

Ane Sequeiros; Luis Serrano; Jalel Labidi

Bromination of guaiacol and syringol using ionic liquids to obtain bromindes (poster)

CHISA 2016

27-31 August, Prague, Czech Republic

Ane Sequeiros; Jalel Labidi

Bromination of guaiacol and syringol to obtain bromides (poster)

Cost FP1306 Second Workshop

4-6 April, Dubrovnik, Croatia

Ane Sequeiros; Luis Serrano; Jalel Labidi.

Different extraction methods to obtain lignin from almond shell (poster)

3rd International Symposium on Green Chemistry (ISGC), 3-7 May 2015, La Rochelle, France

Ane Sequeiros

Different extraction methods to obtain lignin from almond shell (Flash oral presentation)

COST FP1306, 3-5 February 2015

Belgrade, Serbia

Ane Sequeiros

Oral presentation of the research group

1st meeting of COST FP1306, Valorization of lignocellulosic biomass side streams for suitable production of chemicals, materials and fuels using low environmental impact technologies

27-28 October 2014, Warsaw, Poland

Rodrigo Briones, F. Valdebenito, Ane Sequeiros; Y. Saravia.

Liquefied agricultural wastes for film elaboration (Oral)

Renewable resources and Biorefieneries RRB-10

4-6 June 2014, Valladolid, Spain

Ane Sequeiros, Alberto Darci Gatto, Jalel Labidi, Luis Serrano.

Influence of microwave heating on the chemical properties of liquefied lignocellulosic residues (poster)

Renewable resources and Biorefineries RRB10

4-6 June 2014, Valladolid, Spain

Ane Sequeiros; Maria Gonzánez; Darci Alberto Gatto; Jalel Labidi; Luis Serrano.

Lignin liquefaction under microwave heating (poster)

4th International Conference on biodegradable and biobased polymers

1-4 October 2013, Roma, Italy

Ane Sequeiros; Luis Serrano; Jalel Labidi.

Lignin liquefaction under microwave heating (poster)

COST FP0901 Biorefinery analytics-outcomes

17-18 September 2013, Turku-Abo, Finland

Rodrigo Briones; Luis Serrano; Ane Sequeiros; Jalel Labidi.

Influence of microwave activation on chemical properties of liquefied lignocellulosic residues (poster).

20th International Congress of Chemical and Process Engineering and PRESS-15th PRESS Conference

25-29 August 2012, Prague, Czech Republic

Appendix

1. Appendix I

1.1. Characterization procedures of lignocellulosic biomass and solid fractions

The lignocellulosic biomass and the solid fractions were characterized using the procedures described in the standards by Technical Association of Pulp and Paper Industries (TAPPI), as detailed below:

1.1.1. Sample preparation (TAPPI T257-cm85)

The objective of this standard is to set the suitable size conditions of the raw material or sample so that it is homogeneous and suitable for the chemical treatments which will be performed to determine the chemical composition of the fibers

The sample preparation consists of grinding the sample in a mill Retsch 2000 with a sieve of 4 mm, neglecting the fractions with a size less than 0.25 mm. raw material is selected with a size between 0.4 and 0.25 mm.

1.1.2. Moisture content (TAPPI T264-cm97)

This moisture content corresponds to the equilibrium moisture content of the sample, and will be taken into account in subsequent analysis. The procedure to determine the moisture consists of:

- Carefully clean the empty crucible and dry it in an over at 105 ±3 °C for 30-60 minutes. Cool slightly and then place in a desiccators. When cooled to room temperature, weight the dried crucible on the analytical balance to the nearest 0.1 mg.
- Accurately weight 2.00 ±0.001 g of the sample.
- Place it in the oven at 105 ±3 °C for 24 hours.
- After that time, samples were transferred to desiccators until cool down to room temperature. After cooling the sample, weighing until the weight of the sample is constant to ± 0.2 mg.

The moisture is determined as follows:

$$Moisture\ (\%) = \frac{S_0 - S_f}{S_0}$$

S_0= initial sample

S_f= final sample

1.1.3. Ash content at 525 ºC (TAPPI T211-om93)

The ash content of the sample may consist of: various residues from chemicals used in its manufacture, metallic matter from piping and machinery, mineral matter in the pulp from which the paper was made and filling, coating, pigmenting and/or other added materials. The amount and composition of the ash is a function of the presence or absence of any of these materials or other singly or in combination.

The procedure to determine the ash content at 525 °C consists of:

- The test samples, 1 g moisture free, shall be weighted on an analytical balance to the nearest 0.1 mg.

- Carefully clean the empty crucible and ignite in a muffle furnace at 525±25 °C for 30-60 minutes. After ignition, cool slightly and then place in a desiccators. When cooled to room temperature, weight the ignited crucible on an analytical balance to the nearest 0.1 mg.
- Transfer the test sample to the crucible. Place the crucible with a cover in a furnace at about 100 °C. Raise the temperature to 525 °C slowly so that the sample becomes carbonized without flaming. Sample must be charred, not burned so that the temperature of the samples does not exceed 525 °C. When the residue has ceased to char, place the crucible with the sample into the furnace at 525 ± 25 °C and remove the cover after the crucible seems to have reached the temperature of the furnace.
- When the sample is completely combusted as indicated by the absence of black particles, remove the crucible from the furnace, replace the cover, and allow to cool down somewhat; then place in a desiccators to cool to room temperature. Weight the crucible with ash to the nearest 0.1 mg.
- Repeat the ignition and weighing until the weight of the ash is constant to ±0.2 mg.

The ash content at 525 °C is determined as follows:

$$Ash\ content\ (\%) = \frac{S_f}{S_0}.100 \quad (2)$$

S_f= sample after the ignition

S_0= initial sample (moisture free)

1.1.4. Solvent extractives (TAPPI T204-cm97)

This method describes the procedure to determine the amount of solvent-soluble, non-volatile material in wood and pulp. Since the pulping process usually removes most water-soluble and volatile compounds that are also soluble in organic solvents, the solvent extractable material in pulp may be considered to consist primarily of resin and fatty acids and their esters, waxes, and unsaponifiable substances.

The procedure to determine the solvent extractives consists of:

- Place 4.0 ± 0.1 g (accurately weight) of dry raw material on an extraction thimble. Cap the thimble with another thimble to prevent sample losses.
- Place extraction thimble with the sample in position in the Soxhlet apparatus. Fill the extraction flask with 150 mL of toluene-ethanol mixture (1:2 v/v).
- Connect the flask to the extraction apparatus, and start water flow to the condenser section. Adjust the heaters to provide a boiling rate which will cycle the samples for not less than 24 extractions over a 4-5 h period. If the extraction is left unattended, a provision should be made to shut off the heat if the water and/or electricity shut off unexpectedly.
- Remove the flask from the apparatus and partially evaporate the solvent in the extraction flask to a volume of 20-25 mL. Transfer the extract to the tared weighing dish by washing with a small amount of fresh solvent. Handle the weighing dish with forceps or tongs.

- Dry the dish and contents in an oven for 1 h at 105 ± 3 ºC, cool to room temperature in a desiccators, and weight to the nearest 0.1 mg.

The percentage of extractives is determined as follows:

$$Extractives\ (\%) = \frac{F_f - F_0}{S_0.\left(\frac{100 - \%H}{100}\right)}.100$$

F_f= flask after the extraction

F_0= flask before the extraction

S_0= initial sample

%H= moisture content

1.1.5. Acid-insoluble lignin (TAPPI T222-om98)

Some of the lignin dissolved in acid solution during the test is not included in the test results. In softwoods (coniferous woods) and in sulfate pulps, the amount of soluble lignin is small, about 0.2 to 0.5%. In hadwoods (deciduous woods) non-wood fibers, and in sulfite pulps, the content of soluble lignin is about 3 to 5%. The carbohydrates in wood and pulp are hydrolyzed and solubilized by sulfuric acid.

The procedure to determine the acid-insoluble lignin consists of:

- Weigh out two test samples to the nearest 0.1 mg as follows: for wood 1.0 ± 0.1 g; for pulp, 2.0 ± 0.1 g, and equivalent to oven-dry weight. Place the test samples in 100 mL beakers. Samples should be previously extracted.

- Add to the beakers containing the test samples cold (10 to 15 ºC) 72% sulphuric acid, 15.0 mL for wood and 40.0 mL for pulp specimen. Add the acid gradually in small increments while stirring and macerating the material with a glass rod. Keep the beaker in a bath at 20 ± 1 ºC for 2 h. Stir the material frequently during this time to ensure complete solution.
- Add about 300 to 400 mL of water to a flask and transfer the material from the beaker to the flask. Rinse and dilute with water to 3% concentration of sulphuric acid, to a total volume of 575 mL for wood, and to 1540 mL for pulps.
- Boil the solution for 4h, maintaining constant volume either by using a reflux condenser or by frequent addition of hot water.
- Allow the insoluble material (lignin) to settle, keeping the flask in an inclined position. If the lignin is finely dispersed, it may require an "overnight" or a longer period to settle. Without stirring up the precipitate, decant or siphon off the supernatant solution through a filtering crucible. Then transfer the lignin quantitatively to the filter, using hot water.
- Dry the crucible with lignin in an oven at 105 ± 3 ºC to constant weight. Cool to room temperature in a desiccators and weight.

The percentage of acid-insoluble lignin is determined as follows:

$$Acid\ insoluble\ lignin\ (\%) = \frac{S_f}{S_0 - (100 - Extractive)} . 100$$

S_f= sample after the treatment

S_0= initial sample

1.1.6. Holocellulose content (Wise and Col.)

Holocellulose is defined as the fraction of water-insoluble carbohydrate present in plant raw materials, grouping cellulose and hemicelluloses present in the fibers. The method of Wise et al. [1] is based on chlorine dioxide which emerges in successive treatments with sodium chloride dissolved lignin while carbohydrates remain unchanged.

The procedure to determine holocellulose consists of:

- Weight 2.5 ± 0.1 g of sample and placed it in a beaker. Add 80 mL of hot distilled water (70-80 °C). The mixture was immersed in a bath at 70 °C and stirred periodically to homogenize.
- Every 60 min, add 0.5 mL of glacial acetic acid and 2.6 mL of 25% sodium chlorite to the beaker. Repeat these conditions till cover a total period of 6-8 hours.
- After that time the mixture is kept in the bath for 12 h without further additions.
- The vessel contents were poured over the filter (previously dried and tared) and filtered under vacuum, washing with hot water until neutral pH.
- Dry the filter with holocellulose in an oven at 105 ± 3°C to constant weight. Cool to room temperature in a desiccators and weigh.

The percentage of holocellulose is determined as follows:

$$Holocellulose\ (\%) = \frac{S_f}{S_0.(100 - Extractive)}.100$$

S_f= sample after the treatment

S_0= initial sample

1.1.7. α-cellulose content (Rowell)

Since the TAPPI T203-om 93 ("Determination of α, β and ɣ cellulose pulp") is defined only for paper pulp, and places special emphasis on it, it was decided to use the protocol proposed by Rowell et al. to determine the content of α-cellulose and hemicelluloses in wood samples. The term "hemicelluloses" is defined in this method as components of plan cell wall that are solubilized by treatment with sodium hydroxide and acetic acid, while the α-cellulose corresponds to the fraction of holocellulose remaining insoluble after such treatment.

The procedure to determine α-cellulose consists of:

- Accurately weigh 2 ± 0.1 g of sample of dry holocellulose free extracts, extracted from the fibers by the previous method.
- Add 10 mL of 17.5% NaOH solution with stirring. Subsequently, add 5 mL of 17.5% NaOH solution every 5 minutes until reaching 15 mL of NaOH solution (3 additions of 5 mL). Wait for 30 minutes to the alkali solution to react with the sample at room temperature.
- Then, add 33 mL of distilled water at room temperature while stirring. Keep the solution at room temperature for 1 hour.
- The vessel contents were poured over the filter (previously dried and tared) and filtered under vacuum.
- The solid residue (α-cellulose) is washed with 100 mL 8.3% of NaOH solution after which, it is washed with distilled water twice.
- Then add 15 mL of 10% acetic acid solution allowing it to react for 3 minutes before connecting the vacuum. Finally wash the fibers with distilled water until the filtrate is free of acid (pH neutral).

- Dry the filter at 105 ± 3 ºC cooled down to room temperature in a desiccators and weighed.

The percentage of α-cellulose is determined as follows:

$$\alpha - cellulose\ (\%) = \frac{S_f}{S_0}.100$$

S_f= sample after the treatment

S_0= initial sample

$$Hemicelluloses\ (\%) = Holocelluloses\ (\%) - \alpha - cellulose\ (\%)$$

1.2. References

1. L.E. Wise, M. Murphy, A.A D'Adieco. A chlorite holocellulose, its fractionation and bearing on summative wood analysis and studies on the hemicelluloses,.*Paper Trade J.* 122 (1946), 35.
2. R. Rowell. The chemistry of solid wood: based on short course and symposium sponsored by the division of cellulose, paper, and textile chemistry at the *185th meeting of the American Chemical Society.* Seattle, Washington, 1983, 70.

2. Appendix II

2.1. Procedures for the characterization of liquid fractions

The obtained liquid fractions were physicochemically characterized using thermal procedures, as detailed below:

2.1.1. pH

The pH of the liquid fraction was determined using a pH meter “CRISON basic 20”.

2.1.2. Density

The density was calculated gravimetrically by measuring the weight of known volume of a volumetric flask filled with the liquid fraction.

2.1.3. Total dissolved solids

Total dissolved solids were determined following an adaptation of the procedure by the National Renewable Energy Laboratory NREL in standard LAP-012.

5 ± 0.001 g of the liquid fraction (m) were weighed in a crucible free of moisture and tared (m_i). The filled crucible was placed in an oven at 105 ± 3°C for 24 hours. After cooling in a desiccators, the crucible was weighed (m_f) until constant weight.

The total dissolved solids were determined as follows:

$$TDS\ (\%) = \left[\frac{(m_f - m_i)}{m}\right].100$$

m_f= weight of the dried crucible (g)

m_i=weight of the crucible after the procedure (g)

m= weight of the liquid fraction (g)

2.1.4. Inorganic and organic matter

The inorganic fraction of the liquid fraction can be determined after the combustion of the sample, adapted procedure of TAPPI standard T211om-93 (ashes at 525 ºC).

The crucible assembly-solid residue obtained in the previous experiment (total dissolved solids) is combusted in the oven at 525 ºC for 3 hours.

Subsequently, after cooling to room temperature in a desiccators, the crucible is weighed assembly (m_f).

The inorganic matter (IM) is determined as follows:

$$IM\ (\%) = \left[\frac{(m_f - m_i)}{m}\right].100$$

m_f= weight of dried crucible (g)

m_i= final weight of the crucible (g)

m= weight of the liquid fraction

The organic matter (OM) is determined as follows:

$$OM\ (\%) = TDS\ (\%) - IM\ (\%)$$

2.1.5. Lignin concentration

The method for determining lignin concentration in the liquid fraction varies depending on the pretreatment applied to the raw material for the lignin extraction. Nevertheless, the principle that governs all isolated procedures is the same, the insolubility of lignin in acid media.

A known volume of liquid fraction (V) is treated with the corresponding lignin isolation procedure. Previously, the filters have to be dried over night at 50 ± 1 °C and then tared

(m_i). The liquid fraction is precipitated and left overnight depending on the isolation procedure. The precipitated liquid fraction is filtered and the filter is dried at 50 ± 1 °C until the lignin gets dried. Once dried, samples were transferred to a desiccators until they cool down. After cooling the samples, weigh (mf) until weight of the sample is constant to ± 0.2 mg.

$$Lignin\ concentration\ (\%) = \left[\frac{(V.100)}{(m_f.m_i)}\right].100$$

V= liquid fraction volume (mL)

m_f= weight of the dried filter + lignin (g)

m_i= weight of the dried filter (g)

3. Appendix III

3.1. Procedures for the lignin characterization

The obtained lignins by different pretreatments were characterized using the procedures described in the standards developed by the International Lignin Institute (ILI) and internal procedures adapted to our facilities, as detailed below:

3.1.1. Acid-insoluble lignin

Acid insoluble lignin (AL) was determined by subjecting lignin to an acid hydrolysis process consisting of two stages. The first acidic hydrolysis was carried out adding 3.75 mL of sulphuric acid 72% to 0.375 g of lignin. The mixture was left for 1 hour at 30 °C. Then it was diluted with 36.25 mL of deionized water for 3 hours at 100 °C. After this time, the solution was cooled for 15 minutes and then filtered using filters over G3 glass filter crucible. The remaining solid is the

acid insoluble lignin. The filtrate is recovered in order to determine acid soluble lignin and sugar content.

The acid-insoluble lignin is determined as follows:

$$IL\ \% = \left[\frac{B - A}{C}\right].100$$

B= weight glass filter crucible + dried residue (g)

A= weight of the dried glass filter crucible (g)

C= initial weight of the sample (g)

3.1.2. Acid-soluble lignin

Acid soluble lignin (ASL) was determined by spectrophotometry (UV absorption at 205 nm). Filtrate samples had to be diluted with 1M H_2SO_4 until the absorbance was between 0.1 and 0.8.

The acid-soluble lignin is determined as follows:

$$Acid\ soluble\ lignin\ (\%) = \frac{A \cdot B \cdot C}{D \cdot E}$$

A = absorbance at 205 nm

B= dilution factor

C= filtrate volume (L)

D= extinction coefficient of lignin (110 $g{\cdot}L^{-1}{\cdot}cm^{-1}$)

E= initial lignin weight (g)

3.1.3. Sugar content

In order to determine the percentage of monosaccharides present in the acid insoluble lignin fraction, the volume of this fraction was measured. Afterwards, a sample was

injected into high performance liquid chromatography (HPLC) determined by Jasco LC Net II/ADC equipped with a photodiodie array detector MD-2018Plus, reflactive index detector RI-2031Plus abd Rezex ROA Organic Acid H^+ (8%) column.Dissolution of 0.005 N H_2SO_4 prepared with 100% deionized and degassed water was used as mobile phase (0.35 mL/min flow, 40ºC and injection volume 20µL). High purity standards of D-(+)-glucose, D-(+)-xylose and D-(-)-arabinose (provided by Fluka, with ≥99% of purity) were used for calibration.

The sugars content is determined as follows:

$$Sugar\ content\ (\%) = \left[\frac{A \cdot B}{1000 \cdot C}\right] \cdot 100$$

A= obtained concentration by HPLC (ppm)

B= filtrate volume (L)

C= the initial lignin weight (g)

3.1.4. Ash content

A Thermogravimetric Analysis (TGA) was carried out in a TGA/SDTA RSI analyzer of Mettler Toledo to determine the ash content. The samples of approximately 7 mg were heated from 25 ºC up to 800 ºC at a rate of 10 ºC/min in air atmosphere.

3.1.5. Total phenolic Content and the Antioxidant Capacity

The total phenolic content was determined by Folin-Ciocalteau spectrophotometric method using gallic acid as

reference compound and DMSO as solvent and was done as it follows:

- Each lignin solution (2g/L in DMSO) was prepared for total phenolic content assay by missing 0.5 mL of sample with 2.5 mL of Folin-Ciocalteau reagent, 5 mL of Na_2CO_3 20% and distilled water up to 50 mL.
- The preparations were kept in a thermostatic bath at 40 °C for 30 min, and afterwards, the absorbance of the samples at 750 nm was measured.

The total phenolic content was determined from the calibration curve made with gallic acid standard solutions (100-1000 mg/L in DMSO), and expressed as the percentage of gallic acid equivalents (GAE) in the lignin solid sample according to the following equation:

$$GAE(\%) = \frac{A_{750}}{C_{sample} \cdot k} \cdot 100$$

A_{750}= absorbance of the lignin solution at 750 nm

k= coefficient of the obtained gallic acid-DMSO calibration curve

c_{sample}= concentration (mg/L) of the analyzed lignin solution

The antioxidant capacity was measured by the ABTS assay which is based on the ability of the antioxidants to interact with the ABTS radical, decreasing its absorbance at 734 nm:

- A radical solution (7mM and 2.45 mM potassium persulfate) was prepared and left to stand in the dark at room-temperature for 12-16 hours before using.
- The solution was then diluted with a mixture of 50% v/v of ethanol-water to an absorbance the spectrophotometric analysis 2 mL of the dilution radical solution were mixed with 20 μL of a DMSO solution of lignin and the absorbance at 734 nm was

reaf after 6 minutes against 50% v/v ethanol-water mixture.

- A black (2mL of the diluted radical solution mixed with 20 µL of DMSO) and an ABTS sample (2 mL of the diluted radical solution) were included in the analysis.

The antioxidant power (AOP) was calculated as the percentage of absorbance at 734 nm:

$$AOP(\%) = \frac{A_{blank} - A_{sample}}{A_{ABTS}} \cdot 100$$

A_{blank}= absorbance value of the blank

A_{sample}= absorbance of the lignin solution

A_{ABTS}= absorbance of the radical solution

4. Appendix IV

Instrumental Characterization

4.1.1. Spectroscopic techniques

Fourier Transformed Infrared Spectroscopy (FTIR) equipped by a Universal Attenuated Total Reflectane accessory with DiCompTM crystal (2.4 refractive index; 1.66 depth of penetration).

Nuclear magnetic resonance (NMR) spectra were recorded at 30 °C on a Bruker Avance 500 MHz equipped with a z gradient BBI probe. Typically, 40 mg of sample were

dissolved in DMSO-d6. The spectral widths were 5000 and 25000 Hz for the 1H and 13C dimensions, respectively.

4.1.2. Chromatography techniques

High Performance Size Exclusion Chromatography (HPSEC) was used to evaluate molecular weight (Mw) and Mw distribution (MWD) using a JASCO instrument equipped with an interface (LC-NetII/ADC) and a reflex index deterctor (RI-2031Plus). Two PolarGel-M columns (300 x 7.5 mm) and PolarGel-M guard (50 x 7.5 mm) were employed. Dimethylformamide + 0.1% lithium bromide was the eluent. The flow rate was 0.7 mL/min and the analyses were carried out at 40 ºC. Calibration was done using polystyrene standards (Sigma-Aldrich) ranging from 266 to 70,000 g/mol.

High Performance Liquid Chromatography (HPLC) Jasco LC-Net II/ADC equipped with a photodiode array detector, refractive index detector and Rezex ROA_Organic Acid H^+ (8%) column. As mobile phase, dissolution of 0.005 N H_2SO_4 prepared with 100 % deionised and degassed water was used (0.35 mL/min flow, 40 ºC and injection volume 20 µL). High purity xylose, glucose, galactose, mannose and arabinose purchased from Sigma-Aldrich were used for calibration. A linear calibration (R^2> 0.999) was obtained for all sugars.

Pyrolysis device was the CDS analytical Pyroprobe 5150. The pyrolysis temperature was set at 500 ºC for 10 seconds with a heating rate of 2 ºC/msec with the interface kept at 250 ºC.

Gas chromatography mass spectra characterization was done in GC (7890A)-MS (5975C inert MSD with Triple-Axis Detector) Agilent equipped with a fused silica capillary

column (HP-5MS, 30m x 0.25 mm x 0.25µm). The temperature program started at 50 ºC then, the temperature was raised to 120 ºC at 10 ºC/min, held 5 min, raised to 280 ºC at 10 ºC/min, held 8 min, raised to 300 ºC at 10 ºC/min and held for 2 min. Helium was used as carrier gas.

Calibration curves were done using pure compounds (Sigma-Aldrich)-phenol, *o*-cresol, *m*-cresol, *p*-cresol, guaiacol, catechol, 4-methylcatechol, syringol, acetovanillone, syringaldehyde, acetosyringone and 4-hydroxy-3-methoxyphenylacetone.

4.1.3. Thermogravimetric techniques

Thermogravimetric analysis (TGA) of lignin was carried out under nitrogen atmosphere using a Mettler Toledo TGA/SDTA RSI analyzer with a dynamic scan from 25 to 800 ºC at a 10 ºC min^{-1} temperature increasing grade.

LIST OF FIGURES

LIST OF TABLES